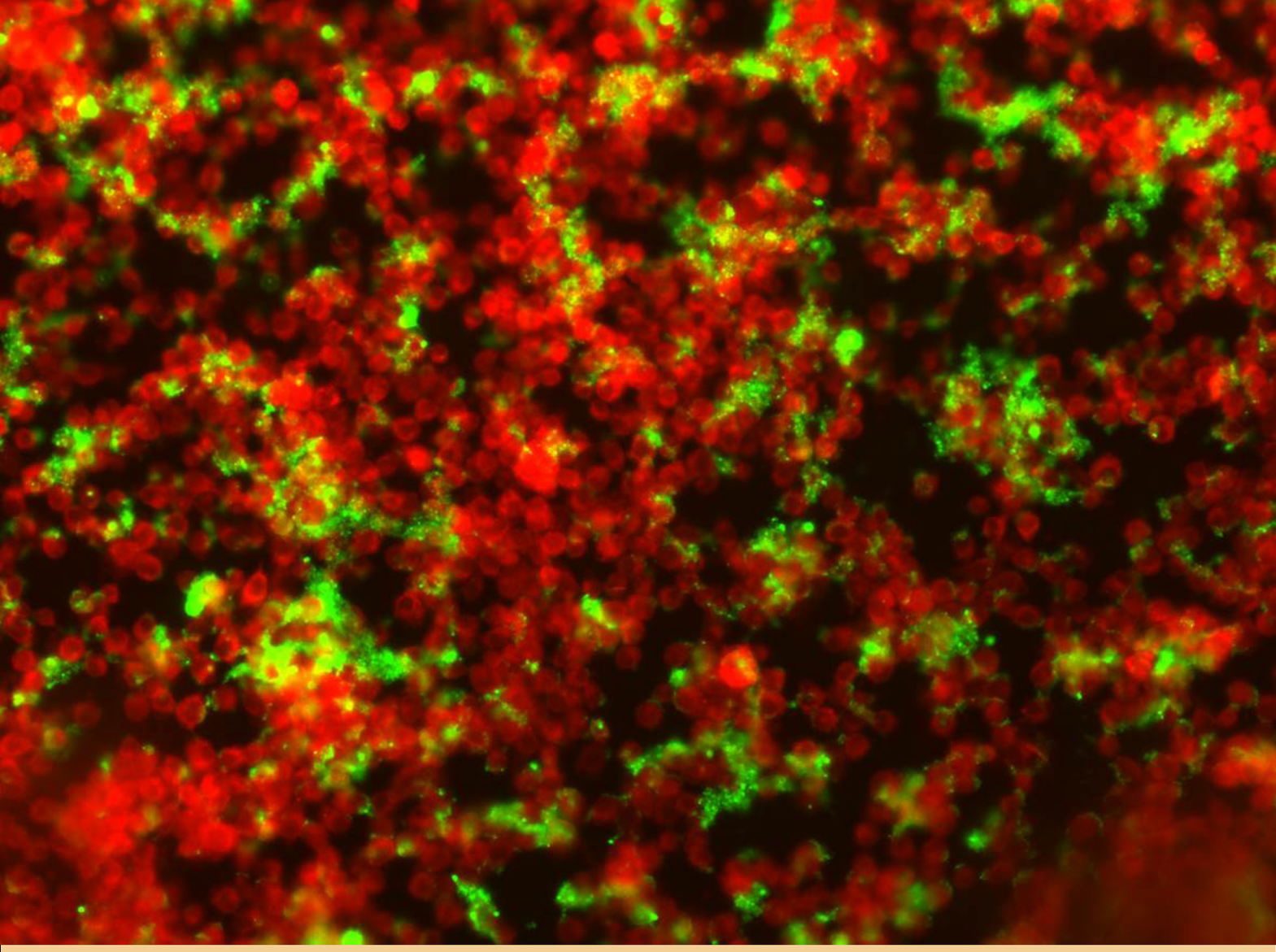

Dulce Marisa Ferreira Bento

Association of compound 48/80 with chitosan based nanoparticles: designing a novel prototypic delivery system for nasal vaccination

Tese de Doutoramento em Ciências Farmacêuticas na área de especialização em Tecnologia Farmacêutica, orientada pela Professora Doutora Olga Borges e apresentada à Faculdade de Farmácia da Universidade de Coimbra

Setembro 2016

· U C ·

Universidade de Coimbra

Association of compound 48/80 with chitosan based nanoparticles: designing a novel prototypic delivery system for nasal vaccination

Dulce Marisa Ferreira Bento

Candidature thesis for doctor degree in Pharmaceutical Sciences, submitted to the Faculty of Pharmacy of the University of Coimbra

Tese de candidatura ao grau de doutor em Ciências Farmacêuticas, apresentada à Faculdade de Farmácia da Universidade de Coimbra

FFUC FACULDADE DE FARMÁCIA
UNIVERSIDADE DE COIMBRA

The experimental work presented in this thesis was developed under the scientific supervision of Professora Doutora Olga Maria Fernandes Borges Ribeiro from Pharmaceutical Technology Laboratory of Faculty of Pharmacy, University of Coimbra and Professora Doutora Teresa Maria Fonseca Oliveira Gonçalves from Medical Microbiology Laboratory of Faculty of Medicine, University of Coimbra. Financial support was given by FEDER funds through the Operational Programme Competitiveness Factors - COMPETE and national funds by FCT - Foundation for Science and Technology under the project PTDC/SAU-FAR/115044/2009, FCT doctoral fellowship SFRH/BD/65141/2009 and strategic project PEst-C/SAU/LA0001/2013-2014.

O trabalho experimental apresentado no âmbito desta tese foi desenvolvido sob a orientação científica da Professora Doutora Olga Maria Fernandes Borges Ribeiro do Laboratório de Tecnologia Farmacêutica da Faculdade de Farmácia da Universidade de Coimbra e da Professora Doutora Teresa Maria Fonseca Oliveira Gonçalves do Laboratório de Microbiologia Médica da Faculdade de Medicina, Universidade de Coimbra. Foi financiado por fundos FEDER através do Programa Operacional Fatores de Competitividade – COMPETE e por Fundos Nacionais através da FCT – Fundação para a Ciência e a Tecnologia no âmbito da bolsa de doutoramento SFRH/BD/65141/2009, do projeto PTDC/SAU-FAR/115044/2009 e do projeto estratégico PEst-C/SAU/LA0001/2013-2014.


FCT
Fundação para a Ciência e a Tecnologia
MINISTÉRIO DA EDUCAÇÃO E CIÊNCIA


QUADRO
DE REFERÊNCIA
ESTRATÉGICO
NACIONAL
PORTUGAL 2007.2013


COMPETE
PROGRAMA OPERACIONAL FACTORES DE COMPETITIVIDADE


UNIÃO EUROPEIA
Fundo Europeu
de Desenvolvimento Regional

"Science knows no country because knowledge belongs to humanity, and is the torch which illuminates the world."

Louis Pasteur

Acknowledgements

Ao longo destes últimos anos foram muitas as pessoas que me apoiaram e que contribuíram para o meu crescimento tanto a nível científico como a nível pessoal. Ao aproximar-me do final desta etapa, sinto um enorme sentimento de satisfação e uma imensa gratidão por todos aqueles que de um modo ou de outro me acompanharam nesta jornada.

Quero expressar o meu agradecimento à Professora Olga Borges, minha orientadora, por fomentar ainda mais em mim o entusiasmo e paixão pela ciência. Recordo-me bem do dia e da satisfação com que recebi o seu convite para me juntar ao seu laboratório. Desde esse dia a Professora Olga tem sido um elemento absolutamente essencial no meu percurso científico. Agradeço a confiança que depositou em mim, o seu incentivo para que eu abraçasse novos desafios, e todo o apoio prestado ao longo destes últimos anos. A sua orientação constante e dedicada foram cruciais para o desenvolvimento do trabalho aqui apresentado.

À Professora Teresa Gonçalves, minha co-orientadora, agradeço pela motivação, sugestões e constante disponibilidade. Agradeço todos os ensinamentos transmitidos, o seu apoio e orientação foram essenciais para completar o trabalho aqui apresentado.

To Professor Gerrit Borchard, I would like to thank for the support and for hosting me in his lab at School of Pharmacy Geneva-Lausanne, Switzerland, for two months.

To Professor Herman Staats, I would like to thank for welcoming me as part of his research laboratory in Duke University, USA, for seven months. I moved to North Carolina just before Christmas and Professor Herman made sure that I felt at home in a place that was totally unknown to me. I'm deeply grateful for all his scientific and personal support. Professor Herman valuable and constructive suggestions were crucial for the planning and execution of the *in vivo* studies presented in this thesis. Working with him and his team in an Immunology lab was a truly enriching experience that broadened my scientific knowledge.

From Duke University, I want also to thank Professor Soman Abraham for the helpful suggestions and for his kindness. I am thankful to Dr. Gregory Sempowski, Scientific Director of Duke Human Vaccine Institute Immune Biocontainment Animal Imaging Shared

Resource, for his support and for providing me access to the facility, and to Kristina Riebe, for the technical support and her valuable help with the *in vivo* imaging studies. I thank Brandi Johnson, Gabrielle Mcrae and Moses Wanyonyi from Herman's lab for all their help and support in the lab. A special acknowledgment to Brandi for her kindness, for her constant good mood and for the enjoyable moments inside and outside the lab.

I also acknowledge Dr. Joseph Butterfield, Mayo Clinic, USA, for his generous gift of the human mast cell line HMC-1.

Agradeço ainda a ajuda prestada no decorrer dos trabalhos realizados pelas técnicas do Centro de Neurociências e Biologia Celular da Universidade de Coimbra, Luísa Cortes, Isabel Nunes e Isabel Dantas.

Um agradecimento muito especial aos elementos do Nanolab, Filipa Lebre, Sandra Jesus e Edna Soares. Filipa, tu sabes bem o quão importante és para mim. Contigo cresci imenso não só a nível científico como pessoal. Enquanto íamos muito dedicadamente aprendendo novas técnicas científicas, viajando juntas para congressos, tomando café na D. Ana, eu fui aprendendo também a conhecer o verdadeiro significado da palavra Amizade. Olhando para trás, não consigo imaginar este trajeto sem ti. Obrigada por me acompanhares nos altos e baixos, pelos desabafos, pelas palavras de incentivo nos momentos certos e por comigo celebrares as minhas conquistas. Fico feliz que os nossos percursos científicos ainda se continuem a cruzar, mas acima de tudo fico feliz e agradeço por fazeres parte da minha vida. Sandra, obrigada pela partilha de ideias ao longo destes anos e pela determinação e perseverança que foste transmitindo. Obrigada também pela amizade e por tão bem perceberes as minhas expressões "à Mortágua"! Não imaginas o quão feliz me fizerem os nossos momentos de extrema eloquência partilhados. Edna, foi um prazer partilhar os meus últimos meses no laboratório contigo, obrigada pelo teu sentido critico e pelas sugestões. Agradeço-te especialmente pela dose extra de loucura e jovialidade com que contagiaste o laboratório. O Nanolab não podia estar em melhores mãos! Quero agradecer-vos pelo apoio científico, pela amizade e por todos os momentos que temos partilhado dentro e fora do laboratório. Vocês as três tornaram este percurso tão mais fácil!

À Ana Fortuna agradeço a amizade, e a energia contagiante no café matinal. Como eu tenho saudades desses cafezinhos! À Carla Vitorino agradeço a boa disposição, a constante disponibilidade para ajudar, as discussões proveitosas e todos os bons momentos partilhados dentro e fora da faculdade. A todos os meus colegas de doutoramento da FFUC: Amélia

Vieira, Ana Serralheiro, Carla Varela, Daniela Gonçalves, Joana Almeida e Sousa, Joana Bicker, João Abrantes, Marisa Gaspar, Raquel Teixeira e Susana Simões o meu agradecimento pelo companheirismo e pelos bons momentos de convívio proporcionados ao longo destes anos.

Agradeço a todos os meus amigos que de um modo ou de outro me acompanharam e apoiaram ao longo destes últimos anos. Um agradecimento especial à Cynthia que mais de perto me acompanhou nesta jornada. Cynthia, obrigada por estares presente nos bons e nos maus momentos, pela amizade, pelas mariscadas e pelos nossos fins-de-tarde no Piolho que tantas vezes salvaram o dia.

Ao Filipe, agradeço o incentivo e acima de tudo a compreensão. O teu apoio incondicional tem sido absolutamente imprescendível nesta fase final. Obrigada pelos sorrisos, pelos mimos, pelo conforto e pelo ânimo para abraçar novas aventuras!

Por último, tendo consciência que nada disto teria sido sem eles, dirigo um especial agradecimento à minha família. Obrigada ao meu irmão, Marco, pela sua amizade, pelas brincadeiras, pelo incentivo e por me fazer sempre acreditar em mim. É um verdadeiro orgulho ter um irmão como tu! Obrigada aos meus avós maternos, Alice e Albertino, que infelizmente partiram durante esta jornada. Obrigada pelo carinho e apoio. Mesmo longe vocês continuam tão perto!... Agradeço aos meus avós paternos, Idalina e Fernando, por serem uns "segundos pais" para mim. Obrigada pelo amor, pelo carinho, pelo incentivo e pela presença constante na minha vida. Aos meus pais, Manuela e Fernando, obrigada pelo amor e apoio incondicionais, pelos conselhos, pela motivação e pela paciência. Obrigada por sempre acreditarem em mim. Agradeço-vos por serem quem são e por terem feito de mim a pessoa que sou. Vocês são os pilares da minha vida e sem vocês não teria sido possível chegar até aqui!

Table of contents

List of abbreviations

APC(s)	Antigen presenting cell(s)
AS	Adjuvant System
ATCC	American Type Culture Collection
ATR	Attenuated total reflection
BALT	Bronchus-associated lymphoid tissue
BCA	Bicinchoninic acid assay
BSA	Bovine serum albumin
C48/80	Compound 48/80
CCL	CC-chemokine ligand
CCR	C-C chemokine receptor type
CD	Cluster of differentiation
c-di-AMP	Cyclic diadenosine monophosphate
c-di-GMP	Cyclic diguanylate monophosphate
Chi NP	Chitosan nanoparticles
Chi/Alg NP	Chitosan/Alginate nanoparticles
Chi/Alg-C48/80 NP	Compound 48/80 loaded Chitosan/Alginate nanoparticles
Chi-C48/80 NP	Compound 48/80 loaded Chitosan nanoparticles
CI	Confidence interval
CMC	Carboxymethyl chitosan
CMIS	Common mucosal immune system
CpG ODN	Cytosine-phosphate-guanine oligodeoxynucleotides
CRM-MenC	Group C meningococcal conjugated vaccine
cryo-SEM	Cryo-scanning electron microscopy
CT	Cholera toxin
CTA1-DD	Cholera toxin subunit A1 fused to a B cell targeting moiety
CTB	Cholera toxin subunit B
CVB3	Coxsackievirus B3
CTL	Cytotoxic T cells
DC(s)	Dendritic cell(s)

DL	Detection limit
DLS	Dynamic light scattering
DMEM	Dulbecco's Modified Eagle's Medium
DMSO	Dimethyl sulfoxide
DLN	Draining lymph nodes
ECACC	European Collection of Authenticated Cell Cultures
ELISA	Enzyme-linked immunosorbent assay
EMA	European Medicines Agency
Ex/Em	Excitation/Emission
FcERI	High affinity Immunoglobulin E receptor
FDA	United States Food and Drug Administration
FITC	Fluorescein isothiocyanate
FITC-BSA	Bovine serum albumin-fluorescein isothiocyanate conjugate
FTIR	Fourier transform infrared spectroscopy
GALT	Gut-associated lymphoid tissue
GM-CSF	Granulocyte–macrophage colony-stimulating factor
GMT	Geometric mean titer
H1N1	Hemagglutinin type 1 and neuraminidase type 1
H5N1	Hemagglutinin type 5 and neuraminidase type 1
HA	Influenza hemagglutinin
HBsAg	Hepatitis B surface antigen
HEPES	4-(2-hydroxyethyl)-1-piperazineethanesulfonic acid
HI	Hemagglutination inhibition
HIV	Human immunodeficiency virus
HMC-1	Human mast cell line-1
HMGB1	High-mobility group box 1
HPV	Human papillomavirus vaccine
IACUC	Institutional Animal Care and Use Committee
ICH	International Conference on Harmonisation
IFN-γ	Interferon-γ
Ig	Immunoglobulin
IL	Interleukin
IP	Isoelectric point
ISCOMs	Immune stimulating complexes

LC	Loading capacity
LE	Loading efficacy
LeTx	Anthrax lethal toxin
LF	Anthrax lethal factor
LMW	Low molecular weight
LPS	Lipopolysaccharide
LT	*Escherichia coli* heat-labile enterotoxin
LTK63	Non-toxic mutant of *Escherichia coli* heat labile enterotoxin
LTN	Lymphotactin
MALT	Mucosal-associated lymphoid tissue
MCDP	Mast cell degranulating peptide
MC(s)	Mast cell(s)
MDP	Muramyl di-peptide
MGC	Methylglycol chitosan
MHC	Major histocompatibility complex
MPL	Monophosphoryl lipid A
MTT	3-[4, 5-dimethylthiazol-2-yl]-2,5-diphenyl tetrazolium bromide
NALT	Nasal-associated lymphoid tissue
NK	Natural killer
NP	Nanoparticle
NT50	Fifty percent neutralization titers
OD	Optical density
OVA	Ovalbumin
PA	Anthrax protective antigen
PAMP	Pathogen-associated molecular patterns
PBDC(s)	Peripheral blood derived dendritic cell(s)
PBMC(s)	Peripheral blood mononuclear cell(s)
PBS	Phosphate buffer saline
PCL	Poly-epsilon-caprolactone
PGA	Polyglycolic acid
PI	Polydispersity index
PLA	Polylactid acid
PLGA	Poly(lactic-co-glycolic) acid
provax-IL-15	IL-15 expressing plasmid

PRR	Pattern recognition receptors
PS	Polystyrene
QL	Quantification limit
QS	Quillaja saponin
ROI	Region-of-interest
RPMI	Roswell Park Memorial Institute medium
RSD	Relative standard deviation
RT	Room temperature
rUre	Recombinant Helicobacter pylori urease
S	Slope
SD	Standard deviation
SEM	Scanning electron microscopy
TCR	T cell receptor
Tfh	Follicular helper T cell
Th	T-helper cells
TLR	Toll-like receptors
TMC	N-trimethyl chitosan
TNF-α	Tumor necrosis factor-α
TPP	Tripolyphosphate
Treg	T-regulatory cells
UV	Ultraviolet
UV-Vis	Ultraviolet-visible
VCAM1	Vascular cell adhesion molecule 1
VLP	Virus-like particles
pVP1	Plasmid encoding the major capsid protein of CVB3
WGA	Wheat Germ Agglutinin
ZP	Zeta Potential
α-galcer	α-galactosylceramide
β-hex	β-hexosaminidase

Abstract

Vaccination is considered one of the greatest medical achievements of modern civilization and large scale immunization programs greatly reduced the global burden of infectious diseases. Therefore, improvement of current vaccines and development of vaccines against diseases for which successful vaccines are not currently available would bring huge benefits for public health and for the society. The development of mucosal vaccines would be highly desirable since it would provide protection at the local of entry of pathogens. However, the development of mucosal vaccination strategies has been delayed for the lack of effective and safe mucosal adjuvants. The objective of this project was to develop a novel prototypic delivery system for nasal vaccination composed by two highly promising mucosal adjuvant candidates: chitosan nanoparticles and the mast cell activator compound 48/80 (C48/80). This is the first time that the combination of C48/80 with nanoparticles in order to develop an improved adjuvant formulation is described.

Two different C48/80 loaded chitosan-based delivery systems were developed: Chitosan-C48/80 NP (Chi-C48/80 NP) and Chitosan/Alginate-C48/80 NP (Chi/Alg-C48/80 NP). The two C48/80 loaded delivery systems were characterized and evaluated *in vitro*. Subsequently, *in vivo* studies assessed their potential as nasal adjuvants.

To support the development of C48/80 loaded nanoparticles, a UV-Vis spectrophotometric method for quantification of C48/80 was developed. This method was validated according to the recommendations of ICH Guidelines for specificity, linearity, range, accuracy, precision and detection and quantification limits.

Chi-C48/80 NP and Chi/Alg-C48/80 NP had a mean size of 501 nm and 564 nm, respectively, and were both positively charged. Loading efficacy of C48/80 was 19 % for Chi-C48/80 NP and 30 % for Chi/Alg-C48/80 NP. Cytotoxicity studies performed in two different cell types showed that incorporation of C48/80 in both formulations resulted in a decreased toxicity of the immunopotentiator compared with C48/80 in solution. *In vitro* uptake studies showed that Chi-C48/80 NP were more efficiently internalized by antigen presenting cells than Chi/Alg-C48/80 NP. The ability of the developed nanoparticles to activate mast cells was tested in vitro using the β-hexosaminidase release assay. Results demonstrated that association of C48/80 with Chi NP but not with Chi/Alg NP enhanced mast cell activation when compared with C48/80 in solution.

To see if the mucoadhesive chitosan-based nanoparticles could increase the residence time of an antigen, an *in vivo* nasal clearance study of fluorescently labelled ovalbumin loaded on nanoparticles was performed. Once again, Chi-C48/80 NP outperformed Chi/Alg-C48/80 NP significantly increasing ovalbumin residence time in the nasal cavity.

Both delivery systems, Chi-C48/80 NP and Chi/Alg NP were then compared for their ability to induce antigen-specific serum IgG, mucosal IgA and serum lethal toxin-neutralizing antibody responses in C57BL/6 mice using nasal immunization with anthrax recombinant protective antigen (PA) as a model system. Nasal immunization with Chi-C48/80 NP as adjuvant elicited high levels of serum anti-PA neutralizing antibodies and higher antigen-specific IgG2c than Chi/Alg-C48/80 NP. The incorporation of C48/80 within Chi NP also promoted a mucosal immunity greater than all the other adjuvanted groups tested. These vaccination studies showed that Chi-C48/80 NP displayed a better performance as nasal adjuvant than Chi/Alg-C48/80 NP. Additionally, an antigen dose-response study showed that Chi-C48/80 NPs allowed a 6-fold decrease of the antigen dose without affecting the levels of specific IgG titers and its neutralizing ability. These results suggest the potential of this novel adjuvant combination to decrease the antigen dose required for vaccination.

Overall, the findings of this project show that the combination of a mast cell activator with chitosan nanoparticles is a promising strategy for nasal immunization inducing potent systemic and mucosal immune responses.

Keywords: nanoparticles, vaccines, C48/80, mast cell activators, chitosan, mucosal vaccination, mucosal vaccination, nasal administration, protective antigen, anthrax vaccine, antigen dose, adjuvant combination.

Resumo

A vacinação é considerada como uma das medidas de saúde publica de controlo de doenças infetocontagiosas mais eficazes na civilização moderna. Os programas de imunização em larga escala diminuíram significativamente a morbilidade e mortalidade atribuídas às doenças infeciosas. A melhoria das vacinas atuais, e o desenvolvimento de vacinas para doenças contra as quais ainda não existem vacinas eficazes, são linhas de investigação de grande importância e com grande impacto na saúde pública e na sociedade. Particularmente, o desenvolvimento de vacinas para administração pelas mucosas será altamente desejável dado que, para além de permitir uma mais fácil administração, permitirá conferir proteção imunológica específica no local de entrada dos patogéneos. A colocação no mercado deste tipo de vacinas tem sido adiada devido à falta de adjuvantes seguros e eficazes para estas vias de administração. O objetivo deste projeto foi desenvolver um novo sistema de entrega de antigénios, com função adjuvante, para vacinação nasal. Este sistema de entrega é composto por dois adjuvantes para as mucosas, os quais, individualmente, em ensaios pré-clínicos, já mostraram ser muito promissores: nanopartículas de quitosano e um ativador de mastócitos, o composto 48/80 (C48/80). Esta é a primeira vez que é descrita a combinação do C48/80 com nanopartículas com o objetivo de desenvolver uma melhor formulação adjuvante para vacinas.

Foram desenvolvidos dois sistemas de entrega, tendo por base o quitosano para a formação de nanopartículas, e nas quais se encapsulou o C48/80: Quitosano-C48/80 NP (Chi-C48/80 NP) e Quitosano/Alginato-C48/80 NP (Chi/Alg-C48/80 NP). As duas formulações foram caracterizadas e avaliadas *in vitro*. *À posteriori*, estudos *in vivo* avaliaram o seu potencial como adjuvantes para vacinas nasais.

Para auxiliar no desenvolvimento das nanopartículas carregadas com C48/80, foi desenvolvido um método colorimétrico com deteção por espetrofotometria UV-Vis para a quantificação do C48/80. Este método foi validado de acordo com as recomendações das normas ICH para os seguintes parâmetros: especificidade, gama de trabalho e linearidade, exatidão, precisão e limites de deteção e de quantificação.

As nanopartículas desenvolvidas no decurso deste projeto, Chi-C48/80 NP e Chi/Alg-C48/80 NP apresentaram um tamanho médio de 501 nm e 564 nm, respetivamente, e ambas apresentaram um potencial zeta positivo. A eficácia de carregamento do C48/80 foi 19 % para as Chi-C48/80 NP e 30 % para as Chi/Alg-C48/80 NP. Estudos de citotoxicidade

demonstraram que a incorporação do C48/80 nos sistemas de entrega diminui a toxicidade do imunopotenciador. Estudos *in vitro* de internalização revelaram que as Chi-C48/80 NP foram internalizadas por células apresentadoras de antigénio mais eficientemente que as Chi/Alg-C48/80 NP. A capacidade das nanopartículas desenvolvidas para ativarem mastócitos foi também testada *in vitro* usando o ensaio de libertação de β-hexosaminidase. Os resultados demonstraram que a associação do C48/80 com as Chi NP, mas não com as Chi/Alg NP, resultou numa maior ativação de mastócitos quando comparado com o C48/80 em solução.

Para avaliar se as particulas mucoadesivas, à base de quitosano, conseguiam aumentar o tempo de residência do antigénio na cavidade nasal, foi realizado um estudo *in vivo* de clearance nasal. Com esse objetivo foi usada ovalbumina marcada com fluorescência, adsorvida às nanopartículas. Neste estudo as Chi-C48/80 NP superaram novamente as Chi/Alg-C48/80 NP aumentando significativamente o tempo de residência do antigénio na cavidade nasal.

A aptidão das nanopartículas desenvolvidas para potenciarem uma resposta imune, foi avaliada em murganhos C57BL/6 usando a imunização nasal com o antigénio protetor (PA) do *B. anthracis* como sistema modelo. A imunização usando as Chi-C48/80 NP como adjuvante induziu títulos elevados de anticorpos neutralizantes anti-PA no soro e títulos de anticorpos IgG2c anti-PA mais elevados do que as Chi/Alg-C48/80 NP. A incorporação do C48/80 nas Chi NP também promoveu uma imunidade nas mucosas melhor que a induzida por todos os outros grupos testados. Estes estudos de vacinação demonstraram que as Chi-C48/80 NP exibiram um desempenho melhor como adjuvante para a mucosa nasal que as Chi/Alg-C48/80 NP. Além disso, um estudo de dose-resposta revelou que as Chi-C48/80 NP permitiram diminuir seis vezes a dose de antigénio usada, sem afetar os títulos de anticorpos IgG específicos e neutralizantes. Estes resultados sugerem que esta inovadora combinação de adjuvantes, Chi NP com C48/80, tem potencial para diminuir a dose de antigénio necessário a incluir numa formulação comercial da vacina.

De um modo geral, os resultados obtidos com este projeto demonstram que a combinação de nanopartículas de quitosano com um ativador de mastócitos é uma estratégia promissora para a imunização nasal, induzindo uma resposta imune potente, tanto sistemicamente como nas mucosas.

Keywords: nanoparticulas, vacinas, C48/80, ativadores de mastócitos, quitosano, vacinas de mucosas, administração nasal, antigénio protetor, vacina para o anthrax, dose de antigénio, combinação de adjuvantes.

CHAPTER 1

General Introduction

1.1 Vaccines: brief historical overview

In the 18th century, variolation, a technique used in China, spread into Western Europe. The technique, by which healthy people could acquire immunity to smallpox by inserting powdered smallpox pustules into small cuts in the skin [1] was considered, in that time, the most efficient technique to control epidemics of smallpox. In same century the English doctor Edward Jenner, familiarized with variolation, observed that dairymaids who suffered from cowpox were naturally resistant to smallpox [2]. Based on this, he hypothesized that cowpox not only protected against smallpox but could also be transmitted from one person to another as a deliberate mechanism of protection [2]. To prove his theory, he performed a scientific experiment that would lead to the eradication of smallpox and revolutionize the course of infectious diseases. In 1796, Jenner inoculated a child with material from a cowpox pustule from a dairymaid and discovered that inoculation with the cowpox virus provided protection against smallpox infection [1, 3]. He named the cowpox material vaccine, from the Latin *vacca,* meaning cow, introducing the word vaccine for the first time. Although early reports show that Jenner was not the inventor of vaccination, since he was not the first to suggest that infection with cowpox conferred specific immunity to smallpox or even the first to attempt cowpox inoculation for this purpose [3], he was the one responsible for the popularization of the practice. His work represents the first scientific attempt to control an infectious disease by the deliberate use of vaccination. In fact, the terms vaccine and vaccination were originally used to refer exclusively Jenner's method to prevent smallpox, but almost 100 years later, in 1880s, Louis Pasteur broadened the terms to designate preventive inoculation with other agents [1].

Nowadays, vaccination is considered one of the greatest medical achievements of modern civilization. Large scale immunization programs lead to the eradication of smallpox, the near elimination of polio and control of many other major human diseases, such as measles, mumps, rubella and diphtheria, greatly reducing the global burden of infectious diseases (Fig. 1.1). Vaccination is regarded as one of most cost-effective health interventions and, according to World Health Organization (WHO), prevents an estimated 2.5 million child deaths each year [4]. Nevertheless, there are still challenges to be overcome regarding vaccines. While successful vaccines do exist, there are several infectious diseases that cause considerable morbidity and mortality for which no effective vaccine is available (e.g., malaria, human immunodeficiency virus (HIV)) or for which existing vaccines provide insufficient immunity (e.g., tuberculosis, whooping cough). Many vaccine-preventable diseases have been controlled in the developed world but are still a major public health problem in developing countries [5,

6]. Factors like poor health services, the requirement for cold chain storage and high cost of vaccination represent some of the challenges faced by these countries [6]. Additionally, in the last few years the development of bacterial resistance to antibiotics, as well as the emergence of new human infectious diseases, has reinforced the need for sustained development and improvement of vaccination strategies. Optimal worldwide control of infectious diseases through vaccination could be facilitated by the development of vaccines that do not require a cold chain and do not require delivery through needles [6].

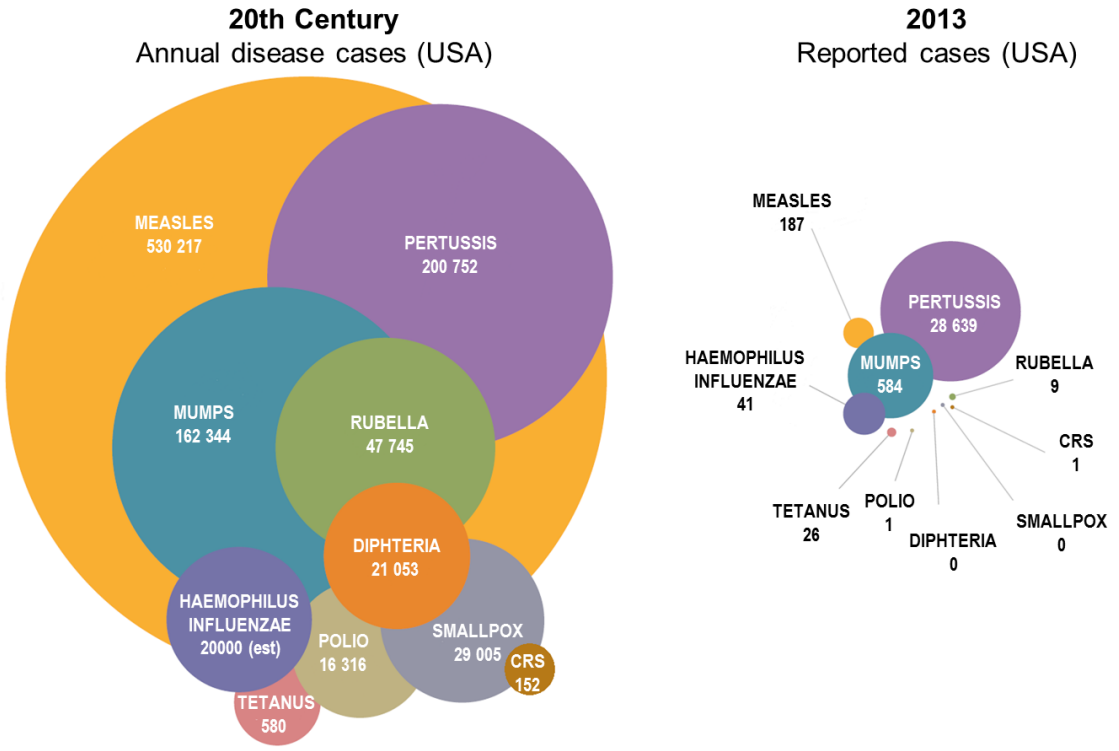

Figure 1.1 - Impact of vaccines in the 20th and 21st centuries. Annual number of reported cases of diseases in the USA during the 1990s versus 2013 [7]. Adapted from infographic - *Vaccines Work* by Sanofi Pasteur, 2015.

1.2 Key cellular actors in the immune system

The immune system is typically divided in two arms: the innate and the adaptive immune systems. The innate immune cells are composed by granulocytes, monocytes, eosinophils, macrophages, dendritic cells, mast cells and natural killer (NK) cells and functions as a quick first line of defense against microorganisms. Additional components, like epithelial cell barriers, complement system, antimicrobial peptides and other soluble factor are also part of the innate immune system. Innate immune cells express receptors that recognize molecular patterns present on microorganisms or released upon tissue damage. Among these receptors,

the most studied are Toll-like receptors (TLR). Stimulation of TLRs leads to activation of transcription factors, inducing the expression of cytokines that modulate the adaptive immune response. The function of innate immune cells are not limited to controlling infections before the onset of adaptive immune responses and initiating of adaptive immune responses, they also contribute to the removal of pathogens that have been targeted by an adaptive immune response [8].

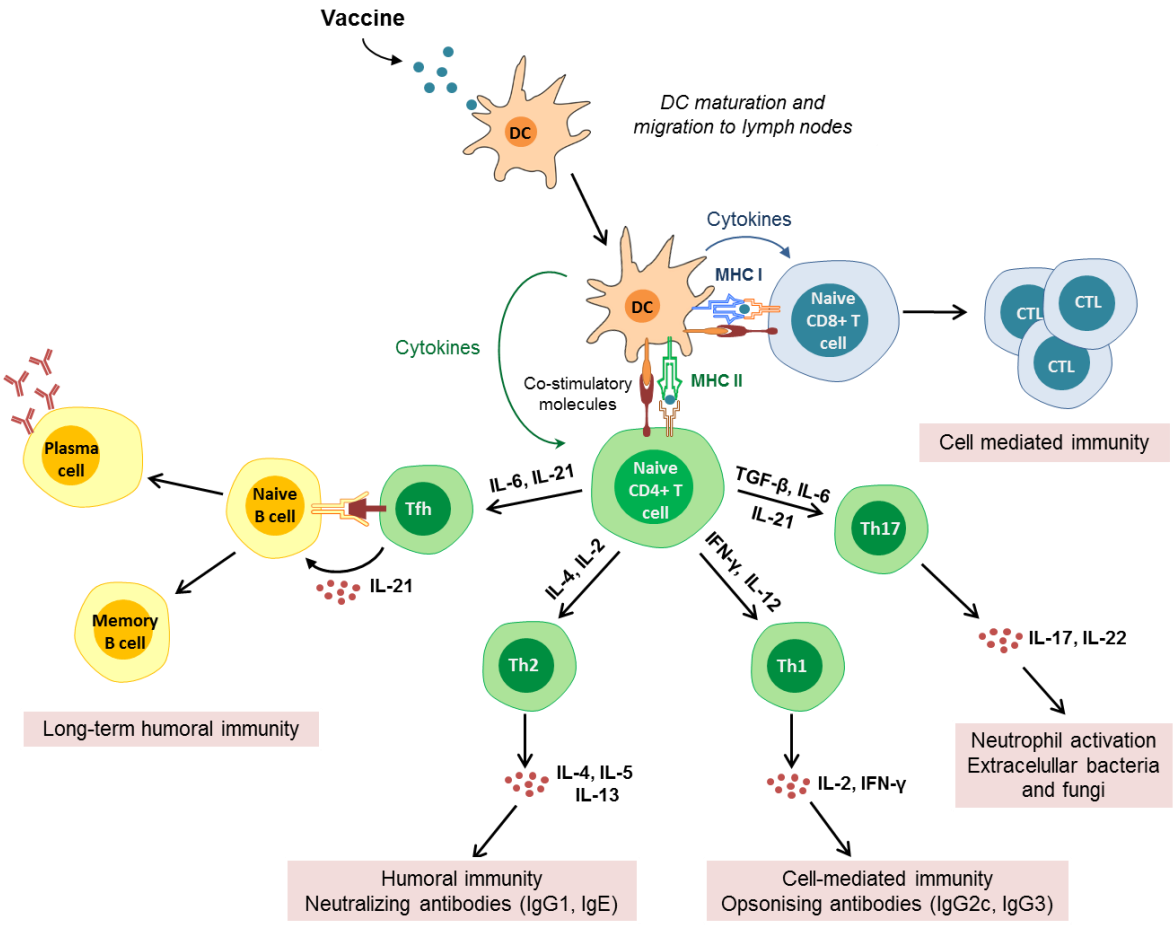

Figure 1.2 – Induction of adaptive immune responses to vaccines. Following vaccine administration, antigen is recognized and processed by dendritic cells (DCs), or by other antigen presenting cells, that then migrate to lymph nodes (LN). In the LN, activated DCs can present the antigen to two distinct populations of T cells: CD4+ and CD8+ T cells via MHC class II and I, respectively. Simultaneously, DCs express co-stimulatory molecules and secrete cytokines that stimulate T cell activation and differentiation. Depending on the cytokine milieu, CD4+ T cells may differentiate into different T helper (Th) cell subtypes, such as Th1, Th2, Th17, Treg or Tfh cells. In turn, these subsets release distinct sets of cytokines that mediate different functions (adapted from [9]).

The adaptive immune response is slower to develop but is highly specific and establishes an immunological memory which ensures a more rapid and effective response on a subsequent encounter with the same pathogen. The adaptive immune system is composed by the antibody

secreting B cells and by T cells, including CD8+ and CD4+ T cells. CD8+ T cells, also called cytotoxic T cells (CTL), recognize and destroy cells infected by intracellular pathogens or tumoral cells. On the other hand, CD4+ T cells are also known as T-helper cells (Th) because they secrete cytokines that provide help to other cells of the immune system. Naïve Th cells upon activation differentiate into different subsets depending on the surrounding cytokine milieu (Fig. 1.2). These different T cells subsets include T-helper 1 cells (Th1), T-helper 2 cells (Th2), T-helper 17 cells (Th17), follicular helper T cell (Tfh) and T-regulatory cells (Treg), and each one of this subtypes has distinct functions mediated by the cytokines they secrete. For example, Th1 cells secrete interferon-γ (IFN-γ) and tumor necrosis factor-α (*TNF*-α) that activate CD8+ T cells and instruct macrophages to clear infections. IFN-γ also stimulates B cells to secrete specific subclasses of IgG antibodies, mainly IgG2a or IgG2c. On the other hand, Th2 cells secrete cytokines like IL-4, IL-5 and IL-13 which mediate the induction of strong humoral immune responses, including IgG1 and IgE [10] . Th17 cells play a role in host defense against pathogens at mucosal sites and produce cytokines such as IL-17, IL-21 and IL-22.

For a long time the ability to induce a memory immune response was considered one of the hallmarks of the adaptive immune system, while it was assumed that innate immune responses lacked immunological memory. However, this paradigm has been changed due to the recent recognition that some innate cells can show memory-like behavior, which suggests that innate immunity can also display adaptive characteristics [11]. These findings are transforming our understanding of the immune system and may challenge the classic definition of innate and adaptive immunity.

1.2.1 Bridging innate and adaptive immunity

As professional antigen presenting cells (APCs), dendritic cells (DCs) are the main link between innate and adaptive immune system (Fig.1.2). After capture and processing of antigen, DCs migrate to the draining lymph nodes (DLN) where they present the antigen to T cell. T cells became then activated to exert their effector actions. Simultaneous, DCs express co-stimulatory molecules (e.g. CD80, CD86, major histocompatibility complex class II (MHC II) and CD40) and release cytokines that amplify T cell receptor (TCR) signaling and promote T cell activation and polarization. The ability of the adaptive immune system to elicit antigen-specific CD4+ and CD8+ T cells is based on the presentation of antigen in MHC molecules (the peptide–MHC complex) and its recognition by the T cell receptor. Typically, an exogenous antigen is internalized by APCs, processed and presented on class MHC II

molecules to CD4+ T cells. On the other hand, endogenous antigens are presented on class MHC I molecules to CD8+ T cells. However, in certain circumstances an exogenous antigen can be presented on MHC class I molecules, by a process called cross-presentation. This mechanism is thought to be vital to the initiation of CD8+ T cell responses to extracellular antigens [12], allowing immunity against most tumors and against viruses that do not readily infect antigen-presenting cells.

While dendritic cells are the main bridge between innate and adaptive immunity, other cells also play an important role at modulating both arms of the immune system. Mast cells (MCs) are a clear example of that. Although MCs are best known for their role in allergic diseases, their functions in defense against pathogens have been increasingly recognized [13-15]. Mast cells are strategically located at the host-environment interface, such as skin and mucosal membranes, and are an early source of inflammatory mediators, therefore they are often recognized as sentinels of the immune system [14, 16]. The activation of MCs by pathogens or other stimuli results in the release of exosomes loaded with pro-inflammatory mediators, which promotes the recruitment of innate immune cells to the local [14]. Mast cells can also secrete products that have direct antimicrobial activity and stimulate mechanisms that hinder pathogen colonization and promote their expulsion, such as enhanced mucus production [14, 15]. Mast cells not only are critical effectors in immune response but also play an important role in the development of an adaptive immune response. Mast cell derived mediators, namely TNF-α, can promote functional maturation of DCs and induce migration of DCs and T cells to DLN [15, 17]. Additionally, MCs can also activate T cells, enhancing T cell proliferation and cytokine secretion [18]. This ability of MCs to change the inflammatory environment and to mobilize immune cells to the site of infection after pathogen recognition, together with the enhancement of DC trafficking to DLN, establishes a role for MCs in bridging innate and adaptive immunity.

1.3 Mucosal immune response

Mucosal surfaces are the major interface between the body and the external environment, constituting the first line of defense against external factors. In addition to the mechanical and chemical cleansing mechanisms, highly specialized innate and adaptive mucosal immune systems protect the body against potential destructive agents and dangerous substances from the environment. Simultaneously, the mucosal immune system has the function of preventing the development of potentially harmful immune responses to innocuous foreign antigens derived from food, airborne matter and commensal microorganisms [19].

Mucosal immune system can be broadly divided into inductive and effector sites. The inductive sites are composed by organized mucosal-associated lymphoid tissue (MALT), located along all the mucosal surfaces, as well as mucosa-draining lymph nodes. MALT includes gut-associated lymphoid tissue (GALT), bronchus-associated lymphoid tissue (BALT) and nasal-associated lymphoid tissue (NALT), and is populated by lymphocytes (T and B cells) and by accessory cells, such as dendritic cells and macrophages, allowing the initiation of specific immune responses. Mucosal effector sites, such as lamina propria and epithelial surfaces, contain antigen-specific mucosal effector cells such as secretory immunoglobulin A (IgA) - producing plasma cells, and memory B and T cells [20]. Immune cells migrate from inductive to effector tissues constituting the common mucosal immune system (CMIS) [21]. Briefly, B and T cells encounter antigens at the inductive sites, leave through the lymph into the bloodstream and then relocate in the selected mucosal sites where they differentiate into memory or effector cells [19]. The anatomical affinity of the sensitized mucosal lymphocytes is dependent on the expression of homing receptors or integrins on the cell surface, tissue-specific receptors or addressins on endothelial cells and chemokines that promote cell migration [20] indicating a compartmentalization of the CMIS. For example, nasal immunization induces the expression of CCR10 and α4β1-integrin by IgA -secreting B cells, allowing them to migrate to the respiratory and genito-urinary tracts, which express the corresponding ligands, CCL28 and VCAM1[22]. Therefore, mucosal vaccination at one mucosal site can induce immune responses in distant multiple effector sites and the mucosal route of immunization should be selected according to the desired location for the mucosal immune response.

Secretory IgA is the main player of the adaptive immune response in mucosal surfaces and is locally produced by B cells in the effector sites. Unlike other antibody isotypes, secretory IgA antibodies have the capacity to form dimers and are resistant to degradation in the protease-rich external environments of mucosal surfaces. Antigen-specific IgA has multiple functions in the mucosal defense against pathogens [23, 24]. It prevents direct contact of the microorganism and antigens with the mucosal surface by entrapping them in the mucus followed by peristaltic or ciliary clearance, a mechanism known as immune exclusion. Additionally, IgA might block or sterically hinder the microbial surface molecules that mediate epithelial attachment or even neutralize incoming pathogens within epithelial-cell vesicular compartments during polymeric immunoglobulin receptor-mediated transport across the epithelial cells. Antigen excretion is other mechanism by which IgA can confer protection. Briefly, mucosal laminal propria contains IgA that binds to antigens that have breached the

epithelial barrier and mediates its transport back to the luminal surface of the mucosal epithelial cells.

1.4 Mucosal vaccination

Mucosal surfaces, with a total surface area of about 400 m^2 [25], are the local of entry for many human pathogens. Actually, many pathogens that initiate infection at a mucosal surface (e.g.: HIV, influenza virus, *Mycobacterium tuberculosis*, *Salmonella typhi*, rotavirus, *Vibrio cholera*, and enterotoxigenic *Escherichia coli*) are a major cause of disease and mortality worldwide [26]. Therefore, there is an increasing drive to administer vaccines through mucosal routes since it would allow the induction of protective mucosal immune responses, while parenteral vaccines are usually poor inducers of mucosal immunity and consequently less effective against mucosal infections [23, 27]. In addition to provide protection at the local of entry of pathogens (mucosal antibodies, such as secretory IgA, and T cell responses), mucosal vaccines are also efficient at inducing systemic immunity, including humoral and cell-mediated responses. But the protective immune response induced by a vaccine is not the only factor determining its success, and mucosal vaccines have several other advantages over parenteral vaccination. Mucosal vaccination does not involve needles, which abolish the requirement of specialized personnel for its administration, makes them attractive for mass vaccination, increase patient compliance and decrease the risk of spread of infectious diseases due to contaminated syringes [28, 29]. Additionally, the potential to develop a heat stable mucosal vaccine would also reduce the logistical burden and be a major benefit for the distribution of vaccines in developing countries were a cold chain infrastructure is usually unavailable.

Despite their clear advantages, only a limited number of mucosal vaccines have been licensed for human use (table 1.1). Most of these approved mucosal vaccines are based on live attenuated pathogens and despite their efficacy there are concerns over their safety, especially in immunocompromised individuals, since there is a risk of residual virulence associated with these vaccines [30]. Furthermore, their requirement for cold-chain storage is an additional limitation to their widespread use. Considering this, the development of new mucosal vaccines has been primarily focused on safer subunit vaccines composed of purified antigenic components of the pathogen, rather than whole cells. However, subunit antigens on its own are poorly immunogenic and when administered in the mucosa may result in mucosal tolerance rather than protective immunity. Tolerance is the natural immune response induced to a soluble antigen at mucosal surfaces that prevents harmful inflammatory responses to innocuous proteins, such as food antigens and antigens from commensal bacterial [28]. Thus,

the use of a potent mucosal adjuvant is essential for the successful design of mucosal vaccines, especially non-living vaccines. In fact, the lack of safe and effective mucosal adjuvants is considered a major obstacle to the development of new effective mucosal vaccines [20, 31].

Table 1.1 – Licensed human vaccines for mucosal administration (adapted from [28]).

Infection	Trade name (manufacturer)	Route	Vaccine type
Influenza	FluMist (MedImmune)	Nasal	Live attenuated influenza virus vaccine
Influenza	Fluenz Tetra (AstraZeneca UK)	Nasal	Live attenuated influenza virus vaccine
Influenza	Nasovac-S (Serum Institute of India)	Nasal	Monovalent live attenuated vaccine
Polio	many	Oral	Live attenuated pentavalent vaccine
Rotavirus	Rotarix (GSK)	Oral	Monovalent live attenuated human rotavirus
Rotavirus	RotaTeq (Merck)	Oral	Live attenuated multivalent reassortant vaccine
Cholera	Dukoral (Crucell)	Oral	Recombinant cholera toxin subunit B + inactivated *V. cholerae*
Cholera	Orochol (Crucell)	Oral	Live attenuated vaccine lacking cholera toxin subunit A
Cholera	Shanchol (Shantha Biotechnics)	Oral	Inactivated cholera vaccine
Typhoid	Vivotif (Crucell)	Oral	Live attenuated S. *Typhi*

1.4.1 Rational for nasal vaccination

Mucosal vaccination comprises different routes, including oral, nasal, vaginal, ocular, rectal and sublingual routes. Most of the research has been focused on oral and nasal administration and, indeed, only the nasal and oral routes have so far been used for licensed human vaccines.

Oral vaccination route is probably the most attractive in terms of patient acceptance but this route is the most challenging for mucosal vaccine development. The acidic gut environment degrades soluble antigens, there is the potential risk of induction of mucosal tolerance and high doses of antigen are required. Besides, oral vaccines, such as vaccines against rotavirus and V. *cholera*, are less effective in developing countries, a phenomenon known as tropical barrier [26]. While the mechanisms for tropical barrier are not completely known, chronic environmental enteropathy, persistent parasitic infections and differences in nutritional status and gut microflora are factors involved with this decreased efficacy [26, 28].

While both nasal and oral routes have the advantages of being a needle-free route, nasal vaccination offers some advantages over oral route. Due to the highly vascularized nasal mucosa, which lacks significant amounts of enzymes, much lower doses of antigen and adjuvants are required compared with oral vaccination [19, 20]. Furthermore, studies have showed that nasal vaccination can induce specific mucosal IgA responses in salivary glands, respiratory tract, small intestine and genital tract [23]. Its ability to induce immune responses

in the genital tract makes nasal vaccination a promising route for the development of vaccines against HIV and other sexually transmitted diseases [32, 33].

Recently, three nasal vaccines against influenza (FluMix, Fluenz Tetra and Nasovac-S) were approved for human use [34], which demonstrates the potential of nasal immunization as a safe and effective vaccination route. These vaccines induce an immune response that more closely resembles the natural immunity than the response elicited by the intramuscular vaccine [19]. The ability to induce both systemic and mucosal immunity is widely recognized as an advantage of mucosal immunization. However, even if a mucosal immune response is not required for protection against the pathogen of interest, the nasal route can still be considered as needle-free method of immunization alternative to parenteral routes [35]. Despite its advantages, the design of subunit nasal vaccines is being delayed by the lack of safe and effective adjuvants able to maximize the induction of antigen-specific immune responses.

1.5 Vaccine adjuvants

Adjuvants are substances capable of enhancing and/or modulating antigen-specific immune responses elicited by a vaccine [36]. They were first described by Ramon in 1920s who notice that the addition of certain substances to vaccines increased their efficacy [37]. Since then, adjuvants have been used to improve vaccine induced immune responses. Traditional live attenuated or inactivated whole-cell vaccines usually do not require the addition of adjuvants since they contain some natural components with adjuvant properties, such as nucleic acids, lipids and cell membrane components [38]. Modern vaccine development has been focused on the design of subunit vaccines composed of highly purified recombinant proteins or peptides. Although these vaccines have a better safety profile than traditional vaccines, they are less immunogenic, requiring the addition of adjuvants to induce a protective long-lasting immune response. The use of adjuvants in vaccines have several benefits that were reviewed by Reed et al.[36] and are summarized on table 1.2.

Adjuvants can be broadly divided in two main groups according to their mode of action [38, 39]: i) immunopotentiators that interact directly with the immune system to improve responses to antigens (e.g. TLR ligands, cytokines, saponins, bacterial toxins, cyclic dinucleotides and mast cell activators); and ii) delivery systems or particulate adjuvants that act by improving the delivery and presentation of antigens to the immune systems, particularly to antigen presenting cells (e.g. mineral salts, emulsions, liposomes, virus-like particles (VLP), immune stimulating complexes (ISCOMs) and biodegradable particles). However, this classification is not strict since some particulate adjuvants also have intrinsic immunostimulant properties [40].

Table 1.2 – Potential benefits of adjuvants in vaccines.

Roles of vaccine adjuvants
• Decrease the dose of antigen in the vaccine, which can potentially increase global vaccine supply
• Reduce the number of vaccine doses necessary
• Generate a faster immune response, which may be crucial in case of pandemic outbreaks or bioterrorism attacks
• Increase magnitude and functionality of antibody responses
• Induce cell-mediated immunity
• Enhance immune responses in the immunocompromised people , such as the young or elderly, who often respond poorly to vaccines
• Induce a broader immune response which can provide cross-protection against related pathogenic strains
• Enable mucosal delivery of vaccines promoting antibody responses at mucosal surfaces

Despite their importance, only a few adjuvants are approved for human use (Table 1.3). The small number of adjuvants available for human use may be explained by the considerable increase in regulatory demands since the initial approval of aluminum salts [38]. Additionally, unacceptable levels of toxicity associated with many new adjuvant candidates have been delaying the approval of new adjuvants. Since prophylactic vaccines are mostly used to immunize healthy individuals, only effective adjuvants that induce minimal adverse effects are acceptable [39].

Table 1.3 – Current licensed adjuvants for human use (adapted from [41]).

Adjuvant (year of approval; agency)	Adjuvant type	Disease (trade name)	Manufacturer
Aluminum salts (1926)	Mineral salt	Various	Various
MF59 (1997; EMA and FDA)	Squalene oil-in-water emulsion	Influenza - seasonal(Fluad, Optaflu) and pandemic (Focetria and Aflunov)	Novartis
Virosomes (2000; EMA)	Liposomes	Seasonal influenza (Inflexal), hepatitis A (Epaxal)	Berna Biotech
AS04 (2005; EMA and FDA)	Aluminum salts plus the TLR4 agonist (MPL)	Hepatitis B (Fendrix), human papilloma virus (Cervarix)	GSK
AS03 (2009; EMA and FDA)	Squalene oil-in-water emulsion plus α-tocopherol	Influenza – pandemic (Pandremix) and pre-pandemic (Prepandrix)	GSK
AS01 (2015; EMA) [42]	Combination of liposomes, MPL and QS21	Malaria (Mosquirix)	GSK
CTB (2004; EMA)	non-toxic enterotoxin derivative	Cholera (Dukoral)	Crucell

Most of the current licensed vaccines, particularly the ones with aluminum salts in their composition, are good at inducing antigen-specific antibodies but are poor inducers of cell-mediated immunity, such as cytotoxic T lymphocytes, a requirement for most of the diseases

for which effective vaccines are not available, such as HIV, tuberculosis and malaria [43, 44]. Furthermore, only one of the current licensed adjuvants (CTB) was approved for mucosal immunization. So, the design of new, safe and improved mucosal adjuvant candidates is essential for the future of vaccine development.

In the next sub-sections, different types of mucosal adjuvants will be briefly described, with focus on the ones used in this thesis: mast cell activators and chitosan nanoparticles.

1.5.1 Immunopotentiators

The best studied and most potent mucosal adjuvants are non-particulate adjuvants, more specifically the bacterial enterotoxins, cholera toxin (CT) and *E. coli* heat-labile toxin (LT). Those molecules have shown to successfully induce mucosal and systemic immunity, including both humoral and cellular immune responses. Despite these advantages, its use has been avoided in humans because some adverse effects, such as severe diarrhea were been observed [23]. Furthermore, Bell's palsy syndrome (facial paralysis) was observed in some individuals immunized with an LT-adjuvanted nasal influenza vaccine [45]. As a result, much effort has been made in the generation of non-toxic derivatives of these molecules, such as CTB, LTK63 and CTA1-DD [20]. While CTB was approved by European Medicines Agency (EMA) in 2004 as an adjuvant in the oral delivered cholera vaccine Dukoral [46], two cases of transient Bell's palsy were reported in Phase 1 clinical trials associated with nasal administration of the non-toxic LT mutant LTK63 [47]. So, although bacterial enterotoxins and their derivatives have already been used as mucosal vaccine adjuvants, there are still some concerns that these molecules may be toxic to the central nervous system when given nasally [48, 49] which may prevent their use in humans, particularly as a nasal adjuvant. There is a recognized need to find safer alternatives and some potential mucosal adjuvants have been investigated.

After the discovery of pattern recognition receptors (PRR) that recognize pathogen-associated molecular patterns (PAMPs), emerged a class of adjuvants that are natural ligands or synthetic agonists for PRR [50]. Toll-like receptors (TLRs) agonists are the better studied in this group. These molecules are potent inducers of innate immune responses leading to subsequent activation of the adaptive immune system. Although several TLR agonists have been explored as potential adjuvant candidates, the only one used in human licensed vaccines is the TLR4 ligand monophosphoryl lipid A (MPL)[51]. The vaccines Cervarix and Fendrix, from GlaxoSmithKline, incorporate the adjuvant system AS04, which combines alum and the MPL. Although initially approved for parenteral administration, *in vivo* studies showed that

MPL has also the potential to be used as an adjuvant in mucosal vaccines [52-54]. Other TLR ligands, including CpG ODN [54-56] and flagellin [57, 58] have also shown the ability to improve immune responses to an antigen after administration through mucosal surfaces.

Besides bacterial enterotoxins derivatives and TLR agonists, there are other small molecules with immunopotentiator properties that have been explored as mucosal adjuvants, including alpha-galactosylceramide (α-galcer) and cyclic dinucleotides, such as c-di-GMP and c-di-AMP [34, 59]. Alpha-galcer, a natural killer T cell agonist, showed the ability to induce efficient mucosal and systemic cell-mediated immunity after immunization by nasal [60-62] or oral route [61]. Cyclic di-nucleotides are bacteria second messengers that have been shown to be quite promising as nasal adjuvants inducing strong mucosal and systemic immune responses, including cytotoxic T-lymphocyte responses [63, 64].

1.5.1.1 Mast cell activators

More recently, mast cell activators emerged as a new class of vaccine adjuvants. As previously described, mast cells are strategically located at the mucosal surfaces and have the ability to promptly respond to pathogen stimulation, releasing preformed mediators that activate the innate immune system to mobilize various immune cells to the site of infection and to draining lymph nodes. In 2008, McLachlan et al. showed that subcutaneous or nasal administration of the mast cell activator compound 48/80 (C48/80) with vaccine antigens resulted in a significant increase of antigen-specific IgG [65]. Additionally, nasal immunization with C48/80 as adjuvant induced high levels of antigen-specific IgA in different mucosal surfaces and provided protection against anthrax lethal toxin challenge *in vitro* and against vaccinia virus infection *in vivo*. This study was the first report that mast cell activators could be used as mucosal vaccine adjuvants providing antigen-specific protective immune responses. Since then, other studies confirmed the immunopotentiator properties of the mast cell activator C48/80. Intradermal immunization of mice with antigen plus C48/80 enhanced neutralizing antibody titers and cell mediated immune responses. Besides, no antigen-specific IgE was detected and minimal injection site inflammation was observed, revealing a good safety profile for C48/80 [66]. Nasal immunization with recombinant hemagglutinin (HA) protein and C48/80 significantly increased the serum IgG and mucosal IgA antibody responses against HA protein, which correlated with stronger and durable neutralizing antibody activities and conferred protection against 2009 pandemic H1N1 influenza virus [67]. C48/80 also demonstrated potential as a mucosal adjuvant in other experiments with different animal models after nasal administration [68-71]. Besides the good safety profile of C48/80

showed in mice [65, 66], previous studies observed that the cutaneous application of C48/80 in humans did not induce any serious long-term adverse reactions [72, 73]. Additionality, the immunomodulatory properties of other vaccine adjuvants, such as IL-18 [74], the cholera toxin derived CTA1-DD [75], imiquimod [76] and alum [77] seem to be somehow mediated by mast cells.

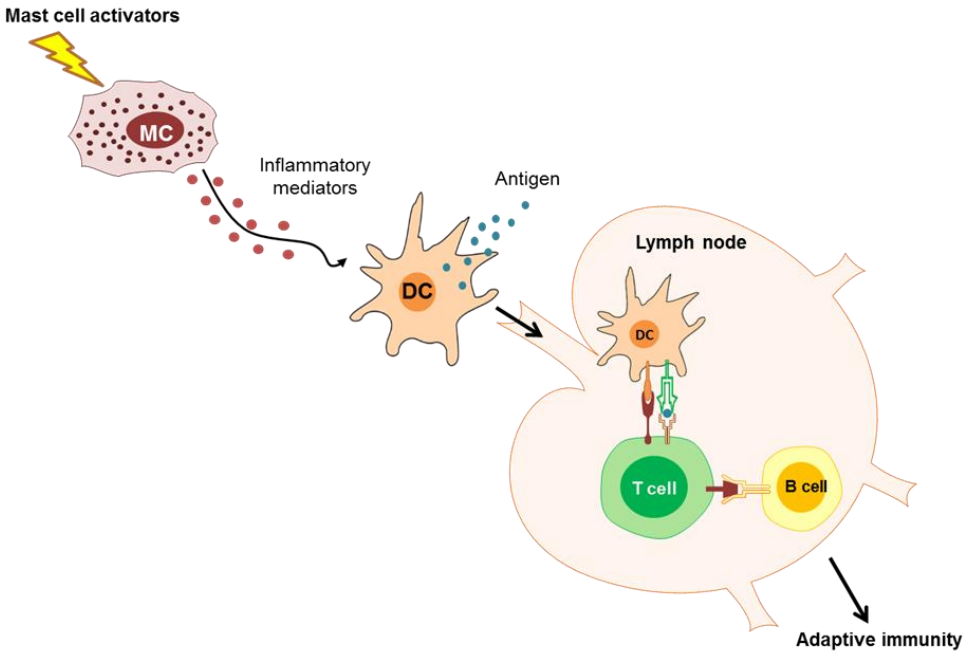

Figure 1.3 – Mast cell activators as vaccine adjuvants. Administration of the mast cell activator C48/80 with an antigen activate MCs and trigger the release of inflammatory mediators, such as TNF-α, inducing migration of DC to DLN. In the lymph node DCs will present the antigen to T cells with further T cell-B cell cooperation resulting in antigen-specific antibody responses (adapted from [78]).

It was suggested that C48/80 acts as an adjuvant by inducing release of inflammatory mediators by mast cells, which enhances the recruitment of DCs and the retention of lymphocytes into draining lymph nodes, promoting the development of antigen-specific immune responses (Fig. 1.3) [14, 65]. Altogether, these studies suggest that using the mast cell activator C48/80 as an adjuvant may be a good strategy for the future development of mucosal vaccines.

1.5.2 Particulate adjuvants/Delivery systems

The use of particulate adjuvants offers several attractive features. Antigens associated with particles have a comparable size to some pathogen, mimicking more closely the nature of antigens, which enhances recognition and uptake by APCs [79, 80]. Other advantages offer by particles include: i) protection of antigen against degradation [81], ii) depot effect with gradual

release of the antigen [82, 83], iii) cross-presentation of antigens [82, 84], iv) improved antigen processing when compared with antigen in solution, which can result in a prolonged antigen presentation [85], v) co-deliver of antigens and adjuvants [79] and vi) modulation of the immune response [82]. Different nano-sized platforms such as virus-like particles [86], liposomes [87], immune stimulating complexes [88, 89], nanoemulsions [90, 91] and polymeric nanoparticles [92, 93] have been explored as potential vaccine delivery systems. These delivery systems are particularly interesting for the design of mucosal vaccines by reducing the rate of dilution and degradation of antigen on mucosal tissues [94]. Besides, particulate antigens are generally more immunogenic than soluble antigens, particularly at mucosal surfaces where soluble antigens are more prone to induce mucosal tolerance [28, 93]. Particle characteristics, such as size, charge and surface chemistry, influence the outcome of the immune response. For example, while studies evaluating the effect of particles size on the immune response are often contradictory, nanoparticles (NP) (< 1000 nm) are generally associated with a better uptake profile and are more prone to induce cell mediated immunity when compared with microparticles [83, 93, 95]. Similarly, in a direct evaluation of the effect of NP surface charge on mucosal immune response positively charged nanoparticles were more potent promoters of systemic and mucosal immune responses than anionic nanoparticles [96]. Despite these preliminary insights on the effect of particle characteristics on the immune response, there is a need for more systematic studies, using different types of particles but the same readouts, to provide a better understanding of the topic.

The use of nanoparticles for vaccine delivery, and more specifically for mucosal immunization, have been extensively reviewed elsewhere [29, 82, 97, 98]. Here it will be described the use of polymeric particles as mucosal adjuvants, more specifically chitosan nanoparticles. The use of polymeric particles as adjuvants is very attractive because it offers flexibility in terms of size, charge and surface characteristics of the vaccine formulation [99]. As a result, several studies have been exploring the use of biocompatible and biodegradable polymers for mucosal vaccine delivery.

Several synthetic polymers, such as poly(epsilon-caprolactone) (PCL), polystyrene (PS), poly(glycolic acid) (PGA), poly(lactid acid) (PLA) or poly(lactic-co-glycolic acid) (PLGA), have been used to prepare nanoparticles [98]. PLGA nanoparticles are probably the most well studied synthetic polymeric particles for vaccine delivery. Although primarily used for parenteral delivery, PLGA NP have been also successfully used for mucosal vaccination. As an example, the entrapment of H1N1 peptides in PLGA nanoparticles enhanced virus specific T cell responses and vaccine efficacy in pigs after nasal vaccination [100]. Similarly,

Binjawadagi B et al. showed that nasal vaccination of pigs with an adjuvanted PLGA NP vaccine formulation resulted in increased humoral and cell-mediated immune responses [101]. However, when compared with other polymers PLGA is not as effective for mucosal vaccination due to its poor mucoadhesive properties. For example, coating of PLGA NP with the mucoadhesive polymer trimethyl chitosan (TMC) resulted in an improved formulation, increasing the levels of antigen-specific antibodies compared to non-coated PLGA NP [102]. However, a direct comparison of PLGA NP with the TMC NP showed that TMC NP are more effective at inducing both systemic and mucosal immune responses after nasal vaccination [103].

Particles formulated with natural polymers such as alginate, hyaluronic acid and chitosan have also been widely investigated as vaccine adjuvants. In particular, chitosan-based nanoparticles have received much interest for mucosal vaccination due to their attractive characteristics.

1.5.2.1 Chitosan

Chitosan, a natural copolymer of β-(1, 4)-linked glucosamine and N-acetylglucosamine, is obtained by deacetylation of chitin (Fig. 1.4), extracted from the exoskeletons of crustacean or the cell walls of fungi. When more than 50 % of acetyl groups are removed from chitin, it is usually considered as chitosan [104] and chitosan characteristic, such as degree of deacetylation and molecular weight, influence its physical and biological properties [104, 105]. Chitosan is biodegradable, biocompatible and bioadhesive and, for these reasons, it has been largely explored for several biomedical applications, particularly drug and vaccine delivery. Chitosan have shown antimicrobial activity [106] and is approved by the US Food and Drug Administration due to its wound healing properties [107]. Chitosan mucoadhesivity is one of its more attractive properties. Due to the presence of amino groups, chitosan is positively charged and interact with the negatively charged mucus and cell membranes [108], facilitating adherence to mucosal membranes. Besides, chitosan is able to reversible open epithelial tight junctions which promote penetration through the mucosa [109, 110], a process usually hindered by the tight arrangement of the epithelial cells. These characteristics make chitosan a good candidate for mucosal delivery of biomolecules [111, 112].

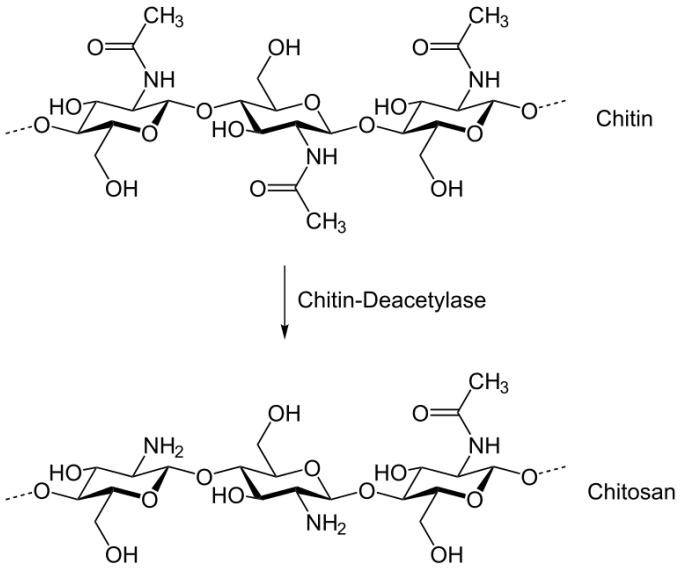

Figure 1.4 - Schematic representation of the preparation of chitosan from deacetylation of chitin.

Following the demonstration that chitosan nanoparticles enhanced the absorption of insulin administered intranasally [113], there was an increased interest in the use of chitosan particles as nasal delivery systems for a wide range of applications, particularly for vaccine delivery. Two of the biggest challenges of nasal vaccine delivery are the short residence time of formulations in the nasal cavity due to mucociliary clearance and inefficient uptake of soluble antigens [108, 111]. Therefore, mucoadhesive chitosan nano- and microparticles are particularly interesting for design of nasal vaccines since they combine the advantages of particulate adjuvants with an increased nasal residence time of the vaccine formulation, resulting in an improved uptake of antigen-loaded particles [111].

The existence of functional groups (amine and hydroxyl) in chitosan allows chemical modification of the polymer and its properties. So, in the recent years, several chitosan derivatives have been synthesized, such as N-trymethyl-chitosan (TMC), carboxymethyl chitosan (CMC) and chitosan hydrochloride salt, to enhance its solubility and/or mucoadhesiveness [108]. Both nano- and microparticles made of chitosan or chitosan derivatives have been successfully used as adjuvants for nasal vaccination. Chitosan based particles improved mucosal and systemic antibody responses after nasal immunization with different antigens, such as tetanus toxoid [114], influenza protein antigens[115, 116], Streptococcus equi antigens [117], pneumococcal surface protein A (PspA) [118] and HBsAg [119, 120] . Similarly, chitosan nanoparticles demonstrated to be effective for nasal delivery of

DNA vaccines [121-123]. The application of chitosan as an adjuvant also showed ability to enhance the immunogenicity of antigens following oral vaccination [124-126].

Vaccination with chitosan as adjuvant not only induces strong mucosal and systemic humoral immune responses but also has the ability to promote cellular immunity [118, 123], namely enhanced antigen-specific IFN-γ production. Besides, chitosan mediated protection against influenza and pneumococcal challenges in murine models [115, 123, 127]. Notably, although mainly used for formulation of delivery systems, chitosan have been shown to possess immunomodulatory effects itself. For example, different chemical compositions of chitosan were found to induce TNF-α production by human monocytes[128]. Koppolu et al. showed that antigen-encapsulated chitosan particles enhanced upregulation of surface activation markers on macrophages and DCs and increased the release of pro-inflammatory cytokines [129]. Recently, Carroll et al. demonstrated that chitosan in solution can promote dendritic cell maturation by inducing type I interferons (IFNs) and enhances antigen-specific Th1 and IgG2c responses following vaccination [118].

While most of the studies using chitosan as mucosal adjuvant were conducted in animal models, data from human studies support the safety profile of chitosan [108, 130] and the potential as nasal adjuvant for use in human vaccines [131-133].

1.6 Combination adjuvants

Recently, the incorporation of two adjuvants in the same vaccine formulation has been recognized as a promising strategy for the design of improved vaccines [40, 134]. While different types of adjuvants have been assessed as part of adjuvant combinations, most of the approaches combine a delivery system with an immunopotentiator. A number of studies demonstrate that the combination of adjuvants can be highly beneficial not only by significantly enhance immune responses induced by a vaccine, but also by modulating the type of immune response desired [79, 134]. The adjuvant systems developed by GSK are a good example of success of the adjuvant combination strategy. Adjuvant systems (AS) are based on the combination of classical adjuvants and were specifically designed to tailor the adaptive immune responses, inducing strong and persistent cellular immune responses against vaccine antigens, while sustaining a high antibody response [135]. AS03, AS04 and AS01 have already been licensed for use in human vaccines (table 1.3). Didierlaurent et al. elucidated the mechanism of action of AS04 and showed that the addition of MPL to aluminum salt enhances the cellular immune responses to a human papillomavirus vaccine (HPV) by rapidly triggering a local cytokine response leading to an optimal activation of APCs [136].

Incorporation of immunopotentiators in nanoparticles can also mediate a decrease of the systemic distribution of the immunopotentiator preventing systemic inflammatory toxicity. For example, Illyinskii et al. showed that association of the TLR agonists R848 and CpG with polymeric nanoparticles resulted in strong immune responses without inducing systemic cytokine release. On the other hand, the same nanoparticles admixed with the TLR agonists led to decreased immunogenicity and induced high levels of inflammatory cytokines in serum [137]. So, combination of particles and immunopotentiators can enhance both efficacy and safety of a vaccine, by reducing adjuvant-related side effects.

1.6.1 Combination of chitosan with immunopotentiators

We made a literature review of the use of chitosan and its derivatives with other immunopotentiators in the development of improved vaccine adjuvants. These studies are summarized on table 1.4 and will be briefly described according to the immunization route.

1.6.1.1 Nasal

Most of the adjuvant combinations tested containing chitosan are intended for nasal vaccine delivery. In 2010, Slutter et al. explored the use of the adjuvant CpG ODN as a crosslinker in TMC nanoparticles in order to modulate the immune response induced by TMC NP [138]. The inclusion of CpG into TMC nanoparticles promoted a Th1 immune response while maintaining the strong OVA specific serum IgG and nasal IgA observed with TMC/TPP nanoparticles. The same group tested different combinations of TMC NP and immunopotentiators for nasal vaccination. They found that while immunization of mice with OVA plus TMC nanoparticles containing LPS or MDP elicited higher IgG, IgG1 and IgA levels than non-adjuvanted particles, nanoparticles containing CTB, PAM3CSK4 or CpG did not [139]. While these results with TMC NP associated with CpG seem to contradict the previous study, the OVA and CpG doses tested here were two-fold lower than in the first study, which may explain the differences observed. The potential of combining chitosan and TLR agonists to develop more effective nasal adjuvants was also explored by other groups. Vicent et al. showed that the co-delivery of HBsAg and the TLR-7 agonist imiquimod using chitosan nanocapsules resulted in increased serum IgG after nasal administration to mice [140].

Dehghan et al. developed a powder formulation of chitosan nanospheres with influenza whole virus and CpG encapsulated that effectively induced humoral and cellular immune responses after nasal administration in rabbits [141]. Similarly, Klas et al. showed that a nasal dry powder anthrax vaccine formulated with chitosan plus MPL significantly protected rabbits

against lethal challenge 9 weeks after a single immunization [142]. The nasal immunization of mice with recombinant Helicobacter pylori urease (rUre) admixed with the PAMP muramyl di-peptide (MDP) and chitosan resulted in elevated serum IgG titers and increased production of the Th1-associated cytokines IL-2 and IFN-γ, following antigen restimulation of splenocytes [143]. This synergy was observed when the mice were immunized intranasally but not intramuscularly suggesting the important role that route of administration plays on the effect of an adjuvant combination. Chitosan has been also shown to improve the immunopotentiator effect of other molecules. The formulation of the conjugated CRM-MenC vaccine with LTK63, a non-toxic LT mutant, and chitosan microparticles induced systemic immune responses as high as the subcutaneous vaccine adjuvanted with alum. Moreover, higher anti-MenC IgA titers in serum and nasal washes were observed in the mice vaccinated with the microparticle conjugated vaccine formulated together with LTK63 [144]. The same group tested the concomitant use of LTK63 and TMC as a nasal vaccine adjuvant [145]. The positive effect of this combination was less evident at higher doses of adjuvants tested, but a dose-response study demonstrated that the concomitant use of TMC allowed a reduction of the LTK63 dose from 10 μg to 0.1 μg without significantly affecting the bactericidal antibody titers. This suggests that the intrinsic mucosal adjuvanticity of LTK63 can be efficiently enhanced by formulating LTK63 with chitosan or chitosan derivatives. Svindland et al. evaluated the potential of combining chitosan and the bacterial second messenger (3', 5')-cyclic dimeric guanylic acid (c-di-GMP) for the development of an intranasal influenza H5N1 vaccine [146]. At the highest dose of antigen tested, the adjuvant combination was as effective at boosting the humoral immune responses as c-di-GMP alone, but gave rise to lower Th1 (IL-2 and IFN-γ) and higher Th2 (IL-5 and IL-10) cytokine concentrations than c-di-GMP adjuvanted vaccine. So, this adjuvant combination provided similar humoral immune responses as the c-di-GMP adjuvant, but a more balanced Th response. However, at the lower doses of antigen tested, c-di-GMP alone was more effective at inducing humoral and cellular immune responses than the adjuvant combination. This could be related with the study design where, due to formulation compatibility issues, groups immunized with the adjuvant combination received first the antigen mixed with chitosan followed by the c-di-GMP. The adjuvant combination strategy has also been used to improve the immune response to chitosan adjuvanted DNA vaccines. Nasal delivery of chitosan encapsulated provax-IL-15 plasmid with pcD-VP1 against foot-and-mouth disease virus (FMDV) induced strong systemic and mucosal antibody responses. Cellular immune responses, including antigen specific T-cell proliferation, cytotoxic responses *in vivo* and production of IFN-γ by CD4+ and

CD8+ T cells were also significantly improved [147]. Co-immunization of mice with the chitosan-pVP1 DNA vaccine against Coxsackievirus B3 (CVB3) plus lymphotactin (LTN) gene (T cell-attractive-chemokine) incorporated in chitosan particles significantly enhanced antibody and T cell immune responses in systemic and mucosal immune compartments [148]. Furthermore, this adjuvant combination improved resistance to CVB3-induced acute myocarditis after CVB3 challenge, as evidenced by reduced myocardial viral load and increased the survival rate of mice. These results were confirmed by a second study also from Yue et al. in which they tested different combinations of the adjuvant LTN and antigen VP1 [149]. The two genes were either cloned in separate vectors, as in the first study, or co-expressed in the same vector before encapsulation in chitosan nanoparticles. Nasal co-immunization with VP1 and LTN as separate chitosan-DNA showed to be the most effective combination for enhancement of both antibody and T cell immune responses. After the success of this adjuvant combination, and based on a similar principle, the same group pursued to test new adjuvant combinations for a nasal vaccine against CVB3. The co-immunization of mice with the adjuvant combinations chitosan-pAIM2 (absent in melanoma 2) [150] or with chitosan-HMGB1 (high-mobility group box 1) [151] plus chitosan-pVP1 both lead to enhanced immune responses and alleviate CVB3-induced myocarditis.

Table 1.4 – Summary of studies using chitosan in combination with other immunopotentiators for vaccination purposes.

Chitosan type and formulation	Immunopotentiator	Antigen	Dose	Immunization schedule and animal model	Immune response induced	Ref.
Nasal						
TMC Nanoparticle 304 nm	CpG	OVA	20 µg OVA, 20 µg CpG	Days 0, 21, 42 BALB/c mice	**Humoral:** IgG and IgG2a; nasal IgA **Cellular:** IFN-γ	[138]
TMC Nanoparticle 300 to 420 nm	LPS, CpG, PAM3CSK4, MDP or CT	OVA	10 µg OVA, 10 µg immunopotentiator	Days 0, 21 BALB/c mice	**Humoral**: IgG and IgG1; nasal IgA (TMC NP plus LPS or MDP) **Cellular:** NS	[139]
Chitosan glutamate Dry powder ChiSys™	MPL	PA + conj.	150 µg PA + 150 µg conj., 50 µg MPL, 20 mg of powder	Day 0 (single immunization) Challenged at week 9 New Zealand White rabbits	**Humoral:** IgG; toxin neutralizing antibody titers **Cellular:** NS Increased survival rate	[142]
Chitosan Dry powder nanosphere 581 nm	CpG or QS	Influenza /H1N1 whole virus (WV)	45 µg of virus, 10 µg of CpG ODN or QS in 5 mg of powder	Days 0, 45, 60: In, day 75: Im New Zealand White rabbits	**Humoral:** Serum HI titer and IgG; nasal IgA **Cellular:** IL-2 and IFN-γ (Chi plus CpG)	[141]
Chitosan hydrochloride salt Nanocapsule 200 nm	Imiquimod	HBsAg	10 µg HBsAg, 10 µg imiquimod	Weeks 0, 4 and 28 BALB/c mice	**Humoral:** IgG **Cellular:** NS	[140]
Chitosan Microparticle 5 µm	LTK63	CRM-MenC conjugate	2.5 µg MenC, 5 µg CRM197, 1 µg LTK63, 20 µg Chi	Days 1, 21, 35 BALB/c mice	**Humoral**: serum IgG and IgA; serum bactericidal antibody titers; nasal IgA **Cellular:** NS	[144]

c-di-GMP: (3', 5')-cyclic dimeric guanylic acid; conj.:10-mer capsule peptide conjugated to BSA; CRM-MenC: Group C meningococcal conjugatedVaccine; CT: cholera toxin; CTB: Cholera toxin B; CTB-UE: multi-epitope vaccine composed of the cholera toxin B subunit and tandem copies of the B and Th cell epitopes from the H. pylori urease A and B subunits; GM-CSF: Granulocyte-macrophage colony-stimulating factor; HA: Influenza hemagglutinin; HBsAg: hepatitis B surface antigen; HI: Hemagglutination inhibition; LPS: Bacterial lipopolysaccharide; LTK63: non-toxic mutant of Escherichia coli heat labile enterotoxin; MDP: muramyl di-peptide; MGC: methylglycol chitosan; NS: not studied; OVA: ovalbumin; PA: anthrax protective antigen; pAIM2: plasmid encoding absent in melanoma 2; pcD-VP1: plasmid encoding the VP1 protein of foot-and-mouth disease virus (FMDV); pHMGB1: plasmid encoding high-mobility group box 1; pLTN: plasmid encoding lymphotactin; provax-IL-15: IL-15 expressing plasmid; QS: Quillaja saponin; TMC: N-trimethyl chitosan; rURE: recombinant Helicobacter pylori urease; VP1: plasmid encoding the major capsid protein of CVB3.

Table 1.4 – Summary of studies using chitosan in combination with other immunopotentiators for vaccination purposes (continued).

Chitosan type and formulation	Immunopotentiator	Antigen	Dose	Immunization schedule and animal model	Immune response induced	Ref.
Nasal						
TMC (solution)	LTK63	Subunit (CRM-MenC)	1-2.5 µg MenC, 2-5 µg CRM197, 0.05, 0.2 or 1 µg LTK63, 10, 20 or 50 µg TMC	Days 0, 21, 35 BALB/c mice	**Humoral**: IgG, serum bactericidal antibody titers **Cellular:** NS	[145]
chitosan chloride (solution)	MDP	rUre	10 µg of rUre, 10 µg of MDP, 0.2% m/v Chitosan	Days 1 and 56 BALB/c mice	**Humoral**: serum IgG and IgA **Cellular:** IFN-γ and IL-2	[143]
chitosan glutamate (solution)	c-di-GMP	HA	7.5, 1.5 or 0.3 µg HA; 82.5 µg chitosan; 5µg c-di-GMP	Days 1 and 21 BALB/c mice	**Humoral**: serum IgG and IgA (with 7.5 ug of HA) **Cellular:** increased Il-10 and IL-5, decreased IFN-γ and IL-2 when compared with c-di-GMP (with 7.5 µg of HA)	[146]
Chitosan (Chitosan-DNA complexes 255 nm)	provax-IL-15	pcD-VP1 (DNA vaccine)	100 µg pcD-VP1 and 100 µg provax-IL-15	Days 0, 14 and 28 BALB/c mice	**Humoral:** IgG; vaginal IgA and lung IgA **Cellular:** antigen specific T cell proliferation, IFN-γ and IL-4	[147]
Chitosan (Chitosan-DNA complexes 200 – 400 nm)	pLTN	pVP1 (DNA vaccine)	50 µg chitosan pVP1 and 50 µg chitosan-pLTN	4 times, biweekly; challenged 4 weeks after final immunization BALB/c mice	**Humoral:** IgG and IgG2a; fecal IgA; serum and fecal antibody neutralization titers **Cellular:** IFN-γ and IL-12 Increased survival rate	[148]

c-di-GMP: (3', 5')-cyclic dimeric guanylic acid; conj.:10-mer capsule peptide conjugated to BSA; CRM-MenC: Group C meningococcal conjugatedVaccine; CT: cholera toxin; CTB: Cholera toxin B; CTB-UE: multi-epitope vaccine composed of the cholera toxin B subunit and tandem copies of the B and Th cell epitopes from the H. pylori urease A and B subunits; GM-CSF: Granulocyte-macrophage colony-stimulating factor; HA: Influenza hemagglutinin; HBsAg: hepatitis B surface antigen; HI: Hemagglutination inhibition; LPS: Bacterial lipopolysaccharide; LTK63: non-toxic mutant of Escherichia coli heat labile enterotoxin; MDP: muramyl di-peptide; MGC: methylglycol chitosan; NS: not studied; OVA: ovalbumin; PA: anthrax protective antigen; pAIM2: plasmid encoding absent in melanoma 2; pcD-VP1: plasmid encoding the VP1 protein of foot-and-mouth disease virus (FMDV); pHMGB1: plasmid encoding high-mobility group box 1; pLTN: plasmid encoding lymphotactin; provax-IL-15: IL-15 expressing plasmid; QS: Quillaja saponin; TMC: N-trimethyl chitosan; rURE: recombinant Helicobacter pylori urease; VP1: plasmid encoding the major capsid protein of CVB3.

Table 1.4 – Summary of studies using chitosan in combination with other immunopotentiators for vaccination purposes (continued).

Chitosan type and formulation	Immunopotentiator	Antigen	Dose	Immunization schedule and animal model	Immune response induced	Ref.
Nasal						
Chitosan (Chitosan-DNA complexes)	pAIM2	pVP1 (DNA vaccine)	50 µg chitosan pVP1 and 50 µg chitosan-pAIM2	4 times, biweekly; challenged 2 weeks after final immunization BALB/c mice	**Humoral:** fecal IgA and neutralizing titers **Cellular:** NS Increased survival rate	[150]
Chitosan (Chitosan-DNA complexes)	pHMGB1	pVP1 (DNA vaccine)	50 µg chitosan pVP1 and 50 µg chitosan-pHMGB1	4 times, biweekly; challenged 4 weeks after final immunization BALB/c mice	**Humoral:** IgG**;** fecal IgA; serum and fecal antibody neutralization titers **Cellular:** T cell proliferation, IFN-γ Increased survival rate	[151]
Oral						
Chitosan (solution)	CpG and CTB (present in CTB-UE)	CTB-UE	150 µg CTB-UE, 50 mg chitosan, 50 µg CpG	Weeks 0 and 3 BALB/c mice	**Humoral:** Serum IgG, IgG2a and IgA; IgA in stomach, intestine and feces **Cellular:** IFN-γ, IL-4 and IL-17	[152]
Sublingual						
MGC (MGC-CRX-601 complexes)	CRX-601	H3N2 detergent-split flu (A/Victoria /210/2009)	3 µg flu antigen, 5 or 25 µg MGC, 0.01 to 5 µg CRX-601	Days 0, 21 and 42 BALB/c mice	**Humoral:** IgG, serum functional antibody titers; vaginal and tracheal IgA **Cellular:** NS	[153]
Intradermal						
TMC Nanoparticle 300 to 420 nm	LPS, CpG, PAM3CSK4, MDP or CT	OVA	2 µg OVA, 2 µg immunopotentiator	Days 1 and 21 BALB/c mice	**Humoral**: IgG (TMC NP plus LPS), IgG2a (TMC NP plus CpG) **Cellular:** NS	[139]

c-di-GMP: (3', 5')-cyclic dimeric guanylic acid; conj.:10-mer capsule peptide conjugated to BSA; CRM-MenC: Group C meningococcal conjugatedVaccine; CT: cholera toxin; CTB: Cholera toxin B; CTB-UE: multi-epitope vaccine composed of the cholera toxin B subunit and tandem copies of the B and Th cell epitopes from the H. pylori urease A and B subunits; GM-CSF: Granulocyte-macrophage colony-stimulating factor; HA: Influenza hemagglutinin; HBsAg: hepatitis B surface antigen; HI: Hemagglutination inhibition; LPS: Bacterial lipopolysaccharide; LTK63: non-toxic mutant of Escherichia coli heat labile enterotoxin; MDP: muramyl di-peptide; MGC: methylglycol chitosan; NS: not studied; OVA: ovalbumin; PA: anthrax protective antigen; pAIM2: plasmid encoding absent in melanoma 2; pcD-VP1: plasmid encoding the VP1 protein of foot-and-mouth disease virus (FMDV); pHMGB1: plasmid encoding high-mobility group box 1; pLTN: plasmid encoding lymphotactin; provax-IL-15: IL-15 expressing plasmid; QS: Quillaja saponin; TMC: N-trimethyl chitosan; rURE: recombinant Helicobacter pylori urease; VP1: plasmid encoding the major capsid protein of CVB3.

Table 1.4 – Summary of studies using chitosan in combination with other immunopotentiators for vaccination purposes (continued).

Chitosan type and formulation	Immunopotentiator	Antigen	Dose	Immunization schedule and animal model	Immune response induced	
Subcutaneous						
Chitosan glutamate (solution)	GM-CSF	β-galactosidase and UV-inactivated influenza A virus	5µg UV-inactivated influenza or 100 µg β-galactosidase, 20 µg or 80 µg of GM-CSF	Weeks 0 and 1 C57BL/6 mice	**Humoral:** IgG **Cellular:** antigen – specific CD4+ and CD8+ T cell responses	[154]
Chitosan glutamate (solution)	IL-12	OVA	75 ug OVA, 0.25,1 or 4 ug IL-12, 1.5 mg chitosan	Days 1 and 14 C57BL/6 mice	**Humoral:** IgG, IgG2a, IgG2b, IgG1 **Cellular:** OVA-specific CD4+ and CD8+ T cell responses	[155]

c-di-GMP: (3', 5')-cyclic dimeric guanylic acid; conj.:10-mer capsule peptide conjugated to BSA; CRM-MenC: Group C meningococcal conjugatedVaccine; CT: cholera toxin; CTB: Cholera toxin B; CTB-UE: multi-epitope vaccine composed of the cholera toxin B subunit and tandem copies of the B and Th cell epitopes from the H. pylori urease A and B subunits; GM-CSF: Granulocyte-macrophage colony-stimulating factor; HA: Influenza hemagglutinin; HBsAg: hepatitis B surface antigen; HI: Hemagglutination inhibition; LPS: Bacterial lipopolysaccharide; LTK63: non-toxic mutant of Escherichia coli heat labile enterotoxin; MDP: muramyl di-peptide; MGC: methylglycol chitosan; NS: not studied; OVA: ovalbumin; PA: anthrax protective antigen; pAIM2: plasmid encoding absent in melanoma 2; pcD-VP1: plasmid encoding the VP1 protein of foot-and-mouth disease virus (FMDV); pHMGB1: plasmid encoding high-mobility group box 1; pLTN: plasmid encoding lymphotactin; provax-IL-15: IL-15 expressing plasmid; QS: Quillaja saponin; TMC: N-trimethyl chitosan; rURE: recombinant Helicobacter pylori urease; VP1: plasmid encoding the major capsid protein of CVB3.

1.6.1.2 Other immunization routes

Due to its properties, such as mucoadhesiveness, chitosan is an ideal polymer for nasal delivery which probably explains why most of the adjuvant combinations containing chitosan are intended for nasal immunization. However, chitosan has also been used together with other immunopotentiators for vaccination through alternative routes. Xing et al. showed that oral immunization of mice with chitosan plus CpG and CTB enhanced the immunogenicity of a vaccine against *Helicobacter pylori* [152]. This combination promoted both systemic and mucosal immune responses, increased the ratio of IgG2a/IgG1 and induced significantly high levels of antigen-specific IFN-γ and IL-17 cytokines associated with Th1 and Th17 immune responses, respectively. Sublingual vaccination with methylglycol chitosan and the TLR-4 agonist CRX-601 also elicited an improved mucosal response to an influenza vaccine and a systemic immune response at least equivalent to that induced by a flu vaccine delivered intramuscularly [153]. Only a few adjuvant combinations with chitosan were tested for parenteral immunization. Bal et al. showed that intradermal vaccination of mice with OVA plus TMC nanoparticles containing CpG or LPS provoked higher IgG titers than plain TMC

particles [139]. Additionally, TMC plus CpG resulted in significantly higher serum IgG2a. Subcutaneously, chitosan demonstrated to be effective at improving the immunomodulatory properties of GM-CSF [154] and IL-12 [155], enhancing both humoral and T cell mediated immunity.

Altogether these results show that chitosan can not only function as an adjuvant itself but also function as an enhancer to other adjuvants that are already effective on its own. This reinforces the use of adjuvant combinations containing chitosan as a promising strategy for future vaccine development, particularly for mucosal vaccination.

1.7 Aim and outline of the thesis

The aim of this project was to develop chitosan based nanoparticles associated with the mast cell activator C48/80 as a novel delivery system for nasal vaccination. We hypothesized that the mucoadhesive chitosan nanoparticles would extend the residence time of the antigen on the nasal cavity. Simultaneously, the mast cell activation would promote a local microenvironment favorable to the devolvement of an immune response. The use of mast cell activators as vaccine adjuvants is a recent field and this is the first time that C48/80 was combined with nanoparticles. Two different delivery systems were prepared and evaluated in parallel:

Chapter 2 describes the optimization of a colorimetric method for quantification of C48/80 loaded on nanoparticles.

Chapter 3 describes the design, characterization and preliminary *in vitro* evaluation of C48/80 loaded chitosan nanoparticles.

Chapter 4 describes the design, characterization and preliminary *in vitro* evaluation of C48/80 loaded chitosan/alginate nanoparticles.

Chapter 5 compares and evaluates the potential of C48/80 loaded chitosan nanoparticles and C48/80 loaded chitosan/alginate nanoparticles as adjuvants for nasal vaccination.

Chapter 6 evaluates the potential of Chi-C48/80 NP to induce antigen sparing.

Chapter 7 presents the concluding remarks of the thesis.

References

1. Baxby, D., *The Jenner bicentenary: the introduction and early distribution of smallpox vaccine.* FEMS Immunol Med Microbiol, 1996. **16**(1): p. 1-10.
2. Riedel, S., *Edward Jenner and the history of smallpox and vaccination.* Proc (Bayl Univ Med Cent), 2005. **18**(1): p. 21-5.
3. Hilleman, M.R., *Vaccines in historic evolution and perspective: a narrative of vaccine discoveries.* Vaccine, 2000. **18**(15): p. 1436-47.
4. WHO, U., World Bank, *State of the world's vaccines and immunization*. 3rd ed2009, Geneva: WHO.
5. Ogra, P.L., H. Faden, and R.C. Welliver, *Vaccination strategies for mucosal immune responses.* Clin Microbiol Rev, 2001. **14**(2): p. 430-45.
6. Orenstein, W.A., et al., *Contemporary vaccine challenges: improving global health one shot at a time.* Sci Transl Med, 2014. **6**(253): p. 253ps11.
7. Kroger, A., et al., *Epidemiology and Prevention of Vaccine-Preventable Diseases, 13th Edition: The Pink Book*2015: Public Health Foundation.
8. Charles A Janeway, J., Paul Travers, Mark Walport, and Mark J Shlomchik., *Immunobiology: The Immune System in Health and Disease*. 5th ed2001, New York: Garland Science.
9. Desmet, C.J. and K.J. Ishii, *Nucleic acid sensing at the interface between innate and adaptive immunity in vaccination.* Nat Rev Immunol, 2012. **12**(7): p. 479-491.
10. Bruce Alberts, A.J., Julian Lewis, Martin Raff, Keith Roberts, and Peter Walter, *Helper T Cells and Lymphocyte Activation*, in *Molecular Biology of the Cell*

2002, Garland Science: New York.

11. Netea, M.G., et al., *Innate immune memory: a paradigm shift in understanding host defense.* Nat Immunol, 2015. **16**(7): p. 675-9.
12. Joffre, O.P., et al., *Cross-presentation by dendritic cells.* Nat Rev Immunol, 2012. **12**(8): p. 557-569.
13. Metz, M. and M. Maurer, *Mast cells--key effector cells in immune responses.* Trends Immunol, 2007. **28**(5): p. 234-41.
14. Abraham, S.N. and A.L. St John, *Mast cell-orchestrated immunity to pathogens.* Nat Rev Immunol, 2010. **10**(6): p. 440-52.
15. Urb, M. and D.C. Sheppard, *The role of mast cells in the defence against pathogens.* PLoS Pathog, 2012. **8**(4): p. e1002619.
16. Marshall, J.S., *Mast-cell responses to pathogens.* Nat Rev Immunol, 2004. **4**(10): p. 787-99.
17. Galli, S.J., S. Nakae, and M. Tsai, *Mast cells in the development of adaptive immune responses.* Nat Immunol, 2005. **6**(2): p. 135-42.
18. Nakae, S., et al., *Mast cells enhance T cell activation: importance of mast cell costimulatory molecules and secreted TNF.* J Immunol, 2006. **176**(4): p. 2238-48.
19. Holmgren, J. and C. Czerkinsky, *Mucosal immunity and vaccines.* Nat Med, 2005. **11**(4 Suppl): p. S45-53.
20. Gebril, A., et al., *Optimizing efficacy of mucosal vaccines.* Expert Rev Vaccines, 2012. **11**(9): p. 1139-55.
21. Borges, O., et al., *Mucosal vaccines: recent progress in understanding the natural barriers.* Pharm Res, 2010. **27**(2): p. 211-23.
22. Kiyono, H. and S. Fukuyama, *NALT- versus Peyer's-patch-mediated mucosal immunity.* Nat Rev Immunol, 2004. **4**(9): p. 699-710.
23. Neutra, M.R. and P.A. Kozlowski, *Mucosal vaccines: the promise and the challenge.* Nat Rev Immunol, 2006. **6**(2): p. 148-58.
24. Strugnell, R.A. and O.L. Wijburg, *The role of secretory antibodies in infection immunity.* Nat Rev Microbiol, 2010. **8**(9): p. 656-67.

25. Goldsby, R.A., et al., *Kuby immunology*. 4th ed2000, New York: W.H. Freeman. xxv, 670 p.
26. Holmgren, J. and A.M. Svennerholm, *Vaccines against mucosal infections.* Curr Opin Immunol, 2012. **24**(3): p. 343-53.
27. Belyakov, I.M. and J.D. Ahlers, *What role does the route of immunization play in the generation of protective immunity against mucosal pathogens?* J Immunol, 2009. **183**(11): p. 6883-92.
28. Lycke, N., *Recent progress in mucosal vaccine development: potential and limitations.* Nat Rev Immunol, 2012. **12**(8): p. 592-605.
29. Chadwick, S., C. Kriegel, and M. Amiji, *Nanotechnology solutions for mucosal immunization.* Adv Drug Deliv Rev, 2010. **62**(4-5): p. 394-407.
30. *General recommendations on immunization --- recommendations of the Advisory Committee on Immunization Practices (ACIP).* MMWR Recomm Rep, 2011. **60**(2): p. 1-64.
31. Newsted, D., et al., *Advances and challenges in mucosal adjuvant technology.* Vaccine, 2015. **33**(21): p. 2399-405.
32. Arias, M.A., et al., *Glucopyranosyl Lipid Adjuvant (GLA), a Synthetic TLR4 agonist, promotes potent systemic and mucosal responses to intranasal immunization with HIVgp140.* PLoS One, 2012. **7**(7): p. e41144.
33. Gherardi, M.M., et al., *Induction of HIV immunity in the genital tract after intranasal delivery of a MVA vector: enhanced immunogenicity after DNA prime-modified vaccinia virus Ankara boost immunization schedule.* J Immunol, 2004. **172**(10): p. 6209-20.
34. Riese, P., et al., *Intranasal formulations: promising strategy to deliver vaccines.* Expert Opin Drug Deliv, 2014. **11**(10): p. 1619-34.
35. Gwinn, W.M., et al., *Effective induction of protective systemic immunity with nasally administered vaccines adjuvanted with IL-1.* Vaccine, 2010. **28**(42): p. 6901-14.
36. Reed, S.G., M.T. Orr, and C.B. Fox, *Key roles of adjuvants in modern vaccines.* Nat Med, 2013. **19**(12): p. 1597-608.
37. Ramon, G., *Sur l'augmentation anormale de l'antitoxine chez les chevaux producteurs de sérum antidiphtérique*

Bull Soc Centr Med Vet, 1925. **101**: p. 227-234.
38. Reed, S.G., et al., *New horizons in adjuvants for vaccine development.* Trends Immunol, 2009. **30**(1): p. 23-32.
39. Singh, M., A. Chakrapani, and D. O'Hagan, *Nanoparticles and microparticles as vaccine-delivery systems.* Expert Rev Vaccines, 2007. **6**(5): p. 797-808.
40. Guy, B., *The perfect mix: recent progress in adjuvant research.* Nat Rev Microbiol, 2007. **5**(7): p. 505-17.
41. Rappuoli, R., et al., *Vaccines for the twenty-first century society.* Nat Rev Immunol, 2011. **11**(12): p. 865-72.
42. Gosling, R. and L. von Seidlein, *The Future of the RTS,S/AS01 Malaria Vaccine: An Alternative Development Plan.* PLoS Med, 2016. **13**(4): p. e1001994.
43. Rappuoli, R. and A. Aderem, *A 2020 vision for vaccines against HIV, tuberculosis and malaria.* Nature, 2011. **473**(7348): p. 463-9.
44. Seder, R.A. and A.V. Hill, *Vaccines against intracellular infections requiring cellular immunity.* Nature, 2000. **406**(6797): p. 793-8.
45. Mutsch , M., et al., *Use of the Inactivated Intranasal Influenza Vaccine and the Risk of Bell's Palsy in Switzerland.* New England Journal of Medicine, 2004. **350**(9): p. 896-903.
46. Hill, D.R., L. Ford, and D.G. Lalloo, *Oral cholera vaccines: use in clinical practice.* Lancet Infect Dis, 2006. **6**(6): p. 361-73.
47. Lewis, D.J., et al., *Transient facial nerve paralysis (Bell's palsy) following intranasal delivery of a genetically detoxified mutant of Escherichia coli heat labile toxin.* PLoS One, 2009. **4**(9): p. e6999.

48. van Ginkel, F.W., et al., *Cutting edge: the mucosal adjuvant cholera toxin redirects vaccine proteins into olfactory tissues.* J Immunol, 2000. **165**(9): p. 4778-82.
49. Fujihashi, K., et al., *A dilemma for mucosal vaccination: efficacy versus toxicity using enterotoxin-based adjuvants.* Vaccine, 2002. **20**(19-20): p. 2431-8.
50. Coffman, R.L., A. Sher, and R.A. Seder, *Vaccine adjuvants: putting innate immunity to work.* Immunity, 2010. **33**(4): p. 492-503.
51. Maisonneuve, C., et al., *Unleashing the potential of NOD- and Toll-like agonists as vaccine adjuvants.* Proc Natl Acad Sci U S A, 2014. **111**(34): p. 12294-9.
52. Buffa, V., et al., *Evaluation of TLR agonists as potential mucosal adjuvants for HIV gp140 and tetanus toxoid in mice.* PLoS One, 2012. **7**(12): p. e50529.
53. Patil, H.P., et al., *Evaluation of monophosphoryl lipid A as adjuvant for pulmonary delivered influenza vaccine.* J Control Release, 2014. **174**: p. 51-62.
54. Todoroff, J., et al., *Mucosal and systemic immune responses to Mycobacterium tuberculosis antigen 85A following its co-delivery with CpG, MPLA or LTB to the lungs in mice.* PLoS One, 2013. **8**(5): p. e63344.
55. McCluskie, M.J. and H.L. Davis, *CpG DNA is a potent enhancer of systemic and mucosal immune responses against hepatitis B surface antigen with intranasal administration to mice.* J Immunol, 1998. **161**(9): p. 4463-6.
56. Gallichan, W.S., et al., *Intranasal immunization with CpG oligodeoxynucleotides as an adjuvant dramatically increases IgA and protection against herpes simplex virus-2 in the genital tract.* J Immunol, 2001. **166**(5): p. 3451-7.
57. Lee, S.E., et al., *A bacterial flagellin, Vibrio vulnificus FlaB, has a strong mucosal adjuvant activity to induce protective immunity.* Infect Immun, 2006. **74**(1): p. 694-702.
58. Munoz, N., et al., *Mucosal administration of flagellin protects mice from Streptococcus pneumoniae lung infection.* Infect Immun, 2010. **78**(10): p. 4226-33.
59. Wang, S., et al., *Intranasal and oral vaccination with protein-based antigens: advantages, challenges and formulation strategies.* Protein Cell, 2015. **6**(7): p. 480-503.
60. Courtney, A.N., et al., *Intranasal but not intravenous delivery of the adjuvant alpha-galactosylceramide permits repeated stimulation of natural killer T cells in the lung.* Eur J Immunol, 2011. **41**(11): p. 3312-22.
61. Courtney, A.N., et al., *Alpha-galactosylceramide is an effective mucosal adjuvant for repeated intranasal or oral delivery of HIV peptide antigens.* Vaccine, 2009. **27**(25-26): p. 3335-41.
62. Ko, S.Y., et al., *alpha-Galactosylceramide can act as a nasal vaccine adjuvant inducing protective immune responses against viral infection and tumor.* J Immunol, 2005. **175**(5): p. 3309-17.
63. Madhun, A.S., et al., *Intranasal c-di-GMP-adjuvanted plant-derived H5 influenza vaccine induces multifunctional Th1 CD4+ cells and strong mucosal and systemic antibody responses in mice.* Vaccine, 2011. **29**(31): p. 4973-82.
64. Ebensen, T., et al., *The bacterial second messenger cdiGMP exhibits promising activity as a mucosal adjuvant.* Clin Vaccine Immunol, 2007. **14**(8): p. 952-8.
65. McLachlan, J.B., et al., *Mast cell activators: a new class of highly effective vaccine adjuvants.* Nat Med, 2008. **14**(5): p. 536-41.
66. McGowen, A.L., et al., *The mast cell activator compound 48/80 is safe and effective when used as an adjuvant for intradermal immunization with Bacillus anthracis protective antigen.* Vaccine, 2009. **27**(27): p. 3544-52.
67. Meng, S., et al., *Intranasal immunization with recombinant HA and mast cell activator C48/80 elicits protective immunity against 2009 pandemic H1N1 influenza in mice.* PLoS One, 2011. **6**(5): p. e19863.
68. Wang, S.H., et al., *Stable dry powder formulation for nasal delivery of anthrax vaccine.* J Pharm Sci, 2012. **101**(1): p. 31-47.

69. Staats, H.F., et al., *Mucosal targeting of a BoNT/A subunit vaccine adjuvanted with a mast cell activator enhances induction of BoNT/A neutralizing antibodies in rabbits.* PLoS One, 2011. **6**(1): p. e16532.
70. Zheng, M., et al., *Cross-protection against influenza virus infection by intranasal administration of nucleoprotein-based vaccine with compound 48/80 adjuvant.* Hum Vaccin Immunother, 2015. **11**(2): p. 397-406.
71. Gwinn, W.M., et al., *A comparison of non-toxin vaccine adjuvants for their ability to enhance the immunogenicity of nasally-administered anthrax recombinant protective antigen.* Vaccine, 2013. **31**(11): p. 1480-9.
72. Brunet, C., P.M. Bedard, and J. Hebert, *Analysis of compound 48/80-induced skin histamine release and leukotriene production in chronic urticaria.* J Allergy Clin Immunol, 1988. **82**(3 Pt 1): p. 398-402.
73. Dor, P.J., et al., *Induction of late cutaneous reaction by kallikrein injection: comparison with allergic-like late response to compound 48/80.* J Allergy Clin Immunol, 1983. **71**(4): p. 363-70.
74. Kayamuro, H., et al., *Interleukin-1 family cytokines as mucosal vaccine adjuvants for induction of protective immunity against influenza virus.* J Virol, 2010. **84**(24): p. 12703-12.
75. Fang, Y., et al., *Mast cells contribute to the mucosal adjuvant effect of CTA1-DD after IgG-complex formation.* J Immunol, 2010. **185**(5): p. 2935-41.
76. Heib, V., et al., *Mast cells are crucial for early inflammation, migration of Langerhans cells, and CTL responses following topical application of TLR7 ligand in mice.* Blood, 2007. **110**(3): p. 946-53.
77. McKee, A.S., et al., *Alum induces innate immune responses through macrophage and mast cell sensors, but these sensors are not required for alum to act as an adjuvant for specific immunity.* J Immunol, 2009. **183**(7): p. 4403-14.
78. Pulendran, B. and S.J. Ono, *A shot in the arm for mast cells.* Nat Med, 2008. **14**(5): p. 489-90.
79. De Temmerman, M.L., et al., *Particulate vaccines: on the quest for optimal delivery and immune response.* Drug Discov Today, 2011. **16**(13-14): p. 569-82.
80. Zhao, L., et al., *Nanoparticle vaccines.* Vaccine, 2014. **32**(3): p. 327-37.
81. Akagi, T., F. Shima, and M. Akashi, *Intracellular degradation and distribution of protein-encapsulated amphiphilic poly(amino acid) nanoparticles.* Biomaterials, 2011. **32**(21): p. 4959-67.
82. Smith, D.M., J.K. Simon, and J.R. Baker, Jr., *Applications of nanotechnology for immunology.* Nat Rev Immunol, 2013. **13**(8): p. 592-605.
83. Oyewumi, M.O., A. Kumar, and Z. Cui, *Nano-microparticles as immune adjuvants: correlating particle sizes and the resultant immune responses.* Expert Rev Vaccines, 2010. **9**(9): p. 1095-107.
84. Shen, H., et al., *Enhanced and prolonged cross-presentation following endosomal escape of exogenous antigens encapsulated in biodegradable nanoparticles.* Immunology, 2006. **117**(1): p. 78-88.
85. Thomann-Harwood, L.J., et al., *Nanogel vaccines targeting dendritic cells: contributions of the surface decoration and vaccine cargo on cell targeting and activation.* J Control Release, 2013. **166**(2): p. 95-105.
86. Vacher, G., et al., *Recent advances in mucosal immunization using virus-like particles.* Mol Pharm, 2013. **10**(5): p. 1596-609.
87. Tada, R., et al., *Intranasal Immunization with DOTAP Cationic Liposomes Combined with DC-Cholesterol Induces Potent Antigen-Specific Mucosal and Systemic Immune Responses in Mice.* PLoS One, 2015. **10**(10): p. e0139785.
88. Coulter, A., et al., *Intranasal vaccination with ISCOMATRIX adjuvanted influenza vaccine.* Vaccine, 2003. **21**(9-10): p. 946-9.

89. Cibulski, S.P., et al., *Novel ISCOMs from Quillaja brasiliensis saponins induce mucosal and systemic antibody production, T-cell responses and improved antigen uptake.* Vaccine, 2016. **34**(9): p. 1162-71.
90. Makidon, P.E., et al., *Pre-clinical evaluation of a novel nanoemulsion-based hepatitis B mucosal vaccine.* PLoS One, 2008. **3**(8): p. e2954.
91. Das, S.C., et al., *Nanoemulsion W805EC improves immune responses upon intranasal delivery of an inactivated pandemic H1N1 influenza vaccine.* Vaccine, 2012. **30**(48): p. 6871-7.
92. Sharma, R., et al., *Polymer nanotechnology based approaches in mucosal vaccine delivery: challenges and opportunities.* Biotechnol Adv, 2015. **33**(1): p. 64-79.
93. Rice-Ficht, A.C., et al., *Polymeric particles in vaccine delivery.* Curr Opin Microbiol, 2010. **13**(1): p. 106-12.
94. Vajdy, M., et al., *Mucosal adjuvants and delivery systems for protein-, DNA- and RNA-based vaccines.* Immunol Cell Biol, 2004. **82**(6): p. 617-27.
95. Shah, R.R., et al., *The impact of size on particulate vaccine adjuvants.* Nanomedicine (Lond), 2014. **9**(17): p. 2671-81.
96. Fromen, C.A., et al., *Controlled analysis of nanoparticle charge on mucosal and systemic antibody responses following pulmonary immunization.* Proc Natl Acad Sci U S A, 2015. **112**(2): p. 488-93.
97. Csaba, N., M. Garcia-Fuentes, and M.J. Alonso, *Nanoparticles for nasal vaccination.* Adv Drug Deliv Rev, 2009. **61**(2): p. 140-57.
98. Lebre, F., C.H. Hearnden, and E.C. Lavelle, *Modulation of Immune Responses by Particulate Materials.* Adv Mater, 2016.
99. Lawson, L.B., E.B. Norton, and J.D. Clements, *Defending the mucosa: adjuvant and carrier formulations for mucosal immunity.* Curr Opin Immunol, 2011. **23**(3): p. 414-20.
100. Hiremath, J., et al., *Entrapment of H1N1 Influenza Virus Derived Conserved Peptides in PLGA Nanoparticles Enhances T Cell Response and Vaccine Efficacy in Pigs.* PLoS One, 2016. **11**(4): p. e0151922.
101. Binjawadagi, B., et al., *Adjuvanted poly(lactic-co-glycolic) acid nanoparticle-entrapped inactivated porcine reproductive and respiratory syndrome virus vaccine elicits cross-protective immune response in pigs.* Int J Nanomedicine, 2014. **9**: p. 679-94.
102. Pawar, D., et al., *Evaluation of mucoadhesive PLGA microparticles for nasal immunization.* AAPS J, 2010. **12**(2): p. 130-7.
103. Slutter, B., et al., *Nasal vaccination with N-trimethyl chitosan and PLGA based nanoparticles: nanoparticle characteristics determine quality and strength of the antibody response in mice against the encapsulated antigen.* Vaccine, 2010. **28**(38): p. 6282-91.
104. Vasiliev, Y.M., *Chitosan-based vaccine adjuvants: incomplete characterization complicates preclinical and clinical evaluation.* Expert Rev Vaccines, 2015. **14**(1): p. 37-53.
105. Arca, H.C., M. Gunbeyaz, and S. Senel, *Chitosan-based systems for the delivery of vaccine antigens.* Expert Rev Vaccines, 2009. **8**(7): p. 937-53.
106. Jeon, S.J., et al., *Underlying mechanism of antimicrobial activity of chitosan microparticles and implications for the treatment of infectious diseases.* PLoS One, 2014. **9**(3): p. e92723.
107. Croisier, F. and C. Jérôme, *Chitosan-based biomaterials for tissue engineering.* European Polymer Journal, 2013. **49**(4): p. 780-792.
108. Jabbal-Gill, I., P. Watts, and A. Smith, *Chitosan-based delivery systems for mucosal vaccines.* Expert Opin Drug Deliv, 2012. **9**(9): p. 1051-67.
109. Artursson, P., et al., *Effect of chitosan on the permeability of monolayers of intestinal epithelial cells (Caco-2).* Pharm Res, 1994. **11**(9): p. 1358-61.
110. Sonaje, K., et al., *Opening of epithelial tight junctions and enhancement of paracellular permeation by chitosan: microscopic, ultrastructural, and computed-tomographic observations.* Mol Pharm, 2012. **9**(5): p. 1271-9.

111. Amidi, M., et al., *Chitosan-based delivery systems for protein therapeutics and antigens.* Adv Drug Deliv Rev, 2010. **62**(1): p. 59-82.
112. Xia, Y., et al., *Chitosan-based mucosal adjuvants: Sunrise on the ocean.* Vaccine, 2015. **33**(44): p. 5997-6010.
113. Fernandez-Urrusuno, R., et al., *Enhancement of nasal absorption of insulin using chitosan nanoparticles.* Pharm Res, 1999. **16**(10): p. 1576-81.
114. Vila, A., et al., *Low molecular weight chitosan nanoparticles as new carriers for nasal vaccine delivery in mice.* Eur J Pharm Biopharm, 2004. **57**(1): p. 123-31.
115. Sawaengsak, C., et al., *Chitosan nanoparticle encapsulated hemagglutinin-split influenza virus mucosal vaccine.* AAPS PharmSciTech, 2014. **15**(2): p. 317-25.
116. Liu, Q., et al., *Conjugating influenza a (H1N1) antigen to n-trimethylaminoethylmethacrylate chitosan nanoparticles improves the immunogenicity of the antigen after nasal administration.* J Med Virol, 2015. **87**(11): p. 1807-15.
117. Figueiredo, L., et al., *Intranasal immunisation of mice against Streptococcus equi using positively charged nanoparticulate carrier systems.* Vaccine, 2012. **30**(46): p. 6551-8.
118. Carroll, E.C., et al., *The Vaccine Adjuvant Chitosan Promotes Cellular Immunity via DNA Sensor cGAS-STING-Dependent Induction of Type I Interferons.* Immunity, 2016. **44**(3): p. 597-608.
119. Pawar, D. and K.S. Jaganathan, *Mucoadhesive glycol chitosan nanoparticles for intranasal delivery of hepatitis B vaccine: enhancement of mucosal and systemic immune response.* Drug Deliv, 2016. **23**(1): p. 185-94.
120. Borges, O., et al., *Immune response by nasal delivery of hepatitis B surface antigen and codelivery of a CpG ODN in alginate coated chitosan nanoparticles.* Eur J Pharm Biopharm, 2008. **69**(2): p. 405-16.
121. Ai, W., et al., *Enhanced protection against pulmonary mycobacterial challenge by chitosan-formulated polyepitope gene vaccine is associated with increased pulmonary secretory IgA and gamma-interferon(+) T cell responses.* Microbiol Immunol, 2013. **57**(3): p. 224-35.
122. Lebre, F., et al., *Intranasal Administration of Novel Chitosan Nanoparticle/DNA Complexes Induces Antibody Response to Hepatitis B Surface Antigen in Mice.* Mol Pharm, 2016.
123. Xu, J., et al., *Intranasal vaccination with chitosan-DNA nanoparticles expressing pneumococcal surface antigen a protects mice against nasopharyngeal colonization by Streptococcus pneumoniae.* Clin Vaccine Immunol, 2011. **18**(1): p. 75-81.
124. Oliveira, C.R., et al., *A new strategy based on SmRho protein loaded chitosan nanoparticles as a candidate oral vaccine against schistosomiasis.* PLoS Negl Trop Dis, 2012. **6**(11): p. e1894.
125. Borges, O., et al., *Evaluation of the immune response following a short oral vaccination schedule with hepatitis B antigen encapsulated into alginate-coated chitosan nanoparticles.* Eur J Pharm Sci, 2007. **32**(4-5): p. 278-90.
126. Chen, F., et al., *In vitro and in vivo study of N-trimethyl chitosan nanoparticles for oral protein delivery.* Int J Pharm, 2008. **349**(1-2): p. 226-33.
127. Wang, X., et al., *Intranasal immunization with live attenuated influenza vaccine plus chitosan as an adjuvant protects mice against homologous and heterologous virus challenge.* Arch Virol, 2012. **157**(8): p. 1451-61.
128. Nishimura, K., et al., *Immunological activity of chitin and its derivatives.* Vaccine, 1984. **2**(1): p. 93-9.
129. Koppolu, B. and D.A. Zaharoff, *The effect of antigen encapsulation in chitosan particles on uptake, activation and presentation by antigen presenting cells.* Biomaterials, 2013. **34**(9): p. 2359-69.
130. Smith, A., M. Perelman, and M. Hinchcliffe, *Chitosan: a promising safe and immune-enhancing adjuvant for intranasal vaccines.* Hum Vaccin Immunother, 2014. **10**(3): p. 797-807.

131. McNeela, E.A., et al., *Intranasal immunization with genetically detoxified diphtheria toxin induces T cell responses in humans: enhancement of Th2 responses and toxin-neutralizing antibodies by formulation with chitosan.* Vaccine, 2004. **22**(8): p. 909-14.
132. Huo, Z., et al., *Induction of protective serum meningococcal bactericidal and diphtheria-neutralizing antibodies and mucosal immunoglobulin A in volunteers by nasal insufflations of the Neisseria meningitidis serogroup C polysaccharide-CRM197 conjugate vaccine mixed with chitosan.* Infect Immun, 2005. **73**(12): p. 8256-65.
133. Read, R.C., et al., *Effective nasal influenza vaccine delivery using chitosan.* Vaccine, 2005. **23**(35): p. 4367-74.
134. Mutwiri, G., et al., *Combination adjuvants: the next generation of adjuvants?* Expert Rev Vaccines, 2011. **10**(1): p. 95-107.
135. Garcon, N., P. Chomez, and M. Van Mechelen, *GlaxoSmithKline Adjuvant Systems in vaccines: concepts, achievements and perspectives.* Expert Rev Vaccines, 2007. **6**(5): p. 723-39.
136. Didierlaurent, A.M., et al., *AS04, an aluminum salt- and TLR4 agonist-based adjuvant system, induces a transient localized innate immune response leading to enhanced adaptive immunity.* J Immunol, 2009. **183**(10): p. 6186-97.
137. Ilyinskii, P.O., et al., *Adjuvant-carrying synthetic vaccine particles augment the immune response to encapsulated antigen and exhibit strong local immune activation without inducing systemic cytokine release.* Vaccine, 2014. **32**(24): p. 2882-95.
138. Slutter, B. and W. Jiskoot, *Dual role of CpG as immune modulator and physical crosslinker in ovalbumin loaded N-trimethyl chitosan (TMC) nanoparticles for nasal vaccination.* J Control Release, 2010. **148**(1): p. 117-21.
139. Bal, S.M., et al., *Adjuvanted, antigen loaded N-trimethyl chitosan nanoparticles for nasal and intradermal vaccination: adjuvant- and site-dependent immunogenicity in mice.* Eur J Pharm Sci, 2012. **45**(4): p. 475-81.
140. Vicente, S., et al., *Co-delivery of viral proteins and a TLR7 agonist from polysaccharide nanocapsules: a needle-free vaccination strategy.* J Control Release, 2013. **172**(3): p. 773-81.
141. Dehghan, S., et al., *Rabbit nasal immunization against influenza by dry-powder form of chitosan nanospheres encapsulated with influenza whole virus and adjuvants.* Int J Pharm, 2014. **475**(1-2): p. 1-8.
142. Klas, S.D., et al., *A single immunization with a dry powder anthrax vaccine protects rabbits against lethal aerosol challenge.* Vaccine, 2008. **26**(43): p. 5494-502.
143. Moschos, S.A., et al., *Comparative immunomodulatory properties of a chitosan-MDP adjuvant combination following intranasal or intramuscular immunisation.* Vaccine, 2005. **23**(16): p. 1923-30.
144. Baudner, B.C., et al., *The concomitant use of the LTK63 mucosal adjuvant and of chitosan-based delivery system enhances the immunogenicity and efficacy of intranasally administered vaccines.* Vaccine, 2003. **21**(25-26): p. 3837-44.
145. Baudner, B.C., et al., *Modulation of immune response to group C meningococcal conjugate vaccine given intranasally to mice together with the LTK63 mucosal adjuvant and the trimethyl chitosan delivery system.* J Infect Dis, 2004. **189**(5): p. 828-32.
146. Svindland, S.C., et al., *A study of Chitosan and c-di-GMP as mucosal adjuvants for intranasal influenza H5N1 vaccine.* Influenza Other Respir Viruses, 2013. **7**(6): p. 1181-93.
147. Wang, X., et al., *Interleukin-15 enhance DNA vaccine elicited mucosal and systemic immunity against foot and mouth disease virus.* Vaccine, 2008. **26**(40): p. 5135-44.
148. Yue, Y., et al., *Enhanced resistance to coxsackievirus B3-induced myocarditis by intranasal co-immunization of lymphotactin gene encapsulated in chitosan particle.* Virology, 2009. **386**(2): p. 438-47.

149. Yue, Y., W. Xu, and S. Xiong, *Modulation of immunogenicity and immunoprotection of mucosal vaccine against coxsackievirus B3 by optimizing the coadministration mode of lymphotactin adjuvant.* DNA Cell Biol, 2012. **31**(4): p. 479-88.
150. Chai, D., et al., *Mucosal co-immunization with AIM2 enhances protective SIgA response and increases prophylactic efficacy of chitosan-DNA vaccine against coxsackievirus B3-induced myocarditis.* Hum Vaccin Immunother, 2014. **10**(5): p. 1284-94.
151. Wang, M., et al., *Mucosal immunization with high-mobility group box 1 in chitosan enhances DNA vaccine-induced protection against coxsackievirus B3-induced myocarditis.* Clin Vaccine Immunol, 2013. **20**(11): p. 1743-51.
152. Xing, Y., et al., *Immunogenicity characterization of the multi-epitope vaccine CTB-UE with chitosan-CpG as combination adjuvants against Helicobacter pylori.* Biochem Biophys Res Commun, 2015. **462**(3): p. 269-74.
153. Spinner, J.L., et al., *Methylglycol chitosan and a synthetic TLR4 agonist enhance immune responses to influenza vaccine administered sublingually.* Vaccine, 2015. **33**(43): p. 5845-53.
154. Zaharoff, D.A., et al., *Chitosan solution enhances the immunoadjuvant properties of GM-CSF.* Vaccine, 2007. **25**(52): p. 8673-86.
155. Heffernan, M.J., et al., *In vivo efficacy of a chitosan/IL-12 adjuvant system for protein-based vaccines.* Biomaterials, 2011. **32**(3): p. 926-32.

CHAPTER 2

Development and validation of a spectrophotometric method for quantification of C48/80 associated with particles

This chapter was adapted from:

Bento D, Borchard G, Gonçalves T, Borges O. Validation of a new 96-well plate spectrophotometric method for the quantification of compound 48/80 associated with particles. AAPS PharmSciTech, 2013. 14(2): p. 649-55.

Abstract

A new, simple, inexpensive and rapid 96-well plate UV-spectrophotometric method was developed and validated for the quantification of C48/80 associated with particles. C48/80 was quantified at 570 nm after reaction with acetaldehyde and sodium nitroprusside in an alkaline solution (pH = 9.6). The method was validated according to the recommendations of ICH Guidelines for specificity, linearity, range, accuracy, precision and detection and quantification limits. All the validation parameters were assessed in three different solvents i.e. distilled water, blank matrix of chitosan nanoparticles and blank matrix of chitosan/alginate nanoparticles. The method was found to be linear in the concentration range of 5 μg/mL to 160 μg/mL ($R^2 > 0.9994$). Intra- and inter-day precision was adequate with RSD lower than those given by the Horwitz equation. The mean recoveries of C48/80 from spiked samples ranged between 98.1 % and 105.9 % for calibration curves done with the blank matrices and between 89.3 % and 103.3 % for calibration curves done with water, respectively. The detection limits were lower than 1.01 μg/mL and the quantification limits lower than 3.30 μg/mL. The results showed that the developed method is sensitive, linear, precise and accurate for its intended use with the additional advantage to be cost and time effective, allowing the use of small volume samples and the simultaneous analysis of a large number of samples. The proposed method was successfully applied to evaluate the loading efficacy of C48/80 chitosan-based nanoparticles and can easily be applied during the development of other C48/80 based formulations.

2.1 Introduction

Compound 48/80 (polymer formed from p-Methoxy-n-methyl-phenethylamine monomers) is a mast cell activator that has been widely used in allergies related studies due to its ability to induce the release of histamine [1]. More recently it was demonstrated that C48/80 can also act as a vaccine adjuvant by inducing dendritic cell migration to draining lymph nodes via a mast cell dependent mechanism [2]. In fact, different studies showed that the co-administration of C48/80 with an antigen improves the immunogenicity of the antigen resulting in higher titers of specific antibodies compared to the antigen alone [2-5].

The delivery of C48/80 to target cells could result in an improvement of the adjuvant effect. This can be achieved by the incorporation of the mast cell activator in nanoparticles. The development of a technique to encapsulate C48/80 into particles can only be possible if an efficient method for measurement C48/80 exists, since the evaluation of the loading efficacy of the compound in the delivery system is imperative. To our better knowledge, no method has been described so far for the quantification of C48/80, neither in the supernatant of centrifuged particles nor in any other solvent or matrix. Therefore, to support pharmaceutical formulation development efforts, a method for the measurement of the compound 48/80 needs to be established.

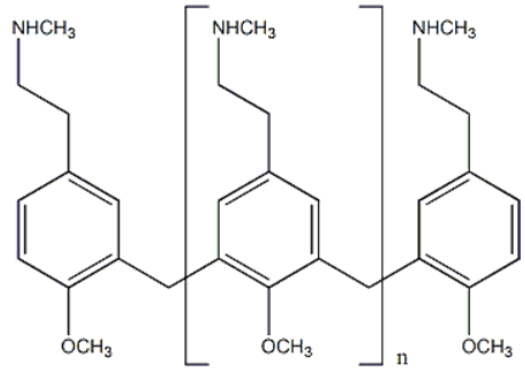

Figure 2.1 – Chemical structure of compound 48/80.

C48/80 is cationic polymer with secondary amine groups produced by the condensation of N-methyl-p-methoxyphenethylamine with formaldehyde [6] (Fig. 2.1). It is known that secondary amines in an alkaline solution react with acetaldehyde and sodium nitroprusside to form a blue-violet compound, a reaction that can be used to quantify secondary amines such as dialkylamines by spectrophotometry [7, 8]. This reaction is also routinely used in forensic laboratories as a preliminary test, called Simon's test, for the qualitative detection of secondary amines used as drugs of abuse, namely 3,4-methylenedixoymethamphetamine (MDMA) and

methamphetamine [9]. Therefore, based on this theoretical hypothesis, a quantitative method for the determination of C48/80 was developed in our laboratory. Optimization of the reaction conditions like concentration of reagents, finding the suitable pH for the formation of the blue-violet compound, reaction time and so on were previously defined as a result of a several experiments in our laboratory. The necessity to evaluate simultaneously an immense number of samples using a small amount of each sample and small amounts of the reagents during the formulation phase of a new C48/80 loaded nanoparticulate delivery systems was the main reason to adapt the method to be performed in 96-well plates. So, here it is described for the first time the optimized protocol for quantification of C48/80 and the validation parameters obtained for three different solvents i.e. distilled water, blank matrix of chitosan nanoparticles and blank matrix of chitosan/alginate nanoparticles. Results of the C48/80 loading efficacy in chitosan-based nanoparticles are reported as a proof of the first application of this simple, reproducible and reliable method.

2.2 Materials and methods

2.2.1 Materials

Compound 48/80 (mixture of low-molecular weight polymers having a degree of polymerization between 3 and 6; mw=153 g/mol (monomer)), sodium nitroprusside dehydrate and acetaldehyde were purchased from Sigma-Aldrich (Sintra, Portugal). LMW chitosan (ChitoClear™) was purchased from Primex Bio-Chemicals AS (Avaldsnes, Norway) and purified as previously described with some modifications [10]. Pharmaceutical grade alginate (MANUCOL LB®) was kindly donated by ISP Technologies Inc. (Surrey, UK). All other reagents were of analytical grade.

2.2.2 Preparation of nanoparticles

Chitosan/alginate particles were prepared using a method described elsewhere [11] with slight modifications introduced. Briefly, a $CaCl_2$ solution 2 mg/mL was added to a 0.063 % (w/v) sodium alginate solution while stirring in order to prepare a pre-gel. The particles were formed upon mixing the pre-gel and 0.05 % (w/v) chitosan solution by high-speed vortexing.

The second delivery system, chitosan particles, was prepared adding a solution 2 mg/mL of Na_2SO_4 dropwise to a 0.1 % chitosan solution. C48/80 loaded chitosan/alginate and chitosan particles were obtained by addition of the compound to chitosan and Na_2SO_4 solutions, respectively, in each preparation method. Subsequently, particles were isolated by centrifugation for 20 min at 12450 g and the supernatants collected. The supernatants of

C48/80 unloaded chitosan and chitosan/alginate particles were used as solvents for establishment of the calibration curve, here named blank matrices. The method for C48/80 quantification was validated using these blank matrices.

2.2.3 Quantification of the C48/80 by UV spectrophotometry

The method was primarily developed in our laboratory to quantify C48/80 in diluted aqueous solutions. Subsequently, the method was applied and validated to quantify C48/80 in samples obtained by the centrifugation of C48/80 loaded particles. In a 96-well plate, 25 µL of 0.85 M carbonate buffer pH = 9.6 were added to 175 µL of sample. Then 50 µL of a 15 % acetaldehyde solution containing 1.5 % of sodium nitroprusside was added and mixed by means of a plate shaker for 30 s. The absorbance was measured after 10 min at 570 nm in a Multiskan EX 96-well plate reader ((Thermo Electron Corporation, Vantaa, Finland).

2.2.4 Calibration curve

One stock solution of 2 mg/mL of compound 48/80 was prepared in distilled water or in the supernatants of unloaded particles. The standards for the calibration curve were prepared using the stock solution as described below (linearity and range).

2.2.5 Analytical method validation

The method was validated according to the recommendations of ICH Guideline Q2(R1) [12] in order to evaluate the specificity, linearity, range, accuracy, precision and finally the detection and quantification limits of the method.

2.2.5.1 Specificity

The supernatants obtained after centrifugation of C48/80 loaded particles will have some unreacted compounds that result from particle production that may possibly interfere with the quantification method. The use of blank matrices (supernatant of unloaded nanoparticles prepared under the same conditions), will more likely simulate the solvent of our sample of interest. Therefore, C48/80 at a concentration of 80 µg/mL was prepared in distilled water and in supernatant of both unloaded chitosan and chitosan/alginate particles and analyzed at a wavelength of 570 nm (n=9) according to the described method. The means of the resultant absorbance values were compared by student's t-test at 95 % confidence level.

2.2.5.2 Linearity and Range

For the determination of linearity, seven different concentrations of C48/80 were prepared from the stock solution and analyzed. The stock solution of C48/80 was prepared in distilled water at the concentration of 2 mg/mL and the calibration standards were prepared by diluting the stock solutions to 5, 10, 20, 40, 80, 120 and 160 μg/mL. In a similar way, the calibration curves were prepared using the supernatants of chitosan and chitosan/alginate unloaded particles. The linearity of the method in the proposed range was evaluated by least square regression analysis. The linearity and range of the proposed methods were evaluated in three independent experiments.

2.2.5.3 Accuracy

The accuracy of the proposed method was investigated by spiking the supernatants of unloaded particles with known concentrations of C48/80 at 3 different levels (lower, intermediate and higher concentration) corresponding to C48/80 final concentrations of 10, 80 and 160 μg/mL (n=6), respectively. The % recovery of the added compound was calculated using equation 2.1.

$$\text{Recovery (\%)} = \frac{\text{Concentration measured}}{\text{Concentration added}} \text{x } 100 \quad \text{(Equation 2.1)}$$

2.2.5.4 Precision

The intra-day precision was evaluated by measuring different levels of C48/80 concentration (10, 80 and 160 μg/mL) in triplicates at the same day under the same experimental conditions. The inter-day precision was evaluated following the same procedure for the 3 different days (n=9). The precision of the measurements was reported as relative standard deviation (% RSD).

2.2.5.5 Detection and quantification limits

Detection limit (DL) and quantification limit (QL) were determined based on the standard deviation of the response and on the slope of the calibration curve, according to equation 2.2 and equation 2.3, respectively:

$$\text{DL} = \frac{3.3\ \sigma}{\text{S}} \quad \text{(Equation 2.2)}$$

$$QL = \frac{10\,\sigma}{S} \quad \text{(Equation 2.3)}$$

Where S is the slope of the calibration curve and σ is the standard deviation of y-intercept of the regression equation (n=9).

2.2.6 Application of the method

The developed method was applied for the determination of C48/80 loading efficacy in chitosan and chitosan/alginate particles. Compound 48/80 loaded particles were prepared as described above and the supernatant collected by centrifugation. C48/80 loading efficacy (LE) was determined by an indirect way, quantifying the C48/80 not associated with particles (in the supernatant) using the equation 2.4.

$$LE\ (\%) = \frac{\text{total}_{C48/80}\ (\mu g/mL) - \text{free}_{C48/80}\ \text{in supernatant}\ (\mu g/mL)}{\text{total}_{C48/80}\ (\mu g/mL)}\ x\ 100 \quad \text{(Equation 2.4)}$$

The supernatants of unloaded particles were used as solvents for the calibration curve. Blank matrix of chitosan/alginate particles was used for the determination of C48/80 LE in chitosan/alginate particles and the blank matrix of chitosan particles was used for the C48/80 LE assessment in chitosan particles.

2.2.7 Statistical analysis

All data analyses described above were done using GraphPad Prism v 5.03 (GraphPad Software Inc., La Jolla, CA, USA).

2.3 Results and discussion

Microplate readers detect and process biological and chemical data using absorbance, luminescence and fluorescence for a great number of samples simultaneously. Microplate readers using absorbance (UV-Vis) are widely used in laboratories because the reagents used in protocols are less expensive, when compared to fluorescence or luminescence detection. For that reason, the first-line detection method is the determination of absorbance, and frequently, the protocols indicate the utilization of 96-well plates as a physical support to measure simultaneously 96 small-volume samples (maximum volume around 250 μL). What appears to be a detail constitutes an important and decisive advantage of the microplate readers over conventional spectrophotometer protocols. Examples of standard protocols, which are

routinely used in laboratories using microplate readers, with absorbance as the detection method, are protocols for nucleic acids, enzyme activity and protein quantification. In this paper, we describe the validation of a spectrophotometric method, using 96-well plate, for the quantification of C48/80. The method was also validated for samples obtained by centrifugation of freshly prepared C48/80 loaded particles. During the development of this method the effect of several parameters was evaluated by modifying one parameter and maintaining the others unchanged. Factors such as reaction time, concentration of the acetaldehyde or the sodium nitroprusside and buffer solution characteristics were studied and the most favourable conditions established and followed on validation experiments. The optimal pH for the reaction was described elsewhere [8] as to be between 9.6 and 10.2. We found that the pH is the most critical factor and the selected carbonate buffer should be freshly prepared (once weekly). The samples were measured 10 min after the formation of C48/80-acetaldehyde-sodium nitroprusside complex. During this period there is no need to concern about the light-sensitivity. Similar to the BCA-protein assay, this reaction does not reach a true end-point, so colour development will continue after the recommended measurement time. Finally, the observation of the correct storage of acetaldehyde is also a critical factor. It should be stored under an inert atmosphere since aldehyde oxidation easily occurs, which would compromise the final colour development.

2.3.1 Specificity

The assay was performed with C48/80 solutions at 80 μg/mL in order to confirm the suitability of the method to unequivocally determine the concentration of C48/80 in the presence of other components that may be present (for example, compounds that were not incorporated during the preparation of the particles or compounds that were released after particle preparation). The statistical treatment of the results showed that the calculated t-values were higher than the tabulated t-values indicating that there are statistical differences between the mean absorbance of the C48/80 in water or in the presence of the nanoparticle constituents (table 2.1). These differences are possibly related to the interaction of the matrix components with C48/80 affecting the results measured. In order to minimize the interference of other constituents present in the formulations, all validation parameters were evaluated not only with distilled water but also with the supernatants of unloaded chitosan and chitosan/alginate nanoparticles. So, the suitability of these matrices as solvents for C48/80 quantification could be assessed.

Table 2.1 – Statistical data of the regression equations and resume of validation parameters for compound 48/80 (n=9).

Parameter	H_2O	Chi NP supernatant	Chi/Alg NP supernatant
Optical characteristics			
Molar absorptivity, λ =570 nm (l mol^{-1} cm^{-1})[a]	122.10	99.14	113.78
Regression analysis (n=9)			
Slope	0.005197 ± 3.124 $x10^{-5}$	0.005267 ± 5.733 $x10^{-5}$	0.005269 ± 4.455e-005
95% confidence interval of slope	0.005116 to 0.005277	0.005119 to 0.005414	0.005155 to 0.005384
Intercept	0.009681 ± 0.002601	- 0.0008062 ± 0.004773	0.00022210 ± 0.003710
95% confidence interval of intercept	0.005186 to 0.01214	- 0.01308 to 0.01147	-0.009315 to 0.009759
Regression coefficient (R2)	0.9998	0.9994	0.9996
SD of the residuals (sy.x)	0.00458	0.008405	0.006532
Validation parameters			
Specificity, tcal (tcrit)[b]		20.58 (2.12)	5.887 (2.12)
Linearity (µg/mL)	5 -160	5 - 160	5 - 160
Detection Limit (µg/mL)	0.93	0.71	1.01
Quantification limit (µg/mL)	2.80	2.15	3.30

[a] Molar absorptivity for the monomer of C48/80, MW = 153 g/mol

[b] T-test comparing absorbance in supernatant of unloaded nanoparticles to absorbance values in distilled water. t_{cal} is the calculated t-value and t_{crit} is the tabulated t- value based on unpaired t-test at $\alpha = 0.05$ level of significance.

2.3.2 Linearity and range

According to the results of the regression analysis (table 2.1), the method was found to be linear over the concentration range of 5 µg/mL to 160 µg/mL for the three matrices used at good correlation coefficients (0.9994 to 0.9998) (Fig. 2.2). The goodness of fit of the regression equations was supported by the low standard deviations of the residuals (table 2.1).

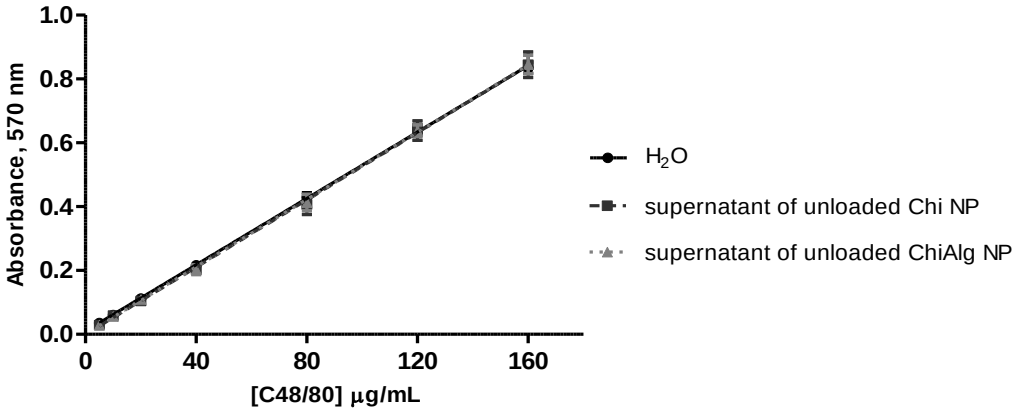

Figure 2.2 – Calibration curves obtained with C48/80 standard solutions in water and in supernatant of unloaded nanoparticles using the purposed spectrophotometric method (n =9).

2.3.3 Accuracy

Accuracy was assessed by the recovery of the C48/80 added as a spike into the supernatant of unloaded nanoparticles. In order to evaluate the effect of the matrix, the percentage of recovery was assessed by two methods, using the calibration curve done with distilled water and the calibration curve in the correspondent supernatant of unloaded particles. The mean values of the % recovery for each concentration level of C48/80 are shown in table 2.2.

Table 2.2 – Results of recovery (%) for compound 48/80 from spiked samples (n=6).

Sample	Method	C48/80 added (μg/mL)	Measured Concentration (μg/mL) ± SD	% Recovery ± SD	Confidence interval 95%	RSD %
Chi NP	water	10	10.09 ± 1.09	100.95 ± 10.86	± 8.69	10.76
		80	71.45 ± 3.52	89.31 ± 4.40	± 3.52	4.92
		160	148.86 ± 10.02	93.04 ± 4.40	± 5.01	6.73
	NP supernatant	10	10.59 ± 0.90	105.9 ± 9.02	±7.22	8.52
		80	79.92 ± 1.25	101.50 ± 3.49	±2.80	3.44
		160	161.42 ± 1.42	100.88 ± 0.89	± 0.71	0.88
Chi/Alg NP	water	10	9.68 ± 0.59	96.84 ± 5.88	± 4.71	6.08
		80	82.66 ± 1.06	103.32 ± 1.33	± 1.06	1.28
		160	159.13 ± 1.29	99.45 ± 0.81	± 0.65	0.81
	NP supernatant	10	10.12 ± 1.07	101.30 ± 10.76	± 8.61	10.62
		80	80.62 ± 4.27	100.78 ± 4.34	± 4.28	5.30
		160	156.89 ± 2.44	98.05 ± 1.53	± 1.22	1.56

For chitosan particle supernatants, mean recoveries of 89.31 % to 100.95 % and 100.88 % to 105.90 % were found, calculated applying the calibration curve prepared in water and in particle supernatant, respectively. In chitosan/alginate particle supernatant, recoveries of the C48/80 were 96.84 % to 103.32 % and 98.05 % to 101.30 % for determinations with calibration curve in water and in particle supernatants, respectively. When the calibration curve in water is used for the determination of the percentage of C48/80 recovery in chitosan particle supernatants, the mean recovery values obtained for concentrations of 80 μg/mL and 160 μg/mL (89.31 % and 93.04 %, respectively) are out of the suggested acceptable range often considered to be between 98 % and 101 %. However, when using the calibration curve in the supernatant of unloaded particles, the mean recovery values (Table 2.3) were within the acceptable range [13] and % RSD values were lower than the recommended values predicted from the Horwitz equation (Table 2.3 adapted from [14]).

Table 2.3 – Summarize of acceptance criteria for RSD according to Horwitz equation (% RSD = 2 (1 - 0.5 logC)) and for mean recovery (%) for each one of concentration levels assayed.

[Analyte] µg/mL	Analyte %	Analyte ratio	Horwitz % RSD	Mean recovery (%)
10	0.001	1.00E - 05	< 11.3	80 – 110
80	0.008	8.00E - 05	< 8.3	90 – 107
160	0.016	1.60E - 04	< 7.5	95 – 105

2.3.4 Precision

The precision of the proposed method was evaluated by the assessment of the repeatability (intra-day) and intermediate precision (inter-day). The precision was evaluated in three different matrices: distilled water, unloaded chitosan particle supernatant and unloaded chitosan/alginate particle supernatant. The results are shown in table 2.4, 2.5 and 2.6, respectively.

Table 2.4 – Intra-day and inter-day precision results for the method using water as the solvent.

Standard solution (µg/mL)	Day	Measured (µg/mL)	SD	RSD %	Confidence Interval 95 %
Intra-day variation (n=3)					
10	1	9.52	0.34	3.57	0.38
	2	9.60	0.69	7.23	0.78
	3	10.36	0.68	6.56	0.77
80	1	80.89	1.22	1.51	1.39
	2	79.34	1.61	2.03	1.83
	3	81.62	1.28	1.57	1.45
160	1	160.82	1.18	0.73	1.34
	2	156.26	0.44	0.28	0.50
	3	159.04	0.68	0.43	0.77
Inter-day (n=9)					
10		9.83	0.66	6.67	0.43
80		80.62	1.57	1.94	1.02
160		158.71	2.12	1.33	1.38

The repeatability refers to the precision of the method carried out under the same operating conditions over a short interval of time. For the three analytical methods, repeatability (RSD) ranged from 1.62 % to 7.48 % at 10 µg/mL concentration level of C48/80, from 0.98 % to 2.09 % at 80 µg/mL and from 0.28 % to 1.10 % at 160 µg/mL. The intermediate precision hints at within-laboratory variation and was evaluated using the same method on identical test samples in the same laboratory and equipment but on different days. Intermediate precision (RSD) ranged from 4.43 % to 7.08 %, from 1.94 % to 3.59 % and

from 0.58 % to 1.33 %, at lower, intermediate and higher concentration levels, respectively. RSD values (%) found for the three analytical methods were within the acceptable range indicating that these methods have good repeatability and intermediate precision.

Table 2.5 – Intra-day and inter-day precision results for the method using the supernatant of unloaded Chi NP as the solvent.

Standard solution (µg/mL)	Day	Measured (µg/mL)	SD	RSD	Confidence Interval 95%
Intra-day variation (n=3)					
10	1	11.35	0.85	7.48	0.96
	2	11.23	0.18	1.62	0.21
	3	11.25	0.65	5.78	0.74
80	1	75.98	0.89	1.17	1.01
	2	75.17	0.73	0.98	0.83
	3	80.88	1.39	1.72	1.57
160	1	161.56	0.51	0.32	0.58
	2	159.72	1.00	0.63	1.13
	3	160.32	1.18	0.73	1.33
Inter-day (n=9)					
10		11.88	0.53	4.43	0.34
80		77.53	2.78	3.59	1.82
160		160.40	0.93	0.58	0.61

Table 2.6 – Intra-day and inter-day precision result for the method using the supernatant of unloaded Chi/Alg NP was the solvent.

Standard solution (µg/mL)	Day	Measured (µg/mL)	SD	RSD	Confidence Interval 95%
Intra-day variation (n=3)					
10	1	9.84	0.38	3.85	0.43
	2	11.01	0.48	4.40	0.55
	3	11.05	0.69	6.23	0.78
80	1	82.16	1.03	1.26	1.17
	2	76.84	1.50	1.95	1.70
	3	78.10	1.63	2.09	1.85
160	1	158.64	0.73	0.46	0.83
	2	162.40	1.79	1.10	2.02
	3	160.00	1.68	1.05	1.90
Inter-day (n=9)					
10		10.63	0.75	7.08	0.49
80		79.04	2.70	3.42	1.77
160		160.42	2.12	1.32	1.39

2.3.5 Detection and Quantification limits

The DL and QL for C48/80 in water were 0.93 μg/mL and 2.80 μg/mL, respectively. In the supernatant of unloaded chitosan particles the detection and quantification limits were found to be 0.71 μg/mL and 2.15 μg/mL and in the supernatant of unloaded chitosan/alginate particles 1.01 μg/mL and 3.30 μg/mL, respectively. These values indicate that the method is sufficiently sensitive to evaluate the concentration of the C48/80 in the supernatants of particles and so, indirectly, the extent of incorporation of the mast cell activator in the delivery systems.

2.3.6 Application of the method

The proposed method was applied to determine the C48/80 loading efficacy into two chitosan based delivery systems – chitosan particles and chitosan/alginate particles. Recovery studies revealed that the method was more accurate when utilizing the blank matrices of the particles to establish the calibration curve to evaluate the amounts of C48/80 present in the particle supernatants. Since the quantification method in supernatants of unloaded nanoparticles was found to be linear, precise, sensitive and accurate for the determination of C48/80, these matrices were used instead of distilled water for the quantification of C48/80 in the supernatant of loaded particles. C48/80 loading efficacy was found to be 18.65 ± 2.99 % for chitosan particles and 29.56 ± 1.59 % for chitosan/alginate particles (mean ± SD; $n \geq 12$).

2.4 Conclusions

An inexpensive, rapid, sensitive, precise and accurate small-volume UV spectrophotometric method for the determination of C48/80 was developed and validated. The simplicity of the method and the small amounts of sample and solvents required make this method attractive for C48/80 quantification in pharmaceutical dosage forms. When applied to quantification of C48/80 in chitosan based particles, a small effect of the other particle components was observed but was compensated by using the supernatants of unloaded formulations to establish the calibration curve. We could demonstrate that the developed method is accurate for the quantification of C48/80 in the samples of interest and so sufficient specificity of the method can be concluded [15]. The observed matrix effect supports the possible need for partial method revalidation when samples in different matrices are used, as specified in different validation guidelines [12, 16, 17]. The proposed method was already successfully applied for the determination of C48/80 incorporated into two chitosan based delivery

systems and would be useful during the development and characterization of other C48/80 formulations.

References

1. Rothschild, A.M., *Mechanisms of histamine release by compound 48-80.* Br J Pharmacol, 1970. **38**(1): p. 253-62.
2. McLachlan, J.B., et al., *Mast cell activators: a new class of highly effective vaccine adjuvants.* Nat Med, 2008. **14**(5): p. 536-41.
3. Staats, H.F., et al., *Mucosal targeting of a BoNT/A subunit vaccine adjuvanted with a mast cell activator enhances induction of BoNT/A neutralizing antibodies in rabbits.* PLoS One, 2011. **6**(1): p. e16532.
4. McGowen, A.L., et al., *The mast cell activator compound 48/80 is safe and effective when used as an adjuvant for intradermal immunization with Bacillus anthracis protective antigen.* Vaccine, 2009. **27**(27): p. 3544-52.
5. Wang, S.H., et al., *Stable dry powder formulation for nasal delivery of anthrax vaccine.* J Pharm Sci, 2012. **101**(1): p. 31-47.
6. Paton, W.D., *Compound 48/80: a potent histamine liberator.* Br J Pharmacol Chemother, 1951. **6**(3): p. 499-508.
7. Lin, C.M. and C. Wagner, *Quantitative determination of secondary amines: measurement of N-methylalanine.* Anal Biochem, 1974. **60**(1): p. 278-84.
8. Cullis, C.F. and D.J. Waddington, *The colorimetric determination of secondary amines.* Analytica Chimica Acta, 1956. **15**(0): p. 158-163.
9. O'Neal, C.L., D.J. Crouch, and A.A. Fatah, *Validation of twelve chemical spot tests for the detection of drugs of abuse.* Forensic Sci Int, 2000. **109**(3): p. 189-201.
10. Gan, Q. and T. Wang, *Chitosan nanoparticle as protein delivery carrier--systematic examination of fabrication conditions for efficient loading and release.* Colloids Surf B Biointerfaces, 2007. **59**(1): p. 24-34.
11. Rajaonarivony, M., et al., *Development of a new drug carrier made from alginate.* J Pharm Sci, 1993. **82**(9): p. 912-7.
12. *ICH Harmonized Tripartite Guideline, Validation of Analytical Procedures: Text and Methodology Q2(R1)*2005.
13. Huber, L., ed. *Validation and Qualification in Analytical Laboratories*. 2nd ed. 2007, Informa Healthcare: New York.
14. Taverniers, I., M. De Loose, and E. Van Bockstaele, *Trends in quality in the analytical laboratory. II. Analytical method validation and quality assurance.* TrAC Trends in Analytical Chemistry, 2004. **23**(8): p. 535-552.
15. Ermer, J., et al., *Performance Parameters, Calculations and Tests*, in *Method Validation in Pharmaceutical Analysis*2005, Wiley-VCH Verlag GmbH & Co. KGaA. p. 21-194.
16. Michael Thompson, S.E., Roger Wood, *Harmonized guidelines for single-laboratory validation of methods of analysis (IUPAC Technical Report)*, 2002, International Union of Pure and Apllied Chemistry Pure and Applied Chemistry. p. 835-855.
17. *The Fitness for Purpose of Analytical Methods: A Laboratory Guide to Method Validation and Related Topics*, 1998, Eurachem: www.eurachem.org/guides/pdf/valid.pdf

CHAPTER 3

Development, characterization and preliminary evaluation of C48/80 loaded chitosan nanoparticles

Abstract

Current vaccine research is mostly based on subunit antigens instead of traditional whole-cells vaccines. Despite the better toxicity profile of these antigens, they are often poorly immunogenic requiring the concomitant use of adjuvants to improve the immune response to the vaccine. According to this need, the combination of adjuvants has been explored as a strategy to obtain a potent vaccine formulation. Recently, mast cell activators were recognized as a new class of vaccine adjuvants capable of potentiate mucosal and systemic immune responses. In this study a new co-adjuvanted delivery system was developed and characterized, combining the mast cell activator C48/80 with chitosan nanoparticles. C48/80 loaded chitosan nanoparticles were evaluated and the results compared with the plain chitosan nanoparticles. The adsorption of model antigens on the nanoparticles surface as well as the biocompatibility of the system was not affected by the incorporation of C48/80 in the formulation. The stability of the nanoparticles was demonstrated by studying the variation of size and zeta potential at different times and after lyophilization, and the ability to be internalized by antigen presenting cells was confirmed by confocal microscopy. The results suggested that C48/80 can be efficiently incorporated in chitosan nanoparticles without affecting the properties of the polymer confirming the feasibility of formulating a co-adjuvanted vaccine delivery system consisting of chitosan nanoparticles and C48/80.

3.1 Introduction

Traditional vaccines consisting of live attenuated or inactivated pathogens are highly immunogenic but, due to safety concerns, development of new vaccines is being focused on the use of recombinant subunit antigens. Recombinant antigens are safer but they are often poorly immunogenic requiring the use of vaccine adjuvants to enhance the resultant immune response. Therefore, different adjuvant approaches have been studied to enhance and/or modulate vaccine response to subunit antigens. Among them is the use of nanotechnology, a strategy that has been extensively explored and holds great promise [1, 2]. Formulation of antigen in nanoparticles may offer several attractive features, namely: enhanced uptake by antigen presenting cells (APCs) [3], depot effect with gradual release of the antigen [2, 4], cross-presentation of antigens [2, 5], slower antigen processing than antigen in solution, which can result in a prolonged antigen presentation [6] and co-deliver of antigens and adjuvants to the same cell population [1]. Besides, particulate antigens are generally more immunogenic than soluble antigens [7] and can be used to modulate the type of immune response [2]. Different nano-sized platforms such as virus-like particles, liposomes, immune stimulating complexes (ISCOMs), nanoemulsions and polymeric nanoparticles have been explored as potential vaccine delivery systems. Chitosan and its derivatives are among the most studied compounds for development of polymeric vaccines [8, 9] because of their attractive characteristics for biomedical applications. Chitosan is a biocompatible, biodegradable and non-toxic polysaccharide [10], obtained from deacetylation of chitin, consisting of β-(1-4)-linked D-glucosamine and N-acetyl-D-glucosamine monomer units. Its cationic nature, mucoadhesivity and immunostimulating properties [8] make it an attractive polymer, particularly for the design of nanoparticulate vaccines for mucosal delivery.

Despite the potential of nanoparticles as vaccine adjuvants, it is possible to obtain a more potent adjuvant formulation by association with immunopotentiators. In fact, the concept of concomitant delivery of antigens and immunostimulatory molecules through delivery systems gained increased attention and has been appointed as a promising approach in vaccine development [1, 11, 12].

Mast cells (MC), strategically located at the host-environment, have been recognized in recent years as important players in the development of protective immune responses [13-15] and the use of mast cell activators as a new class of vaccine adjuvants began to be explored [16]. Since then, additional studies confirmed the immunopotentiator properties of the mast cell activator compound 48/80 (C48/80) [17-19]. In this study, we explore the feasibility of combining the mast cell activator with chitosan nanoparticles to prepare a new adjuvant

formulation for nasal vaccination. The strategy proposed here could be advantageous because, while chitosan would extend the residence time of the antigen on the administration local, MC activation would promote a local environment favorable to the development of an immune response. Since the lack of knowledge of how to formulate more complex adjuvant systems combining immunopotentiators and delivery systems is appointed has one of the biggest obstacles for vaccine development [20], the publication of novel methodologies for the preparation of these co-adjuvanted formulations is of utmost importance. These approaches would allow other researchers to have access to a broader range of adjuvants to test as vaccine candidates. Considering this, the present chapter describes the design and characterization of a novel co-adjuvanted formulation consisting of chitosan nanoparticles associated with the mast cell activator C48/80. Stability, biocompatibility and uptake by macrophages of the obtained nanoparticles were assessed *in vitro*.

3.2 Materials and Methods

3.2.1 Materials

A low molecular weight Chitosan (deacetylation degree 95 %) was purchased from Primex BioChemicals AS (Avaldsnes, Norway). Compound 48/80, bovine serum albumin (BSA), MTT (3-[4, 5-dimethylthiazol-2-yl]-2,5-diphenyl tetrazolium bromide), albumin-fluorescein isothiocyanate conjugate (FITC-BSA), trehalose, Dulbecco's modified Eagle medium (DMEM) and RPMI 1640 were obtained from Sigma-Aldrich (Sintra, Portugal). Bicinchoninic acid (BCA) assay kit and micro BCA kits were obtained from Pierce Chemical Company (Rockford, IL, USA). FITC was purchased to Santa Cruz Biotechnology (Santa Cruz, CA, USA). Fetal bovine serum (FBS), Wheat Germ Agglutinin Alexa Fluor® 350 Conjugate and Lysotracker® Red DND 99 were obtained from Life Technologies Corporation (Paisley, UK). All other reagents used were of analytical grade.

3.2.2 Chitosan purification

Chitosan was purified by a method described elsewhere [21] with slight modifications. Briefly, 1 g of chitosan was suspended in 10 mL of 1 M NaOH, and stirred for 3 h at 50 °C. The mixture was then filtered (0.45 μm membrane, Millipore), and the resultant pellet washed with 20 mL of water. The recovered chitosan was dissolved in 200 mL of 1 % (v/v) acetic acid solution and stirred for 1 h. The solution was filtered (0.45 μm membrane) and 1 M NaOH was used to adjust the filtrate to pH 8.0, resulting in purified chitosan in the form of

precipitates. Purified chitosan was freeze-dried for 48 h with a Labconco freeze-dryer, model 77530 (Labconco, Kansas City, USA) equipment.

3.2.3 Characterization of the purified chitosan by FTIR

The FTIR spectra of purified and non-purified chitosan were recorded using an FTIR spectrometer (Spectrum 400, PerkinElmer) with attenuated total reflection (ATR) top-plate accessory. The instrument operated with a resolution 2 cm^{-1} and 30 scans were collected for each sample. Spectra were recorded between 650 cm^{-1} and 4000 cm^{-1}.

3.2.4 Preparation of C48/80 loaded chitosan nanoparticles

C48/80 loaded chitosan nanoparticles (Chi-C48/80 NP) were prepared by adding dropwise 3 mL of an alkaline solution (5 mM NaOH) of C48/80 and Na_2SO_4 (0.3 mg/mL and 2.03 mg/mL, respectively) to 3 mL of a chitosan solution (1 mg/mL in acetic acid 0.1 %) under high-speed vortexing. The nanoparticles were formed after further maturation for 60 min under magnetic stirring. Blank chitosan particles (Chi NP) were obtained by preparing nanoparticles exactly in the same conditions but without C48/80.

To evaluate the stability after freeze-drying, nanoparticles were lyophilized with 1 %, 2.5 % or 5 % of trehalose as cryoprotectant. All samples were lyophilized for 48 h with a Labconco freeze-dryer, model 77530 (Labconco, Kansas City, USA), at – 50 ºC and 100 mbar.

3.2.5 Characterization of nanoparticles

3.2.5.1 Size and Zeta Potential

Particle size was measured by dynamic light scattering (DLS) using a Delsa™ Nano C (Beckman Coulter). Samples were diluted in milli-Q water and analyzed at a detection angle of 160° and a temperature of 25 °C. Zeta potential was measured by electrophoretic light scattering, after dispersion of the nanoparticles in a solution of 1 mM NaCl.

3.2.5.2 Morphology

Particle morphology was evaluated by scanning electron microscopy (SEM) in a FEI Quanta 400 FEG ESEM (USA). One drop of nanoparticle suspension was mounted on microscope stub using a double-stick carbon tape and let to dry overnight. Prior to image acquisition, samples were coated with gold.

3.2.5.3 Quantification of C48/80 loading efficacy

In order to evaluate the loading efficacy (LE) of C48/80, nanoparticles were centrifuged 20 min at 8000 g and C48/80 was quantified in the supernatant using the method described in chapter 2. Briefly, 25 µL of carbonate buffer pH 9.6 was added to 175 µL of sample in a 96-well plate. Subsequently, 50 µL of a 15 % acetaldehyde solution containing 1.5 % of sodium nitroprusside was added and the absorbance measured at 570 nm. The loading efficacy was calculated according to equation 3.1.

$$\text{C48/80 LE (\%)} = \frac{\text{total C48/80 (µg/mL)} - \text{free C48/80 in supernatant (µg/mL)}}{\text{total C48/80 (µg/mL)}} \text{ x 100 (Equation 3.1)}$$

3.2.5.4 FTIR analysis

FTIR analysis of lyophilized Chi NP and Chi-C48/80 NP was performed according to the described in section 2.3.

3.2.6 Stability studies

The short term stability of freshly prepared nanoparticle suspensions stored either at 4 ºC or at room temperature (RT) was studied for a period of 15 days. Size, polydispersity index (PI) and zeta potential of 3 independent batches of Chi-C48/80 NP and Chi NP were measured. Samples were withdrawn and characterized at days 0, 3, 5 and 15.

The stability of lyophilized Chi-C48/80 NP was also investigated after storage for a period of 4 months at RT. At the end of the test period, samples were resuspended in milli-Q water, NPs were characterized and the parameters were compared to the values before lyophilization.

3.2.7 Evaluation of loading efficacy and loading capacity of model antigens

Loading of model antigens on nanoparticle surface was made by physical adsorption. Nanoparticles were centrifuged for 30 min at 4500 g and resuspended in acetate buffer pH 5.7, 25 mM. Nanoparticles at a final concentration of 2.5 mg/mL were incubated with BSA, ovalbumin (OVA) or myoglobin in acetate buffer for 60 min at RT. Ratios from 7:1 to 1:1 (NP:protein) were tested for BSA while OVA and myoglobin were incubated at a fixed weight ratio of 7:1. After incubation, particles were centrifuged at 12000 g for 20 min and the supernatant collected. The amount of protein loaded on nanoparticles was determined indirectly by measuring the concentration of non-bound protein in the nanoparticle supernatant using the BCA or Micro-BCA protein assay (Pierce, Thermo Scientific) according

to the manufacturer's instructions. Loading efficacy (LE) and loading capacity (LC) were determined by the equation 3.2 and equation 3.3, respectively.

$$\text{LE (\%)} = \frac{\text{total amount of BSA - non bound BSA}}{\text{total amount of BSA}} \times 100 \text{ (Equation 3.2)}$$

$$\text{LC (\%)} = \frac{\text{total amount of BSA - non bound BSA}}{\text{weight of nanoparticles}} \times 100 \text{ (Equation 3.3)}$$

3.2.8 *In vitro* cytotoxicity studies

Single cell suspensions of spleen cells from 8-week old female C57BL/6 mice (Charles River) were prepared according to a method previously described [22]. Cells were seeded in a 96-well plate at a density of 1 x 10^6 cells/well in complete RPMI 1640 medium (supplemented with 10 % fetal bovine serum, 2 mM glutamine, 1 % Penicillin/Streptomycin and 20 mM HEPES) and incubated with together with different concentrations of nanoparticles. After 24 h of incubation, cellular viability was assessed by MTT assay. Briefly, 20 µL of MTT 5 mg/mL in PBS 7.4 was added to each well and incubated for more 4 h. The plate was centrifuged for 25 min, at 800 g and the supernatants removed. Finally, the formazan crystals produced by viable cells were solubilized with 200 µL of DMSO per well and the optical density values were measured at 540 nm with 630 nm as wavelength reference. The viability of non-treated cells (culture medium only) was defined as 100 % and the relative cell viability calculated using the equation 3.4.

$$\text{Cell viability (\%)} = \frac{\text{OD sample (540 nm) - OD sample (630 nm)}}{\text{OD control (540 nm) - OD control (630 nm)}} \text{ x } 100 \text{ (Equation 3.4)}$$

3.2.9 Particle uptake by macrophages

FITC labeled NPs were prepared by the method described in 2.4 using FITC-labeled chitosan. The synthesis of FITC-labeled chitosan was based on the reaction between the isothiocyanate group of FITC (Ex/Em – 490/525) and the primary amino group of chitosan. Briefly, chitosan was labeled by mixing 35 mL of dehydrated methanol containing 25 mg of FITC to 25 mL of a 1 % (w/v) chitosan in 0.1 M acetic acid. After 3 h of reaction in the dark at RT, the FITC-labeled chitosan was precipitated with 0.2 M NaOH until pH 10. FITC-labeled chitosan was obtained by centrifugation for 30 min at 4500 g and the resultant pellet was washed 3 times with a mixture of methanol:water (70:30, v/v). The labeled chitosan was resuspended in 15 mL of 0.1 M acetic acid and stirred overnight. Polymer solution was

dialyzed in the dark against 2.5 L of distilled water for 3 days before freeze-drying using a freeze dry system (FreezeZone 6, Labconco, Kansas City, MO, US).

The ability of nanoparticles to be internalized by antigen presenting cells was assessed on the mouse macrophage cell line RAW 264.7 (ECACC, Salisbury, UK). Cells were maintained in Dulbecco's modified Eagle medium (DMEM, Sigma) supplemented with 1 mM HEPES, 1 mM sodium pyruvate and 10 % of non-inactivated FBS. To evaluate the uptake of nanoparticles, RAW 264.7 cells were seeded on glass coverslips in 12-well plates at a density of 2.5 x 10^5 cells per well and cultured at 37 ºC in 5 % CO_2 overnight. On the next day, RAW 264.7 were pre-labeled with 300 nM Lysotracker® Red DND 99 (Ex/Em - 577/590 nm) for 30 min at 37 ºC and the culture medium was replaced by a fresh one. The cells were then incubated for 4 h with FITC-Chi NP and FITC-Chi-C48/80 NP at 100 μg/mL or FITC-BSA loaded nanoparticles at 50 μg/mL in DMEM.

Following uptake, cells were washed three times with phosphate-buffered saline pH 7.4 (PBS) and fixed with 4 % paraformaldehyde in PBS for 15 min at 37 ºC. The plasma membrane of pre-fixed cells was then labeled with 5 μg/mL of Wheat Germ Agglutinin (WGA)- Alexa Fluor® 350 conjugate (Ex/Em - 346/442 nm) in PBS for 10 min at RT. After labeling, cells were washed twice with PBS and the coverslips mounted in microscope slides with DAKO mounting medium and examined under an inverted laser scanning confocal microscope (Zeiss LSM 510 META, Carl Zeiss, Oberkochen, Germany) equipped with an imaging software (LSM 510 software, Carl Zeiss).

3.2.10 Statistical analysis

Statistical analysis was performed with GraphPad Prism v 5.03 (GraphPad Software Inc., La Jolla, CA, USA). Student's t-test and ANOVA followed by Tukey's post-test were used for two samples or multiple comparisons, respectively. A P value < 0.05 was considered statistically significant.

3.3 Results and discussion

3.3.1 Purification of chitosan

Before use chitosan was submitted to a purification process to ensure the removal of any possible impurities. FTIR analysis was performed before and after the purification process to confirm the preservation of structure and integrity of the commercial polymer. The spectra obtained were in agreement with previously published data [23, 24]. FTIR spectrum of chitosan showed a broad band between 3500 – 3200 cm^{-1} (Fig. 3.1) corresponding to the

stretching vibration of O-H. The peak of N-H stretching from primary amine groups was overlapped in the same region. The peak at 2869 cm^{-1} indicates the C-H stretching vibrations. Peaks at 1650 cm^{-1} and 1588 cm^{-1} correspond to C=O stretch and N-H bending, respectively. The peak at 1419 cm^{-1} belongs to the N-C stretching and the bands at 1150 cm^{-1} and 1025 cm^{-1} are characteristic of the CO stretching vibration. No differences were observed between the spectra of non-purified and purified chitosan which indicates that the purification process had no effect on the structure of the polymer.

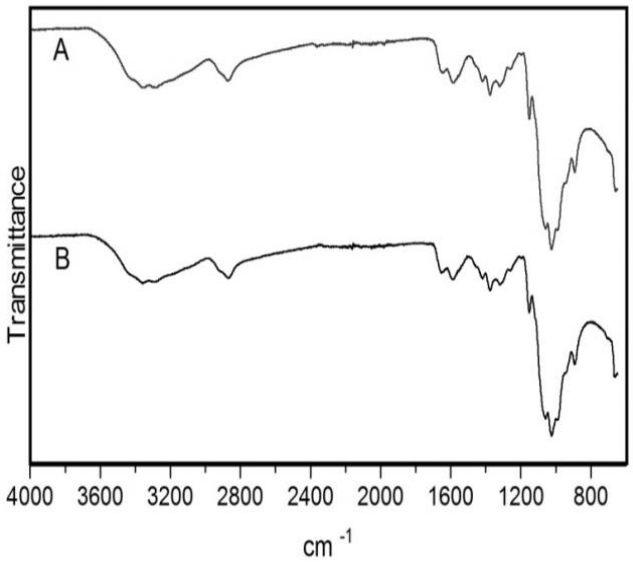

Figure 3.1 – FTIR spectra of chitosan after and before the purification process. (A) Chitosan purified (B) Chitosan non-purified.

3.3.2 Development and physicochemical characterization of C48/80-chitosan nanoparticles

C48/80 loaded chitosan nanoparticles were prepared by ionotropic gelation of cationic chitosan with sulfate anions from Na_2SO_4. Compound 48/80 was added to Na_2SO_4 crosslink solution and entrapped during NPs formation. This method of nanoparticle preparation is extremely simple and involves mixing two aqueous solutions at RT. Despite the simplicity of the method, different conditions were tested in the laboratory before getting the final nanoparticle formulation. Based on previous data collected from our group, different concentrations of the nanoparticles components, as well as different pH and incubation conditions were tested in order to achieve nanoparticles with the desired characteristics: submicron size, a good polydispersity and a reasonable encapsulation of the mast cell activator C48/80. The main challenge was to associate a cationic compound, the mast cell activator C48/80, with the also positively charged chitosan. Typically, interactions with chitosan amine group are electrostatic which favors the interaction of the polymer with anionic compounds.

Consequently, the association of cationic compounds with chitosan can be trickier due to partial repulsion, since both are positively charged [25]. At the end, the preparation of chitosan nanoparticles loaded with the mast cell activator C48/80 was possible by mixing the compound with an alkalinized sodium sulfate solution prior to the preparation of the nanoparticles.

A

Formulation	Size (nm)	PI[a]	ZP (mV) [b]	% LE (C48/80) [c]
Chi-C48/80 NP	500.9 ± 65.2	0.161 ± 0.051	23.83 ± 3.76	18.65 ± 2.99
Chi NP	396.2 ± 35.0	0.156 ± 0.037	21.59 ± 2.81	[d]

[a]Polydispersity index; [b] Zeta Potential; [c] C48/80 loading efficacy; [d] without C48/80

B

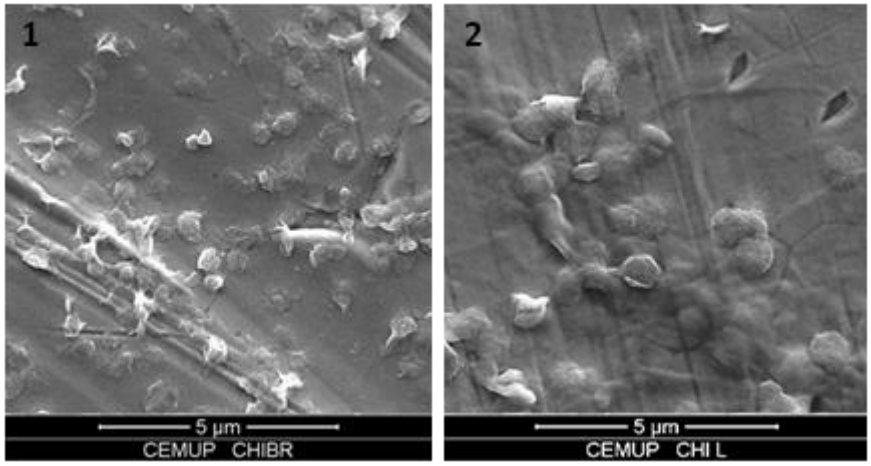

Figure 3.2 – Characterization of C48/80 loaded and unloaded chitosan nanoparticles. (A) Size and zeta potential were measured by dynamic light scattering and electrophoretic light scattering, respectively, with a Delsa™ Nano C. C48/80 loading efficacy was measured by a colorimetric method. Mean ± SD, n ≥ 3. (B) SEM images of (1) Chi NP and (2) Chi-C48/80 NP. Magnification 15 000 x, scale 5 µm.

The unloaded Chi NP had an average size of 396.2 ± 35.0 while the formulation loaded with the mast cell activator, Chi-C48/80 NP, had an average size of 500.9 ± 65.2 nm. Images from scanning electron microscopy confirmed the size measured by DLS (Fig. 3.2B). Both formulations had a narrow size distribution (PI < 0.170) and were positively charged (Fig. 3.2A). The incorporation of C48/80 in Chi NP leaded to an increase of about 100 nm in the nanoparticle size ($p < 0.001$, student's t-test) but the nanoparticle surface charge remains unaltered. The increased mean size was a good indicator of the association of C48/80 in the nanoparticles but the incorporation was definitively confirmed after quantification of the amount of C48/80 in the nanoparticles by a validated method [26]. The results showed that the compound was successfully incorporated into Chi NP with a loading efficacy of 18.6 %.

Even if the attempts to correlate particle size and the resultant immune responses lead to conflicting findings [4, 27], previous studies showed that 500 nm is in the optimal size range for uptake by APCs [28]. So, not only the Chi-C48/80 NP and Chi NP have a suitable size for uptake but also their positive charge is an advantage since it favors mucoadhesion, through interaction with the negatively charged sites on cell surfaces, and should also facilitate the uptake by antigen.

3.3.3 FTIR analysis of nanoparticles

FTIR is an important tool to analyze the interactions between groups and useful for the study of nanomaterial surface [29]. So Chi NP, Chi-C48/80 NP and C48/80 were analyzed by FTIR to characterize any potential interactions in the nanoparticles.

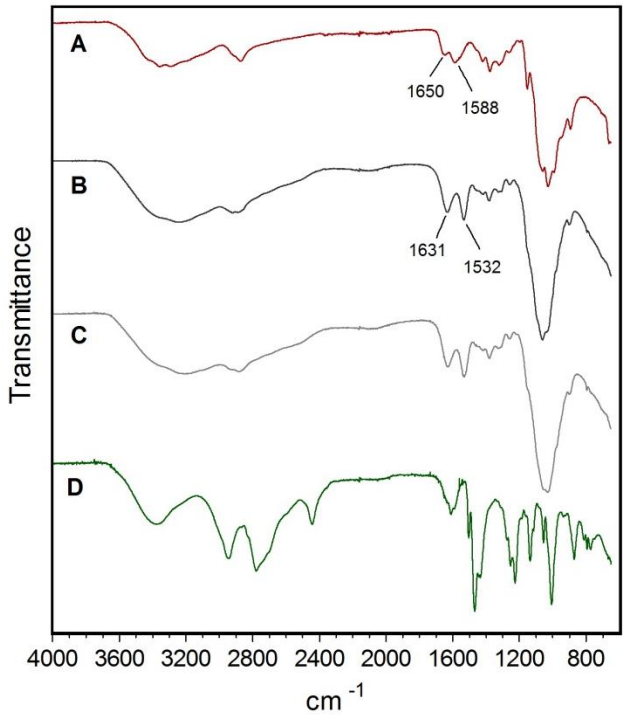

Figure 3.3 – FTIR spectra of (A) Chitosan, (B) Chi NP, (C) Chi-C48/80 NP and (D) C48/80.

Comparison of Chi NP (Fig. 3.3B) with chitosan polymer (Fig. 3.3A) showed a shift of peaks 1650 cm^{-1} and 1588 cm^{-1} to 1631 cm^{-1} and 1532 cm^{-1}, respectively. This difference can be explained by the interaction between the amino groups of chitosan and sulfate ions which resulted in the formation of the NP by ionic cross-link [24]. The broad band between 3500 – 3200 cm^{-1} attributed to O-H and N-H bonds shifted to a lower wavelength in Chi NP indicating an enhancement of the hydrogen bonds interactions [30]. The same band appeared more broadening in Chi-C48/80 NP than in Chi NP (Fig. 3.3) which also indicates enhanced hydrogen bonding in the loaded formulation [23]. No peak exclusively characteristic from

C48/80 was observed on the FTIR spectrum of Chi-C48/80 NP. This may be due to the the small amount of C48/80 and therefore its chemical groups, present in the nanoparticles, which may be masked by the much higher amount of chitosan.

3.3.4 Stability studies of the nanoparticles

A particle based vaccine should be stable in relation to size throughout the process of preparation, storage and administration. Considering this, the short-term stability of aqueous suspensions of Chi-C48/80 NP was assessed by measuring the size, PI and zeta potential during storage at 25 ºC or at 4 ºC for 15 days. Chi-C48/80 NP showed consistent particle size with uniform size distribution during the test period (Fig. 3.4A and 3.4B). Also, no changes in zeta potential of nanoparticles were observed (Fig. 3.4C and 3.4D).

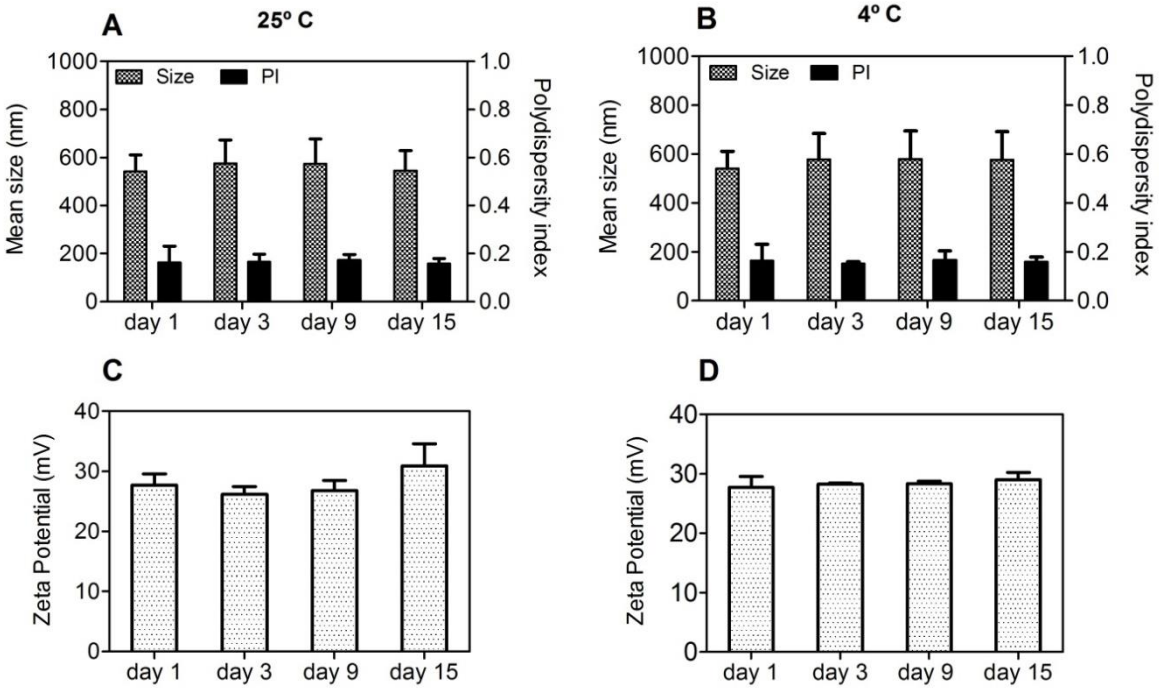

Figure 3.4 – Short-term stability of Chi-C48/80 NP at 25° C (A, C) and 4° C (B, D). Size, polydispersity index (PI) and zeta potential of the C48/80 loaded formulation were measured during storage up to 15 days at 25 °C or at 4 °C. Data are expressed as mean ± SD, n = 3.

The results showed that Chi-C48/80 NP were stable up to 15 days at the tested conditions. However, it should be keep in mind that the target function of these formulation is to act as an adjuvant for nasal vaccination after association with an antigen of interest. It is known that instability during storage of vaccines can lead to physicochemical changes of the formulation and antigen degradation, often requiring additional steps for improving its long-term stability

[4]. One effective way to guarantee this stability and to prevent antigen degradation is to lyophilize the vaccine formulation [31]. It is important that this procedure does not affect the original particle size and size distribution of the formulation since it would also influence the immune responses. Thus, the potential impact of these process should be investigated at early stages of formulation design [4]. Considering this, we explored the feasibility of lyophilizing the developed formulations by evaluating the impact of this technique on the physicochemical properties of Chi-C48/80 NP and Chi NP. The preliminary data obtained revealed that freeze-drying of the developed formulations without any cryoprotectant resulted in great particle aggregation (data not shown). This destabilization of nanoparticle suspensions is very common and most likely is a result of the stress of freezing and dehydration inherent to the technique [32]. So, to avoid that, in this study a fixed concentration of nanoparticles (2 mg/mL) was lyophilized with different concentrations of trehalose (1 %, 2.5 % and 5 % (w/v)). The physicochemical characteristics of the delivery systems were then measured after reconstitution in water and compared to the initial ones (pre-lyophilization), to see if the concentrations of cryoprotectant used were sufficient to stabilize the formulations (Fig. 3.5).

Trehalose was selected as cryoprotectant because it was successfully used before to preserve not only the characteristics of chitosan nanoparticles [30] but also the bioactivity of both C48/80 and an antigen [19]. Size of both Chi-C48/80 NP and Chi NP remain the same after lyophilization with all trehalose concentrations tested (Fig. 3.5A and 3.5B). On the other hand, differences on PI indicate that an adequate reconstitution of nanoparticles was only achieved when using 2.5 % or 5 % of the cryoprotectant. Zeta potential of nanoparticles increased after the lyophilization with trehalose (Fig. 3.5C and 3.5D). This can result from either a change in charge distribution on nanoparticles surface or from the presence of trehalose on the on the nanoparticles suspension. The results suggest that 2.5 % of trehalose was sufficient to achieve a successful cryopreservation of both delivery systems.

To assess if the lyophilized nanoparticles would be feasible to avoid the cold chain, Chi-C48/80 NP lyophilized with 2.5 % of trehalose were characterized after storage at RT for 4 months. Results showed that nanoparticles preserved the initial size and polydispersity for at least 4 months of storage (Fig. 3.5E).

Overall, the results suggest that the stability of Chi NP was not impaired by the association with C48/80. However, is noteworthy that even if these studies on the stability of the nanoparticles provided us with an indication about the potential of the formulations for long-term storage, they do not exclude the requirement of a more complete stability study, including antigen potency evaluation over time, for guarantee that the immunogenicity of the

vaccine candidate is not affected. That would be particularly important during the development of vaccines designed to avoid the cold chain.

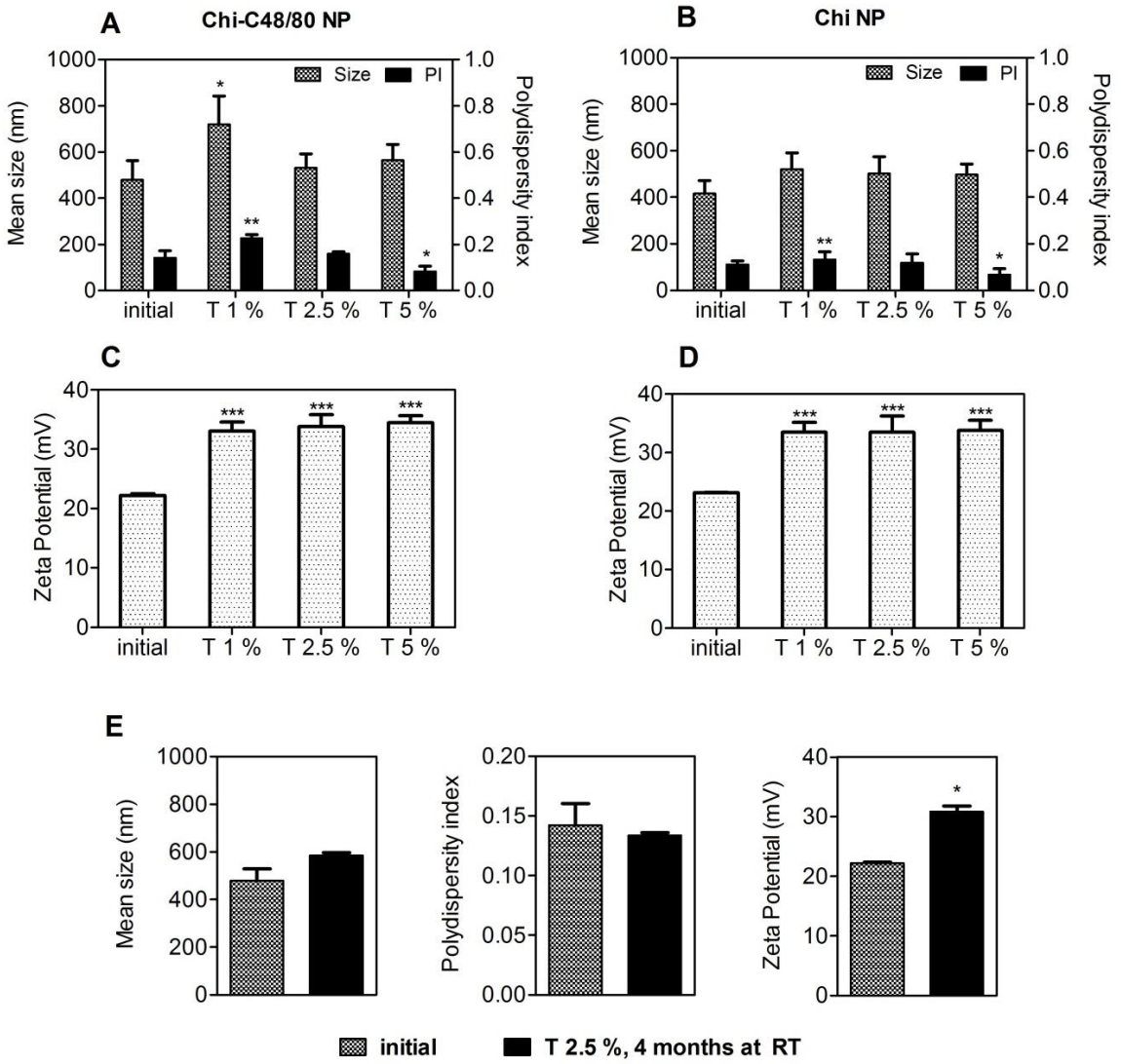

Figure 3.5 – Effect of lyophilization with different concentrations of trehalose on the characteristics of nanoparticles. Size, polydispersity index and zeta potential of Chi-C48/80 NP (A, C) and Chi NP (B, D) were measured before and after lyophilization with 1 %, 2.5 % and 5 % of trehalose. (E) To evaluate the long term stability of the lyophilized nanoparticles, Chi-C48/80 NP plus 2.5 % of trehalose were characterized after 4 months at RT. Data are expressed as mean ± SD, n = 3.

3.3.5 Loading of model antigens

In this study BSA, OVA and myoglobin were used as model antigens to confirm the adsorption of proteins onto the surface of nanoparticles. The use of three different proteins with different isoelectric points allowed us to assess the suitability of the developed delivery

systems for loading different antigens of interest. The loading of proteins on nanoparticles was made by physical adsorption, a mild technique that involves simply the incubation of nanoparticles with an aqueous solution of the antigen. This approach not only helps to preserve the structure of antigen but also allows a repetitive antigen display to the APC, which mimics pathogens [2].

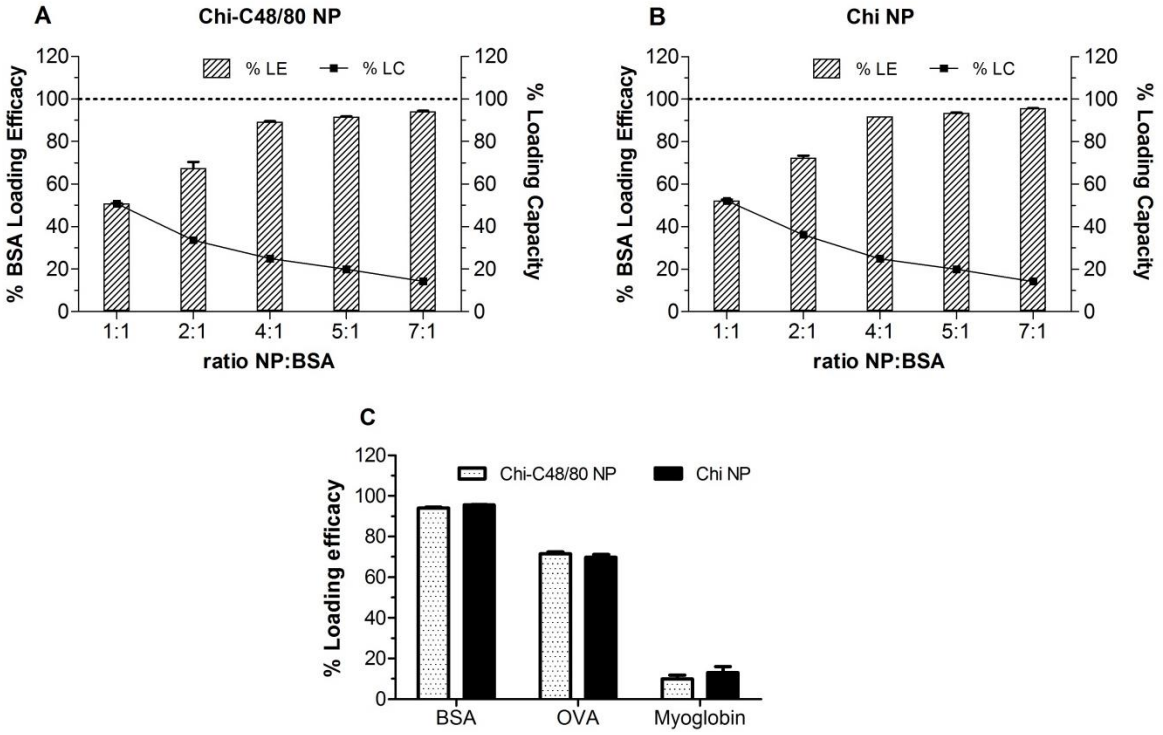

Figure 3.6 – Loading of model antigens. Effect of NP:protein ratio on the protein adsoption to (A) Chi-C48/80 NP and (B) Chi NP. (C) Loading efficacy for BSA, OVA and myoglobin at NP:protein ratio of 7:1. Nanoparticles were incubated with different proteins for 60 min in acetate buffer, pH = 5.7 at RT. Loading efficacy (% LE) and loading capacity (% LC) were determined after quantification of unbound protein in the supernatant using the BCA assay. Bars represent mean ± SD, n=3.

Initially different NP:BSA ratios were tested to evaluate the more efficient weight ratio of NP:protein for loading. BSA loading efficacies were very similar for both Chi-C48/80 NP and Chi NP (Fig. 3.6A and 3.6B). The LE was dependent on the ratio NP:BSA, the higher the ratio, the higher the amount of protein adsorbed on nanoparticles surface, ranging from 50.8 % to 94.1 % and from 52.2 % and 95.5 %, for Chi-C48/80 NP and Chi NP, respectively. The LC of nanoparticles was also calculated, it represents the amount of protein that the nanoparticles are able to carry. Opposing to LE, the LC of the nanoparticles decreased with the increase of the ratio NP:BSA. Loading capacity was maximum at the lower ratio tested (1:1) for both Chi NP and Chi-C48/80 NP. However, even if the incubation with higher amounts of protein allows the nanoparticles to carry an higher amount of the protein of

interest, generally it is preferable to use the NP:protein ratio that allows the highest LE because the antigen is usually the most expensive component of the vaccine. The LE near 95 %, achieved for NP:BSA = 7:1, is very favorable in formulation development since almost the entire amount of antigen used would be associated with the nanoparticles. So, this ratio was selected to test the loading of OVA and myoglobin on nanoparticles surface.

LE of OVA and myoglobin on nanoparticles was around 70 % and 10 %, respectively, for both Chi-C48/80 NP and Chi NP (Fig. 3.6C). These values were significantly lower than the observed for BSA. The isoelectric points (IP) of BSA, OVA and myoglobin (4.7, 4.9 and 7.2, respectively) can help to understand the observed results. High BSA and OVA adsorption efficacies to the surface of can be associated with the electrostatic interactions between the positively charged amino groups of chitosan and the negatively charged carboxyl groups of the proteins. On the other hand, at pH 5.7 both nanoparticles and myoglobin are positively charged which explains the very low LE % observed for this protein. However, despite the similarity of the isoelectric points of BSA and OVA, the adsorption of these proteins was different within the same delivery system. That is because even if the IP is helpful for predicting the loading of proteins on nanoparticles surface, the adsorption is a complex process depending on several other factors [33]. Overall, the results suggested that the developed formulations are suitable for loading negatively charged antigens and that adsorption of protein onto Chi NP surface was not affected by the presence of C48/80.

3.3.6 Cytotoxicity

The cytotoxicity of Chi-C48/80 NP and Chi NP was evaluated in spleen cells using the MTT assay. Spleen cells were chosen because they are a good representative of the different cells of immune system and have been already used to test the toxicity of vaccine delivery systems [22, 34].

As expected, the results show that cytotoxicity was concentration dependent, higher concentrations of nanoparticles resulted in a decreased cell viability (Fig. 3.7). The incorporation of C48/80 in Chi NP didn't affect the toxicity of formulations with both formulations showing no cytotoxicity for concentrations up to 2000 μg/mL. Nevertheless, this concentration is very high and out of the range normally used. These results are in agreement with others that demonstrated that chitosan nanoparticles are non-toxic [22, 35, 36].

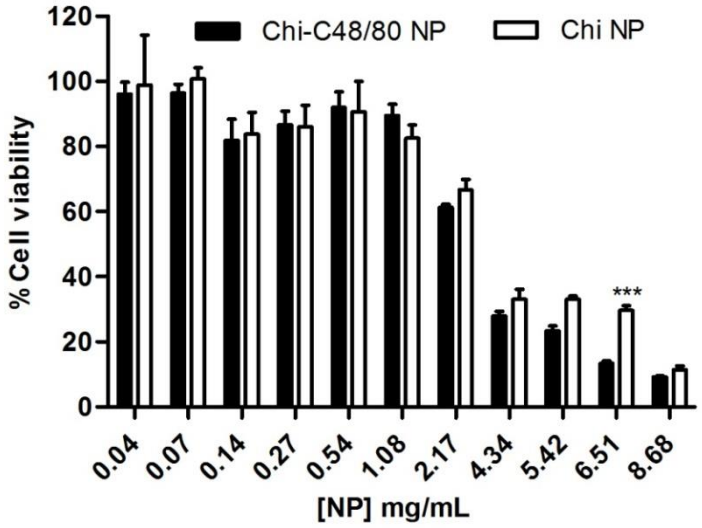

Figure 3.7 – Effect of Chi-C48/80 NP and Chi NP on cell viability. Different concentrations of nanoparticles were incubated with spleen cells for 24 h. The cell viability was measured by MTT assay. Each result is representative of two independent experiments performed in quadruplicate (mean ± SD).

3.3.7 Uptake studies

The uptake of nanoparticles by antigen presenting cells is favorable to an adaptive immune response [35]. Therefore we investigated the ability of both developed formulations to be internalized by RAW 264.7 cells, a macrophage cell line widely used to explore the uptake and immune effect of vaccine delivery systems [3, 7]. To visualize particle uptake by the macrophage cell line RAW 264.7, cells were incubated with FITC labeled Chi NP or Chi-C48/80 NP. The intracellular location of nanoparticles was analyzed by labeling the cells with Lysotracker Red, which accumulates in the acidic endolysosomes. The results showed that the NPs were efficiently taken up by macrophages (Fig. 3.8B). After 4 h of incubation, the FITC-NPs (green) were mostly detected on cell cytoplasm. However, some of the compartments enclosing NPs showed acidification as observed in the merged images between green fluorescent NP and red fluorescent vesicles, appearing in yellow, indicating maturation of the phagolysosome (Fig. 3.8A). To confirm that not only the nanoparticles but also associated antigens would be internalized by antigen presenting cells, uptake studies were repeated with nanoparticles loaded with a fluorescent labeled protein. The confocal images showed an extensive internalization of FITC-BSA loaded on both Chi-C48/80 NP and Chi NP (Fig. 3.8B). Similarly to what was observed with FITC labeled NP, the fluorescence signal of BSA was detected mostly on cell cytoplasm with only a few yellow co-localization signals observed.

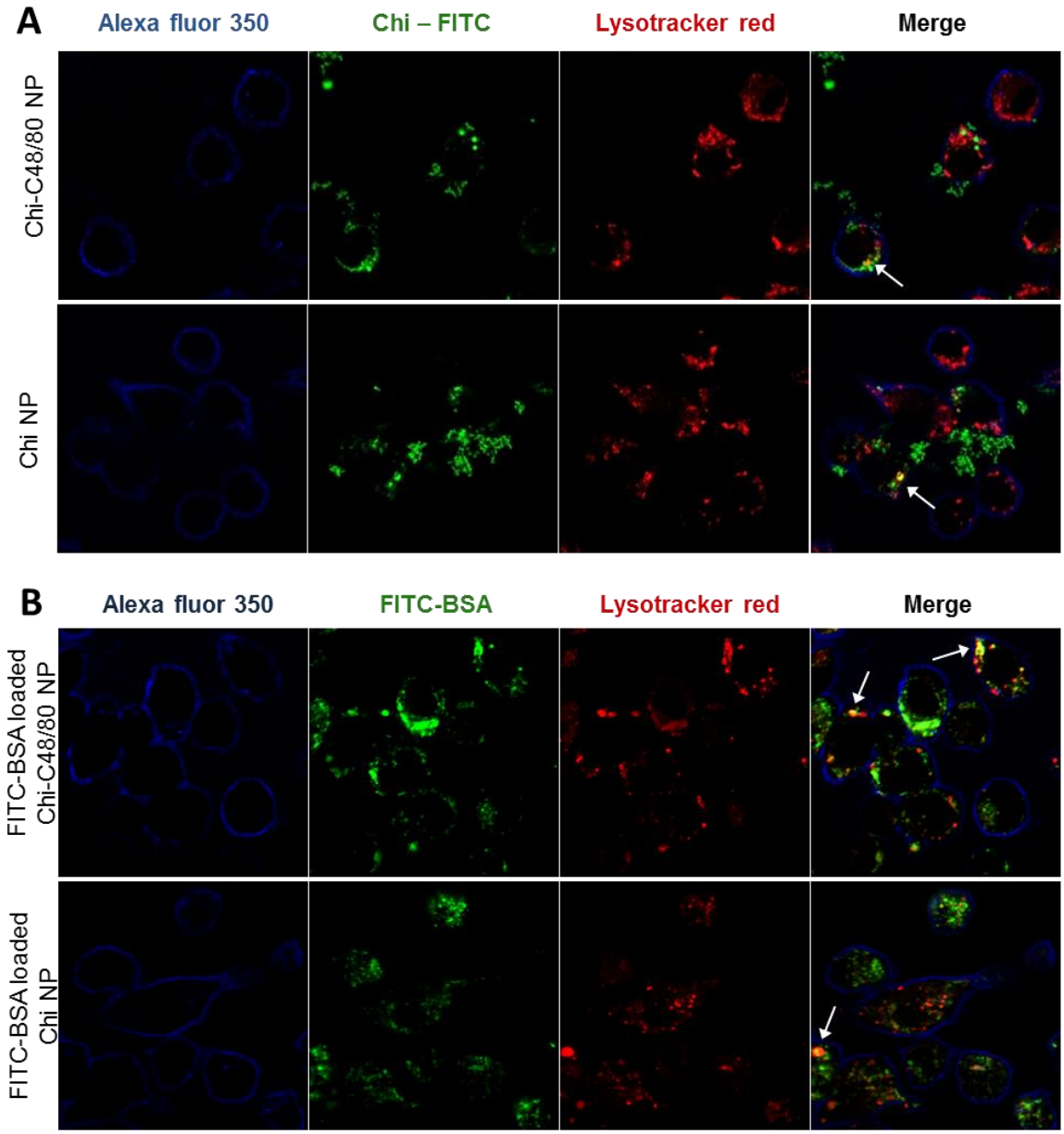

Figure 3.8 – Evaluation of uptake by macrophages. (A) Uptake of nanoparticles was assessed by incubating 4 h, 100 μg/mL RAW 264.7 cells with Chi-C48/80 NP or Chi NP prepared with FITC labeled chitosan (green). (B) Uptake of the antigen loaded on nanoparticles was evaluated by incubating the cells with FITC-BSA loaded Chi-C48/80 NP or Chi NP. Cells were labeled with Alexa Fluor© 350 WGA (blue) to identify the membrane and Lysotracker© Red identifies the acidic *endosomes* and lysosomes. Arrows in the merge image show co-localization.

These results suggest that NP and protein loaded NP might escape from the endosomes to cytoplasm which can facilitate cross-presentation and potentially mediate the MHC I antigen presentation pathway, associated with an induction of CD8+ T cell response [3]. In fact, it was demonstrated by others that chitosan based nanoparticles could escape from endosomes [36]

and that antigens delivered by Chi NP mediate antigen presentation through both MHC I and MHC II pathways [7]. This escape mechanism and consequent cross-presentation of antigens is particularly important for the development of vaccines that require cellular immune response.

Overall, the results showed that there were no significant differences regarding the uptake and distribution of Chi-C48/80 NP and Chi NP. This means that the association of the mast cell activator with the NP not only didn't impair the characteristics of nanoparticle and antigen uptake by antigen presenting cells but also demonstrated to be an effective antigen delivery system.

3.4 CONCLUSIONS

Chitosan is a biomaterial with appealing properties for vaccine delivery. Considering this, we designed and developed a new chitosan based vaccine delivery system by efficiently incorporating the mast cell activator C48/80 into chitosan nanoparticles. Overall, the data obtained demonstrated the versatility of chitosan to be associated with additional adjuvants without significantly affect the physicochemical and biocompatible properties of the polymer. This is a characteristic of chitosan that deserves to be further explored in order to support the design of improved delivery systems for vaccines. The delivery system demonstrated to have interesting features for vaccine delivery, namely, the ability to adsorb high amounts of a model antigen, internalization by antigen presenting cells and stability after lyophilization, which can be useful for the development of a cold chain free vaccine formulation. The present study not only supports the feasibility of associating a mast cell activator with chitosan nanoparticles for test as a vaccine adjuvant but can be helpful for the design of new adjuvant combinations comprising chitosan. Future studies will explore the ability of the developed delivery system to activate immune cells and to enhance the immune responses to vaccine antigens.

References

1. De Temmerman, M.L., et al., *Particulate vaccines: on the quest for optimal delivery and immune response.* Drug Discov Today, 2011. **16**(13-14): p. 569-82.
2. Smith, D.M., J.K. Simon, and J.R. Baker, Jr., *Applications of nanotechnology for immunology.* Nat Rev Immunol, 2013. **13**(8): p. 592-605.
3. Akagi, T., F. Shima, and M. Akashi, *Intracellular degradation and distribution of protein-encapsulated amphiphilic poly(amino acid) nanoparticles.* Biomaterials, 2011. **32**(21): p. 4959-67.
4. Oyewumi, M.O., A. Kumar, and Z. Cui, *Nano-microparticles as immune adjuvants: correlating particle sizes and the resultant immune responses.* Expert Rev Vaccines, 2010. **9**(9): p. 1095-107.

5. Shen, H., et al., *Enhanced and prolonged cross-presentation following endosomal escape of exogenous antigens encapsulated in biodegradable nanoparticles.* Immunology, 2006. **117**(1): p. 78-88.
6. Thomann-Harwood, L.J., et al., *Nanogel vaccines targeting dendritic cells: contributions of the surface decoration and vaccine cargo on cell targeting and activation.* J Control Release, 2013. **166**(2): p. 95-105.
7. Koppolu, B. and D.A. Zaharoff, *The effect of antigen encapsulation in chitosan particles on uptake, activation and presentation by antigen presenting cells.* Biomaterials, 2013. **34**(9): p. 2359-69.
8. Arca, H.C., M. Gunbeyaz, and S. Senel, *Chitosan-based systems for the delivery of vaccine antigens.* Expert Rev Vaccines, 2009. **8**(7): p. 937-53.
9. Amidi, M., et al., *Chitosan-based delivery systems for protein therapeutics and antigens.* Adv Drug Deliv Rev, 2010. **62**(1): p. 59-82.
10. Baldrick, P., *The safety of chitosan as a pharmaceutical excipient.* Regul Toxicol Pharmacol, 2010. **56**(3): p. 290-9.
11. Schijns, V.E. and E.C. Lavelle, *Trends in vaccine adjuvants.* Expert Rev Vaccines, 2011. **10**(4): p. 539-50.
12. Mutwiri, G., et al., *Combination adjuvants: the next generation of adjuvants?* Expert Rev Vaccines, 2011. **10**(1): p. 95-107.
13. Abraham, S.N. and A.L. St John, *Mast cell-orchestrated immunity to pathogens.* Nat Rev Immunol, 2010. **10**(6): p. 440-52.
14. Metz, M. and M. Maurer, *Mast cells--key effector cells in immune responses.* Trends Immunol, 2007. **28**(5): p. 234-41.
15. Marshall, J.S., *Mast-cell responses to pathogens.* Nat Rev Immunol, 2004. **4**(10): p. 787-99.
16. McLachlan, J.B., et al., *Mast cell activators: a new class of highly effective vaccine adjuvants.* Nat Med, 2008. **14**(5): p. 536-41.
17. Staats, H.F., et al., *Mucosal targeting of a BoNT/A subunit vaccine adjuvanted with a mast cell activator enhances induction of BoNT/A neutralizing antibodies in rabbits.* PLoS One, 2011. **6**(1): p. e16532.
18. McGowen, A.L., et al., *The mast cell activator compound 48/80 is safe and effective when used as an adjuvant for intradermal immunization with Bacillus anthracis protective antigen.* Vaccine, 2009. **27**(27): p. 3544-52.
19. Wang, S.H., et al., *Stable dry powder formulation for nasal delivery of anthrax vaccine.* J Pharm Sci, 2012. **101**(1): p. 31-47.
20. Reed, S.G., et al., *New horizons in adjuvants for vaccine development.* Trends Immunol, 2009. **30**(1): p. 23-32.
21. Gan, Q. and T. Wang, *Chitosan nanoparticle as protein delivery carrier—Systematic examination of fabrication conditions for efficient loading and release.* Colloids and Surfaces B: Biointerfaces, 2007. **59**(1): p. 24-34.
22. Borges, O., et al., *Uptake studies in rat Peyer's patches, cytotoxicity and release studies of alginate coated chitosan nanoparticles for mucosal vaccination.* J Control Release, 2006. **114**(3): p. 348-58.
23. Dudhani, A.R. and S.L. Kosaraju, *Bioadhesive chitosan nanoparticles: Preparation and characterization.* Carbohydrate Polymers, 2010. **81**(2): p. 243-251.
24. Borges, O., et al., *Preparation of coated nanoparticles for a new mucosal vaccine delivery system.* Int J Pharm, 2005. **299**(1-2): p. 155-66.
25. Lim, S.T., et al., *Preparation and evaluation of the in vitro drug release properties and mucoadhesion of novel microspheres of hyaluronic acid and chitosan.* J Control Release, 2000. **66**(2-3): p. 281-92.
26. Bento, D., et al., *Validation of a new 96-well plate spectrophotometric method for the quantification of compound 48/80 associated with particles.* AAPS PharmSciTech, 2013. **14**(2): p. 649-55.

27. Zhao, L., et al., *Nanoparticle vaccines.* Vaccine, 2014. **32**(3): p. 327-37.
28. Foged, C., et al., *Particle size and surface charge affect particle uptake by human dendritic cells in an in vitro model.* Int J Pharm, 2005. **298**(2): p. 315-22.
29. Mudunkotuwa, I.A., A.A. Minshid, and V.H. Grassian, *ATR-FTIR spectroscopy as a tool to probe surface adsorption on nanoparticles at the liquid-solid interface in environmentally and biologically relevant media.* Analyst, 2014. **139**(5): p. 870-81.
30. Rampino, A., et al., *Chitosan nanoparticles: preparation, size evolution and stability.* Int J Pharm, 2013. **455**(1-2): p. 219-28.
31. Sloat, B.R., M.A. Sandoval, and Z. Cui, *Towards preserving the immunogenicity of protein antigens carried by nanoparticles while avoiding the cold chain.* Int J Pharm, 2010. **393**(1-2): p. 197-202.
32. Abdelwahed, W., et al., *Freeze-drying of nanoparticles: formulation, process and storage considerations.* Adv Drug Deliv Rev, 2006. **58**(15): p. 1688-713.
33. Dee, K.C., D.A. Puleo, and R. Bizios, *Protein-Surface Interactions*, in *An Introduction To Tissue-Biomaterial Interactions*2003, John Wiley & Sons, Inc. p. 37-52.
34. Eyles, J.E., et al., *Stimulation of spleen cells in vitro by nanospheric particles containing antigen.* J Control Release, 2003. **86**(1): p. 25-32.
35. O'Hagan, D.T. and N.M. Valiante, *Recent advances in the discovery and delivery of vaccine adjuvants.* Nat Rev Drug Discov, 2003. **2**(9): p. 727-35.
36. Yue, Z.G., et al., *Surface charge affects cellular uptake and intracellular trafficking of chitosan-based nanoparticles.* Biomacromolecules, 2011. **12**(7): p. 2440-6.

CHAPTER 4

Development, characterization and preliminary evaluation of C48/80 loaded chitosan/alginate nanoparticles

Abstract

Modern vaccines are mostly based on pure recombinant antigens instead of traditional whole-cells vaccines. These subunit antigens are often poorly immunogenic requiring the concomitant use of adjuvants to improve the immune response to the vaccine. Recently, the combination of adjuvants has been appointed as a promisor strategy to obtain a potent vaccine formulation. Taking advantages of the benefits of nanotechnology in vaccine development, an immunopotentiator can be associated with a particulate delivery system in order to obtain enhanced vaccine adjuvants. In the present study, a new vaccine adjuvant combining the mast cell activator C48/80 with chitosan/alginate particles was developed and characterized. Results showed that particle size and loading of C48/80 can be tuned with different concentrations of chitosan. The optimal formulation had an average size of about 560 nm, was positively charged and was able to adsorb negatively charged model antigens. The association of C48/80 with chitosan/alginate particles significantly affected the characteristics of the formulation including its biocompatibility. Nevertheless, low cytotoxicity was observed for the lower and intermediate concentrations of chitosan/alginate-C48/80 NP. *In vitro* studies in macrophages showed the internalization of FITC-BSA associated with chitosan/alginate-C48/80 NP and a moderate internalization of FITC labelled nanoparticles. These characteristics suggest the potential of chitosan/alginate-C48/80 NP as a new delivery system for vaccine delivery.

4.1 Introduction

Modern vaccines are mainly based on pure recombinant antigens instead of traditional live attenuated or inactivated pathogens. Despite their increased safety profile, these recombinant vaccines are less immunogenic creating a major need to find potent vaccine adjuvants. Over the past decade the use of nanotechnology in vaccinology has been increasing exponentially. Materials such as virus-like particles, liposomes, ISCOMs, polymeric particles can be used either as a delivery system to enhance antigen processing and/or as an immunopotentiator to enhance immunity. In fact, formulation of antigen in nanoparticles may offer several attractive features, namely: enhanced uptake by antigen presenting cells (APCs) [1], depot effect with gradual release of the antigen [2, 3], cross-presentation of antigens [2, 4], slower antigen processing than antigen in solution, which can result in a prolonged antigen presentation [5] and co-deliver of antigen and adjuvant to the same cell [6]. Moreover, generally particulate antigens are more immunogenic than soluble antigens [7] and nanoparticles can be used to modulate the type of immune response [2]. Chitosan and its derivatives are among the most studied compounds for development of polymeric vaccines [8, 9] because of their attracting characteristics for biomedical applications. Chitosan is a biocompatible, biodegradable and non-toxic polysaccharide [10], obtained from deacetylation of chitin, consisting of β-(1-4)-linked D-glucosamine and N-acetyl-D-glucosamine monomer units. Its cationic nature, mucoadhesivity and immunostimulating properties [8] make it an attractive polymer for the design of nanoparticulate vaccines particularly for mucosal delivery. Other polymer widely studied for vaccine delivery is alginate, a biodegradable and a biocompatible natural polyanionic polysaccharide with a good safety profile. Its molecular structure consists in linear copolymers of α-L-guluronate and β-D-mannurate residues. The carboxylic acid groups on these units attribute negative charges to alginate, and thus being able to interact electrostatically with the positively charged molecules like the amino groups of chitosan. In fact, alginate has been quite used in combination with chitosan for preparation of vaccine delivery systems [11-14].

Mast cells were recognized in the last decade as important players in the development of a protective immune response and the immunostimulatory properties of the mast cell activator compound 48/80 (C48/80) is now well recognized [15-20]. The combination of adjuvants, particularly strategies involving the association of particles with immunostimulatory compounds, has recently been appointed as a promising approach in vaccine development [21]. The association of C48/80 with nanoparticles could be advantageous since the nanoparticles would provide a more efficient antigen delivery and simultaneously mast cell

activation would promote a local environment favourable to the development of an immune response. Considering this, we developed a new vaccine delivery system consisting of C48/80 associated with chitosan/alginate nanoparticles. Chitosan was selected because of its mucoadhesive and immunostimulatory properties, and alginate was included in the formulation in order to facilitate the incorporation of the cationic mast cell activator C48/80 into nanoparticles. So, the present paper describes the optimization, characterization and preliminary *in vitro* evaluation of C48/80 loaded chitosan/alginate nanoparticles.

4.2 Materials and Methods

4.2.1 Materials

A low molecular weight Chitosan (deacetylation degree 95 %) was purchased from Primex BioChemicals AS (Avaldsnes, Norway) and used after a purification process, described in chapter 3, section 3.3.2. Alginate (MANUCOL LB®) was kindly donated by ISP Technologies Inc. (Surrey, UK). Compound 48/80, bovine serum albumin (BSA), MTT (3-[4, 5-dimethylthiazol-2-yl]-2,5-diphenyl tetrazolium bromide), albumin-fluorescein isothiocyanate conjugate (FITC-BSA), Dulbecco's modified Eagle medium (DMEM) and RPMI 1640 were obtained from Sigma-Aldrich (Sintra, Portugal). BCA assay kit was obtained from Pierce Chemical Company (Rockford, IL, USA). FITC was purchased to Santa Cruz Biotechnology (Santa Cruz, CA, USA). Fetal bovine serum (FBS), Wheat Germ Agglutinin Alexa Fluor® 350 Conjugate and Lysotracker® Red DND 99 were obtained from Life Technologies Corporation (Paisley, UK). All other reagents used were of analytical grade.

4.2.2 Development of C48/80 loaded chitosan/alginate nanoparticles

C48/80 loaded chitosan/alginate nanoparticles (Chi/Alg-C48/80 NP) were prepared using a two-step method. First, 3 mL of a calcium chloride solution (2 mg/mL) was added dropwise to 47 mL of a sodium alginate solution 0.063 % (pH = 5.1) in a ultrasound bath while stirring for 15 min at 25000 rpm with a homogeneizator (Ystral GmbH D-7801 Dottingen) in order to prepare a pregel. The prepared Ca^{2+}/alginate pregel was stirred for further 20 min in a magnetic stirrer. Finally, the particles were formed upon mixing 3 mL of pregel with an equal volume of a chitosan acidic solution (pH=5.4) containing 300 μg/mL of C48/80. Solutions were mixed during high-speed vortexing and particles obtained after further maturation for 30 min under magnetic stirring. The formulation was optimized testing different concentrations of the chitosan solution (0.02 % to 0.08 %). Blank chitosan/alginate particles (Chi/Alg NP) were obtained preparing nanoparticles exactly in the same conditions but without C48/80.

4.2.3 Characterization of nanoparticles

4.2.3.1 Size and Zeta Potential

Particle size was measured by dynamic light scattering (DLS) using a Delsa™ Nano C (Beckman Coulter). Samples were diluted in milli-Q water and analyzed at a detection angle of 160° and a temperature of 25 °C. Zeta potential was measured by electrophoretic light scattering, after dispersion of the nanoparticles in a solution of 1 mM NaCl.

4.2.3.2 Quantification of C48/80 loading efficacy

To evaluate the loading efficacy (LE) of C48/80, nanoparticles were centrifuged for 20 min at 8000 g and C48/80 was quantified in the supernatant using the method described in section 2. Briefly, 25 µL of carbonate buffer pH = 9.6 was added to 175 µL of sample in a 96-well plate. Subsequently, 50 µL of a 15 % acetaldehyde solution containing 1.5 % of sodium nitroprusside was added and the absorbance measured at 570 nm. The loading efficacy was calculated according to equation 4.1.

$$\text{C48/80 LE (\%)} = \frac{\text{total C48/80 (µg/mL)} - \text{free C48/80 in supernatant (µg/mL)}}{\text{total C48/80 (µg/mL)}} \times 100 \quad \text{(Equation 4.1)}$$

4.2.3.3 FTIR analysis

Chi/Alg NP and Chi/Alg-C48/80 NP were centrifuged for 30 min at 4500 g, washed once and freeze-dried overnight (Labconco, Kansas City, USA). The FTIR spectra of freeze-dryed nanoparticles were recorded using an FTIR spectrometer (Spectrum 400, PerkinElmer) with attenuated total reflection (ATR) top-plate accessory. The instrument operated with a resolution 2 cm^{-1} and 30 scans were collected for each sample. Spectra were recorded between 650 cm^{-1} and 4000 cm^{-1}.

4.2.3.4 Morphology

Particle morphology was evaluated by scanning electron microscopy (SEM) in a FEI Quanta 400 FEG ESEM (USA). One drop of nanoparticle suspension was mounted on microscope stub using a double-stick carbon tape and let to dry overnight. Prior to image acquisition, samples were coated with gold.

4.2.4 Evaluation of loading efficacy and loading capacity of model antigens

Loading of model antigens on nanoparticle surface was made by physical adsorption. Nanoparticles were centrifuged for 30 min at 4500 g and resuspended in acetate buffer pH

5.7, 25 mM. Nanoparticles at a final concentration of 2.5 mg/mL were incubated with BSA, ovalbumin (OVA) or myoglobin in acetate buffer for 60 min at RT. Ratios from 7:1 to 1:1 (NP:protein) were tested for BSA while OVA and myoglobin were incubated at a fixed weight ratio of 7:1. After incubation, particles were centrifuged at 12000 g for 20 min and the supernatant collected. The amount of protein loaded on nanoparticles was determined indirectly by measuring the concentration of non-bound protein in the nanoparticle supernatant using the BCA protein assay (Pierce, Thermo Scientific) according to the manufacturer's instructions. Loading efficacy (LE) and loading capacity (LC) were determined by the equation 4.2 and equation 4.3, respectively.

$$\text{LE (\%)} = \frac{\text{total amount of BSA - non bound BSA}}{\text{total amount of BSA}} \times 100 \quad \text{(Equation 4.2)}$$

$$\text{LC (\%)} = \frac{\text{total amount of BSA (mg)- non bound BSA (mg)}}{\text{weight of nanoparticles (mg)}} \times 100 \quad \text{(Equation 4.3)}$$

4.2.5 Cytotoxicity studies

Single cell suspensions of spleen cells from 8-week old female C57BL/6 mice (Charles River) were prepared according to a method previously described [22]. Cells were seeded in a 96-well plate at a density of 1 x 10^6 cells/well in complete RPMI 1640 medium (supplemented with 10 % fetal bovine serum, 2 mM glutamine, 1 % Penicillin/Streptomycin and 20 mM HEPES buffer) and incubated with different concentrations of nanoparticles. After 24 h of incubation, cellular viability was assessed by MTT assay. Briefly, 20 µL of MTT 5 mg/mL in PBS 7.4 was added to each well and incubated for more 4 h. The plate was centrifuged for 25 min at 800 g and the supernatants removed. Finally, the formazan crystals produced by viable cells were solubilized with 200 µL of DMSO per well and the optical density values were measured at 540 nm with 630 nm as wavelength reference. The viability of non-treated cells (culture medium only) was defined as 100 % and the relative cell viability calculated using the equation 4.4.

$$\text{Cell viability (\%)} = \frac{\text{OD sample (540 nm) - OD sample (630 nm)}}{\text{OD control (540 nm) - OD control (630 nm)}} \text{ x } 100 \quad \text{(Equation 4.4)}$$

4.2.6 Particle uptake by macrophages

FITC labeled NPs were prepared by the method described in section 4.2.3 using FITC-labeled chitosan. The synthesis of FITC-labeled chitosan was based on the reaction between

the isothiocyanate group of FITC (Ex/Em – 490/525) and the primary amino group of chitosan, according to the protocol described in section 3.2.9.

The ability of the developed nanoparticles to be internalized by antigen presenting cells was assessed on mouse macrophage cell line RAW 264.7 (ECACC, Salisbury, UK). Cells were maintained in DMEM supplemented with 1 mM HEPES, 100 mM sodium pyruvate and 10 % of non-inactivated FBS. To evaluate the uptake of nanoparticles, RAW 264.7 cells were seeded on glass coverslips in 12-well plates at a density of 2.5 x 10^5 cells per well and cultured at 37 ºC in 5 % CO_2 overnight. On the next day, RAW 264.7 were pre-labeled with 300 nM Lysotracker® Red DND 99 (Ex/Em - 577/590 nm) for 30 min at 37 ºC and then culture medium was replaced by fresh one. The cells were then incubated for 4 h in DMEM with FITC-Chi/Alg NP and FITC-Chi/Alg-C48/80 NP at 100 μg/mL or FITC-BSA loaded nanoparticles at 50 μg/mL.

Following uptake, cells were washed three times with PBS pH 7.4 and fixed with 4 % paraformaldehyde in PBS for 15 min at 37 ºC. The plasma membrane of pre-fixed cells was then labeled with 5 μg/mL of Wheat Germ Agglutinin - Alexa Fluor® 350 conjugate (Ex/Em - 346/442 nm) in PBS for 10 min at RT. After labeling, cells were washed twice with PBS and the coverslips mounted in microscope slides with DAKO mounting medium and examined under inverted laser scanning confocal microscope (Zeiss LSM 510 META, Carl Zeiss, Oberkochen, Germany) equipped with imaging software (LSM 510 software, Carl Zeiss).

4.2.7 Statistical analysis

Statistical analysis was performed with GraphPad Prism v 5.03 (GraphPad Software Inc., La Jolla, CA, USA). Student's t-test and ANOVA followed by Tukey's post-test were used for two samples or multiple comparisons, respectively. A P value < 0.05 was considered statistically significant.

4.3. Results

4.3.1 Development and optimization of C48/80 loaded Chi/Alg NP

C48/80 loaded Chi/Alg NP were prepared by ionotropic gelation followed by chitosan polyelectrolyte complexation. Different concentrations of chitosan, from 0.2 % to 0.8 %, were tested to establish the conditions at which nanoparticles with desired characteristics were formed. The criteria size, size distribution, colloidal stability and C48/80 loading efficacy were used to select the best formulation parameters to prepare nanoparticles. Characteristics of

Chi/Alg-C48/80 NP prepared with different concentrations of chitosan are summarized in figure 4.1.

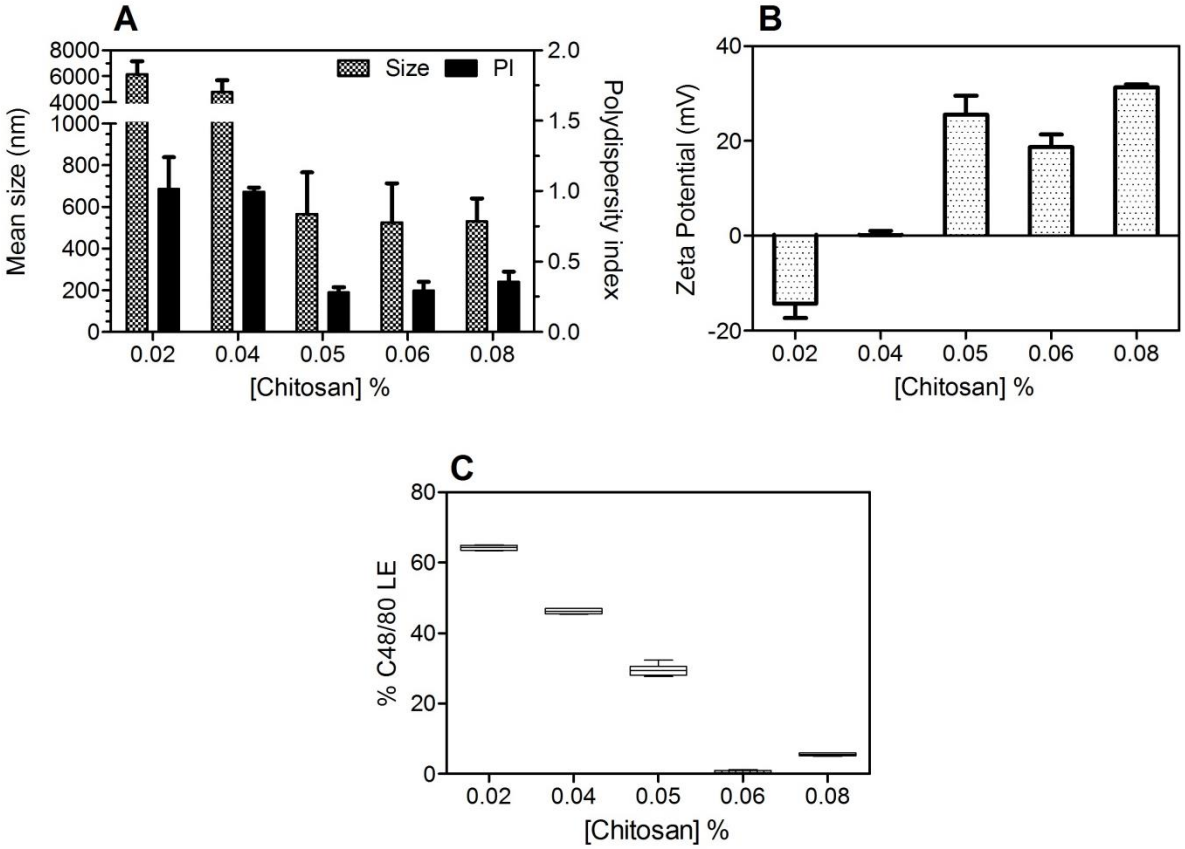

Figure 4.1 – Optimization of Chi/Alg-C48/80 NP. Effect of chitosan concentration on (A) particle size, (B) surface charge and (C) loading efficacy of C48/80. Data are expressed as mean ± SD, n ≥ 3.

A marked influence of chitosan concentration on the characteristics of nanoparticles was observed. At low concentrations of chitosan large particles with low colloidal stability were obtained, while the increase of chitosan concentration resulted in decreased particle size and size distribution (Fig. 4.1A), and increased zeta potential (Fig. 4.1B). Loading efficacy of C48/80 was also affected by the concentration of chitosan used during nanoparticles preparation. The lower amount of chitosan resulted in the higher % of C48/80 loading (Fig 4.1C) while higher chitosan concentrations resulted in poor C48/80 loading efficacy which may be explained to the partial repulsion between chitosan and C48/80 since both are positively charged. In other words, high chitosan concentrations block carboxylic groups from alginate that would be required to interact with C48/80. So, the optimal nanoparticles were formed using a 0.5 % chitosan solution. In these conditions, the particles obtained had a size close to 500 nm - optimal for cellular uptake [23], were positively charged and incorporated an acceptable amount of C48/80. So, this formulation was selected for subsequent studies.

4.3.2 Characterization of optimized C48/80 loaded Chi/Alg-C48/80 NP

The characteristics of optimized Chi/Alg-C48/80 NP and correspondent blank formulation are summarized on figure 4.2.

A

Formulation	Size (nm)	PI[a]	ZP (mV) [b]	% LE (C48/80) [c]
Chi/Alg-C48/80 NP	564.3 ± 201.4	0.280 ± 0.038	25.51 ± 4.04	29.56 ± 1.59
Chi/Alg NP	5752.3 ± 529.6	1.221 ± 0.248	5.33 ± 5.23	[d]

[a] Polydispersity index; [b] Zeta Potential; [c] C48/80 loading efficacy; [d] without C48/80

B

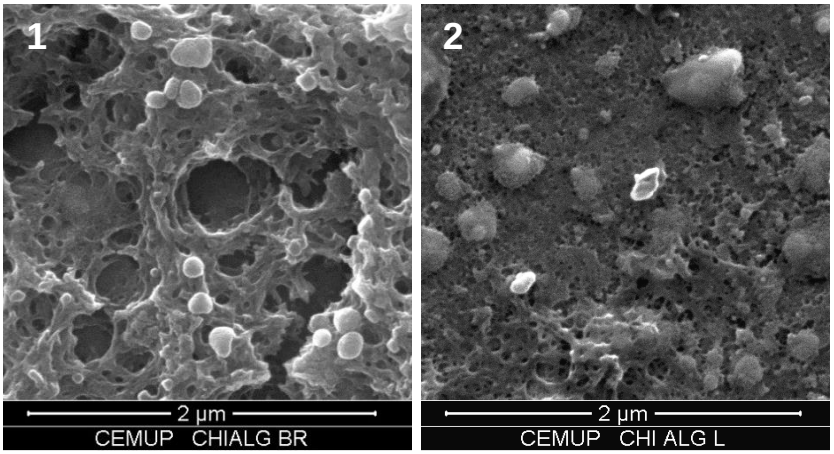

C

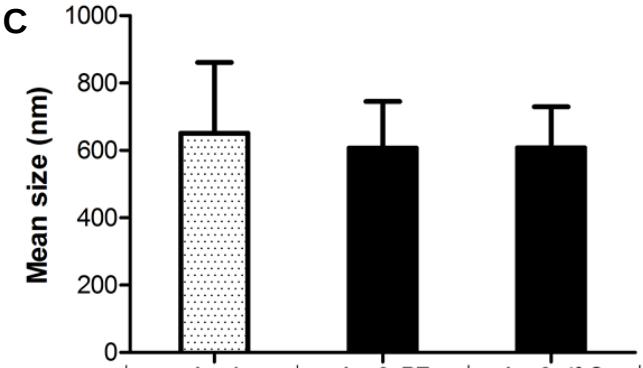

	day 1	day 3, RT	day 3, 4º C
PI	0.272 ± 0.059	0.248 ± 0.049	0.251 ± 0.039
ZP (mV)	+ 28.35 ± 1.58	+ 26.75 ± 1.90	+ 29.92 ± 0.61

Figure 4.2 – Characterization of C48/80 loaded and unloaded chitosan/alginate nanoparticles. (A) Size and zeta potential were measured by dynamic light scattering and electrophoretic light scattering, respectively, with a Delsa™ Nano C. C48/80 loading efficacy was measured by a colorimetric method. Mean ± SD, n ≥ 3. (B) SEM images of (1) Chi/Alg NP and (2) Chi/Alg-C48/80 NP. Magnification 50 000 x, scale 2 µm. (C) Short-term stability of Chi/Alg-C48/80 NP.

The mean size of Chi/Alg-C48/80 NP was 564.3 nm and the zeta potential was + 25.51 mV. Particles prepared by same method (0.5 % of chitosan), excluding C48/80, here referred

as unloaded Chi/Alg NP, revealed to be an unstable formulation with a mean size of 5752.3 nm and a zeta potential of + 5.33 mV. SEM analysis of Chi/Alg NP showed particles with about 200 nm (Fig. 4.2B1) which means that the size measured by DLS for this formulation most likely correspond to particle aggregates. These aggregates were formed due to the low colloidal stability of these unloaded nanoparticles as suggested by its low zeta potential. SEM images of Chi/Alg-C48/80 NP exhibited irregular round shaped particles with a size slightly smaller than the measured by DLS. Since SEM images were taken in the dry solid state while DLS size measurement was done in the swollen state, this may explain the differences observed. Overall, the incorporation of C48/80 in Chi/Alg NP stabilized the particles resulting in a decreased mean particle size and in a significantly increased zeta potential ($p < 0.001$). This difference in surface charge between Chi/Alg-C48/80 NP and Chi/Alg NP suggests that most likely a part of C48/80 is on the surface of NP.

A short-term stability study was performed on Chi/Alg-C48/80 NP suspension. The study was carried out at RT and at 4 °C for 3 days. Neither size nor zeta potential showed significant changes during the tested period (Fig. 4.2C).

4.3.3 FTIR analysis

FTIR was used to confirm the incorporation of chitosan into the alginate pregel and to analyze the potential interactions in the particles. The FTIR spectra of chitosan, alginate, and Chi/Alg NP are illustrated in Figure 4.3. Spectrum of alginate showed two peaks at 1595 cm^{-1} and 1405 cm^{-1} that correspond to asymmetric and symmetric stretch of COO-, respectively. The band at 1024 cm^{-1} is attributed to the saccharide structure of alginate (C-O-C stretching). On Chi/Alg NP, alginate COO- related peaks enlarged and slightly shifted from 1595 cm^{-1} to1588 cm^{-1} and from 1405 cm^{-1} to 1407 cm^{-1}. Also, the band at 1588 cm^{-1} of chitosan attributed to amino groups shifted to 1538 cm^{-1} after reaction with alginate. These results confirm the association of carboxylic groups of alginate with amino groups of chitosan. Chi/Alg NP and Chi/Alg-C48/80 NP were also analyzed by FTIR (Fig. 4.3B). Similarly to what was observed with C48/80 loaded Chi NP (Chapter 3), Chi/Alg-C48/80 NP spectrum did not show any band characteristic of C48/80. C48/80 peaks may have been masked by the bands produced by chitosan and alginate.

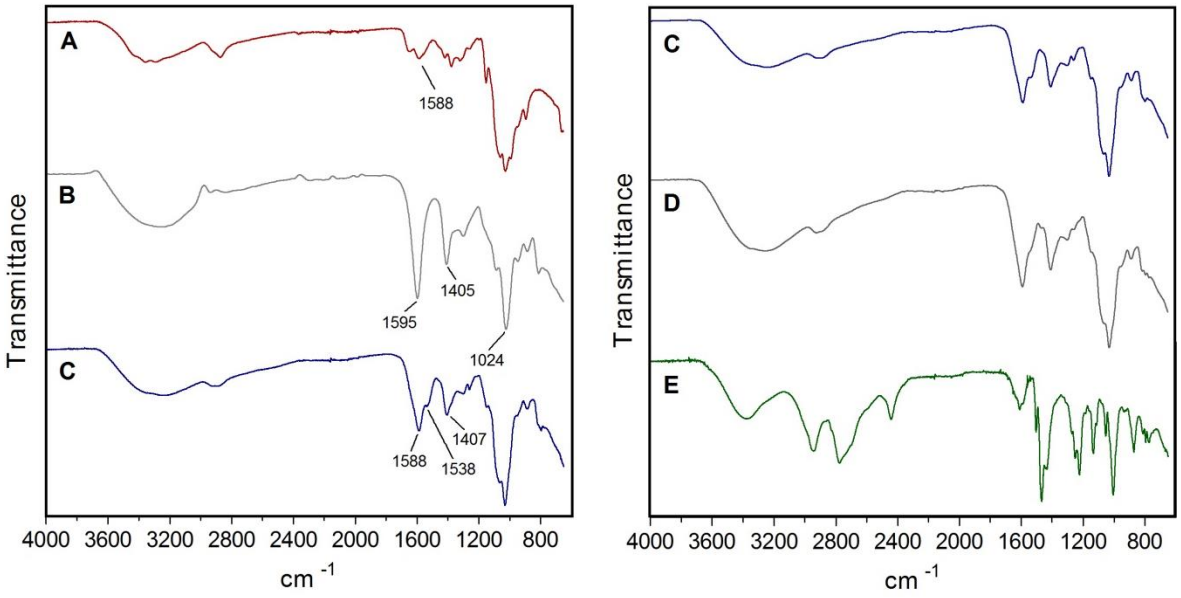

Figure 4.3 – FTIR spectra of (A) Chitosan, (B) Alginate, (C) Chi/Alg NP, (D) Chi/Alg-C48/80 NP and (E) C48/80.

4.3.4 Loading of model antigens

In this study BSA, OVA and myoglobin were used as model antigens to confirm the adsorption of proteins onto the surface of nanoparticles and to evaluate its suitability as vaccine delivery systems. The use of 3 different proteins with different isoelectric points allowed us to assess the suitability of the developed delivery systems for loading different antigens of interest. The loading of proteins on nanoparticles was made by physical adsorption, a mild technique that involves simply the incubation of nanoparticles with an aqueous solution of the antigen. This approach not only helps to preserve the structure of antigen but also allows a repetitive antigen display to the APC, which mimics pathogens [2]. Protein not adsorbed on nanoparticle surface was quantified by BCA assay, and the amount of protein associated with the nanoparticles calculated by difference.

Initially, different ratios NP:BSA were tested to evaluate the proportion that would give an higher percentage of adsorption. LE was dependent on the ratio NP:BSA, the higher the ratio, the higher the amount of protein adsorbed on nanoparticle surface (Fig. 4.4). BSA LE ranged from 25.9 % to 71.6 % and from 37.4 % to 68.7 %, for Chi/Alg-C48/80 NP and Chi/Alg NP, respectively (Fig. 4.4A and 4.4B), with no significant differences between the two formulations. The LC of nanoparticles was also calculated, it represents the amount of protein that the nanoparticles are able to carry. Opposing to LE, the LC of the nanoparticles decreased with the increase of the ratio NP:BSA. Loading capacity was maximum at the lower ratio tested (1:1) for both Chi/Alg NP and Chi/Alg-C48/80 NP. However, even if the

incubation with higher amounts of protein allows the nanoparticles to carry an higher amount of the protein of interest, generally it is preferable to use the NP:protein ratio that allows the highest LE because the antigen is usually the most expensive component of the vaccine. So, the NP:protein ratio of 7:1 was selected to test the loading of OVA and myoglobin on nanoparticles surface.

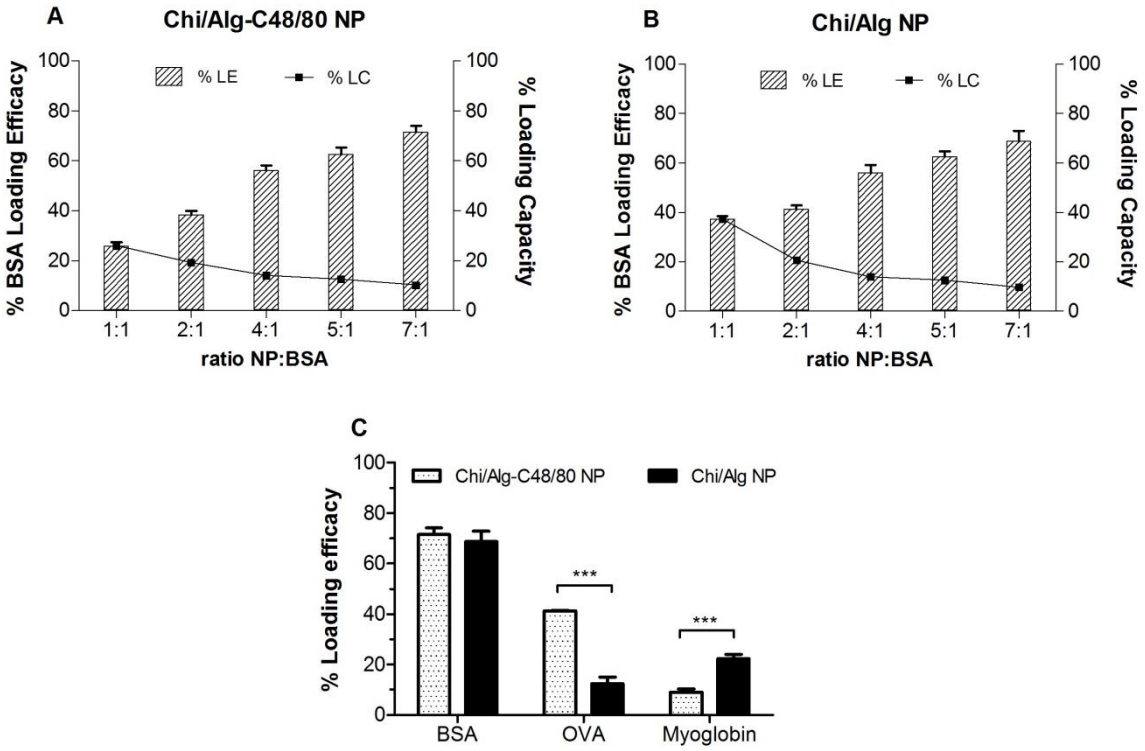

Figure 4.4 – Loading of model antigens. Effect of NP:protein ratio on protein adsorption to (A) Chi/Alg-C48/80 NP and (B) Chi/Alg NP. (C) Loading efficacy for BSA, OVA and Myoglobin at NP:protein ratio of 7:1. Nanoparticles were incubated with different proteins for 60 min in acetate buffer, pH = 5.7 at RT. Loading efficacy (% LE) and loading capacity (% LC) were determined after quantification of unbound protein in the supernatant using the BCA assay. Bars represent mean ± SD, n=3.

Overall, the LE of OVA and myoglobin was significantly lower than the LE of BSA (Fig. 4.4C). Chi/Alg-C48/80 NP adsorbed significantly higher amounts of OVA than Chi/Alg NP, 41.4 % and 12.3 %, respectively. On the other hand, LE of myoglobin on Chi/Alg-C48/80 NP was significantly lower than on Chi/Alg NP, 9.1 % and 22.4 %, respectively. The isoelectric points (IP) of BSA, OVA and myoglobin (4.7, 4.9 and 7.2, respectively) may explain the observed results. At pH 5.7 both BSA and OVA are negatively charged resulting in electrostatic interactions between the proteins and the positively charged particles. On the other hand, at this pH both myoglobin and Chi/Alg-C48/80 NP are positively charged which explains the very low LE of this protein observed for C48/80 loaded formulation. In this case,

the less positively charged surface of unloaded Chi/Alg NP favored the loading of myoglobin. However, IP by itself does not explain the much higher LE of BSA compared with OVA. Different adsorption profiles observed for proteins with similar IP occur because adsorption of protein to surfaces is a complex process depending on several other factors like the structure of the protein [24].

4.3.5 Cytotoxicity

The cytotoxicity of Chi/Alg-C48/80 NP and Chi/Alg NP was evaluated in spleen cells using the MTT assay. No cytotoxic effect was observed for unloaded Chi/Alg NP in the range of concentrations tested, even for concentrations higher as 7 mg/mL (Fig. 4.5). However, the incorporation of C48/80 in Chi/Alg NP affected the cytotoxicity profile of the formulation.

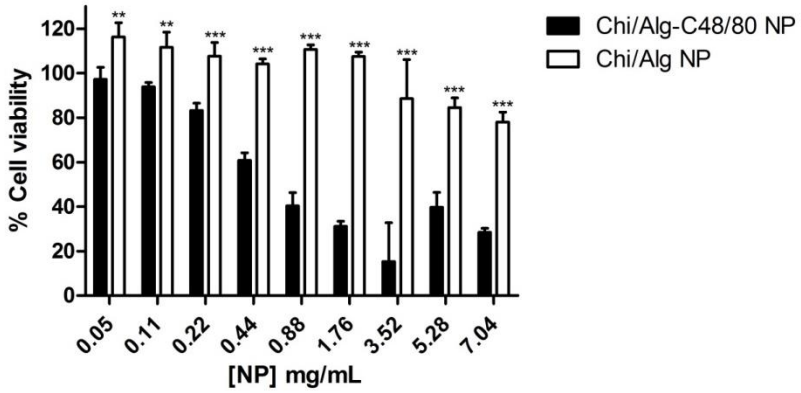

Figure 4.5 – Cytotoxicity of Chi/Alg-C48/80 NP and Chi/Alg NP. Different concentrations of nanoparticles were incubated for 24 h with spleen cells. The cell viability was measured by MTT assay. Each result is representative of at least two independent experiments performed in quadruplicate (mean ± SD).

Cytotoxicity of Chi/Alg-C48/80 was concentration dependent, with concentrations equal and higher than 0.88 mg/mL causing cell viabilities lower than 50 %. This difference in cytotoxicity can be explained not only by the incorporation of C48/80 and the potential toxic effect of this immunopotentiator by itself but also by the distinct physicochemical characteristics of the formulations. Chi/Alg NP are larger in size and have a zeta potential close to neutral. On the other hand, the more cytotoxic Chi/Alg-C48/80 NP are smaller and positively charged. Wan-Kyu Oh et al. compared the cytotoxic effect of cationic, neutral and negative nanoparticles on macrophages and found that the positively charged were the most toxic [25]. The same effect was described in a different study using tri-block copolymer nanoparticles with different surface charges [26]. The stronger interaction of cationic materials

with the negatively charged cellular surface and cell components is one of the mechanisms that can explain the increased toxicity of positively charged particles. Similarly, particle cytotoxicity usually shows a size-dependent cytotoxic pattern. For example, Kyung O Yu et al. tested a wide size-range of silica NP (30, 48, 118 and 535 nm) on a mouse keratinocyte HEL-30 cell line and showed that the smaller nanoparticles showed a much higher toxicity than the bigger ones [27]. The same pattern was observed by Napierska D et al. [28] however smaller particles are not always more toxic than micrometer particles [29]. In this particular case, different parameters may have contributed for the different cytotoxicity profile between Chi/Alg-C48/80 NP and Chi/Alg NP.

4.3.6 Uptake studies

The ability of the developed formulations to interact with macrophages was evaluated by confocal microscopy in RAW 264.7 cell line. Cells were incubated with FITC labeled Chi/Alg-C48/80 NP or Chi/Alg NP and the intracellular location of nanoparticles was analyzed by labeling the cells with Lysotracker © Red, which accumulates in the acidic endo-lysosomes. The results showed that NPs were moderately internalized by macrophages (Fig. 4.6A). After incubation of the NP with the cells for 4h, some FITC fluorescence was detected on cell cytoplasm however no yellow signals correspondent to co-localization of NPs with the lysosomes were identified on confocal images. To confirm if the antigens associated with the nanoparticles would also be internalized by antigen presenting cells together with NP, uptake studies were repeated with nanoparticles loaded with a fluorescent labeled protein. The results showed an extensive internalization of FITC-BSA loaded on both Chi/Alg-C48/80 NP and Chi/Alg NP (Fig. 4.6B). The fluorescence signal of BSA was detected mostly on cell cytoplasm with only a few yellow co-localization signals observed. More fluorescence was detected in the cytoplasm when cells were incubated with nanoparticles loaded with FITC-BSA than with FITC-labeled chitosan nanoparticles. This indicates that most likely some nanoparticles released the protein from outside the cell without being internalized. Kanchan et al. described that while the uptake of nanoparticles by APCs is favorable to the promotion of a cell mediated immune response, the internalization of the delivery system by itself is not required for elicit an antibody response [30]. Therefore, the results suggest that Chi/Alg-C48/80 NP may promote an antibody-biased immune response. Overall, the results showed that there were no significant differences regarding the uptake and distribution of Chi/Alg-C48/80 NP and Chi/Alg NP. This means that despite the different physicochemical

characteristics of C48/80 loaded and unloaded NP, the association of the mast cell activator with the NP did not affect the antigen uptake by antigen presenting cells.

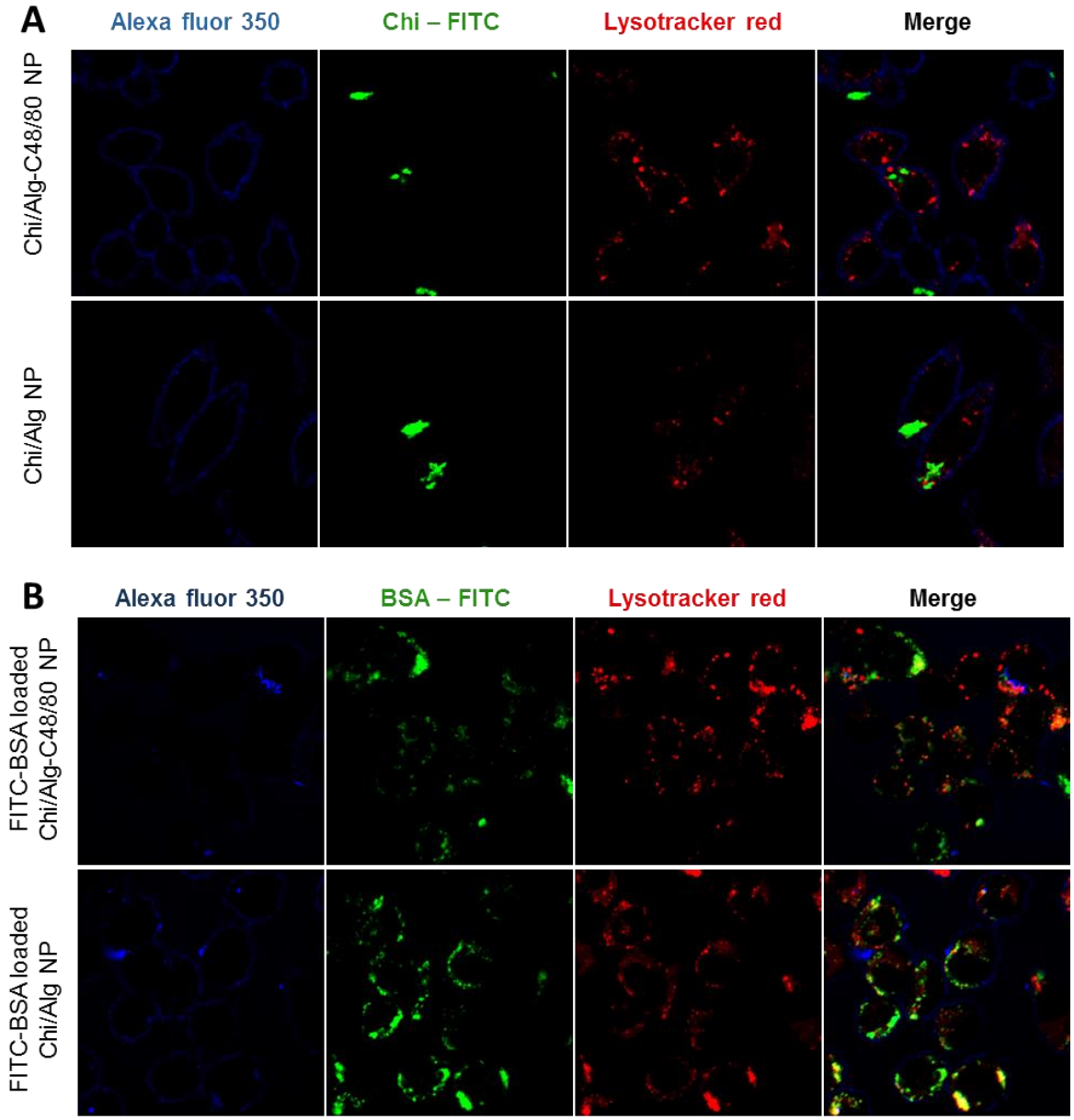

Figure 4.6 – Confocal microscopy analysis of NP interaction with macrophages (A) Uptake of nanoparticles was assessed by incubating 4 h, 100 μg/mL RAW 264.7 cells with Chi/Alg-C48/80 NP or Chi/Alg NP prepared with FITC labeled chitosan (green). (B) Uptake of a model antigen loaded into nanoparticles was assessed by incubating macrophages with NP loaded with FITC labeled BSA for 4 h (50 μg/mL). Cells were labeled with Alexa Fluor© 350 WGA (blue) to identify the membrane and Lysotracker© Red identifies the acidic endosomes and lysosomes.

4.4 Conclusions

This study describes the development and optimization of C48/80 loaded chitosan/alginate nanoparticles as a new vaccine delivery system. Our results indicated that characteristics of particles (mean particle size, surface charge and C48/80 loading efficacy) strongly depended on initial concentration of chitosan used to prepare the nanoparticles. The optimized Chi/Alg-C48/80 NP have a size of 564.3 nm and are positively charged (+ 25.51 mV). Furthermore, Chi/Alg-C48/80 NP showed ability to efficiently load model antigens, low cytotoxicity and were moderately internalized by macrophages. These features make this novel system a candidate for vaccine delivery.

References

1. Akagi, T., F. Shima, and M. Akashi, *Intracellular degradation and distribution of protein-encapsulated amphiphilic poly(amino acid) nanoparticles.* Biomaterials, 2011. **32**(21): p. 4959-67.
2. Smith, D.M., J.K. Simon, and J.R. Baker, Jr., *Applications of nanotechnology for immunology.* Nat Rev Immunol, 2013. **13**(8): p. 592-605.
3. Oyewumi, M.O., A. Kumar, and Z. Cui, *Nano-microparticles as immune adjuvants: correlating particle sizes and the resultant immune responses.* Expert Rev Vaccines, 2010. **9**(9): p. 1095-107.
4. Shen, H., et al., *Enhanced and prolonged cross-presentation following endosomal escape of exogenous antigens encapsulated in biodegradable nanoparticles.* Immunology, 2006. **117**(1): p. 78-88.
5. Thomann-Harwood, L.J., et al., *Nanogel vaccines targeting dendritic cells: contributions of the surface decoration and vaccine cargo on cell targeting and activation.* J Control Release, 2013. **166**(2): p. 95-105.
6. De Temmerman, M.L., et al., *Particulate vaccines: on the quest for optimal delivery and immune response.* Drug Discov Today, 2011. **16**(13-14): p. 569-82.
7. Koppolu, B. and D.A. Zaharoff, *The effect of antigen encapsulation in chitosan particles on uptake, activation and presentation by antigen presenting cells.* Biomaterials, 2013. **34**(9): p. 2359-69.
8. Arca, H.C., M. Gunbeyaz, and S. Senel, *Chitosan-based systems for the delivery of vaccine antigens.* Expert Rev Vaccines, 2009. **8**(7): p. 937-53.
9. Amidi, M., et al., *Chitosan-based delivery systems for protein therapeutics and antigens.* Adv Drug Deliv Rev, 2010. **62**(1): p. 59-82.
10. Baldrick, P., *The safety of chitosan as a pharmaceutical excipient.* Regul Toxicol Pharmacol, 2010. **56**(3): p. 290-9.
11. Borges, O., et al., *Immune response by nasal delivery of hepatitis B surface antigen and codelivery of a CpG ODN in alginate coated chitosan nanoparticles.* Eur J Pharm Biopharm, 2008. **69**(2): p. 405-16.
12. Borges, O., et al., *Alginate coated chitosan nanoparticles are an effective subcutaneous adjuvant for hepatitis B surface antigen.* Int Immunopharmacol, 2008. **8**(13-14): p. 1773-80.
13. Oliveira, C.R., et al., *A new strategy based on SmRho protein loaded chitosan nanoparticles as a candidate oral vaccine against schistosomiasis.* PLoS Negl Trop Dis, 2012. **6**(11): p. e1894.

14. Biswas, S., et al., *Development and characterization of alginate coated low molecular weight chitosan nanoparticles as new carriers for oral vaccine delivery in mice.* Carbohydr Polym, 2015. **121**: p. 403-10.
15. Staats, H.F., et al., *Mucosal targeting of a BoNT/A subunit vaccine adjuvanted with a mast cell activator enhances induction of BoNT/A neutralizing antibodies in rabbits.* PLoS One, 2011. **6**(1): p. e16532.
16. McGowen, A.L., et al., *The mast cell activator compound 48/80 is safe and effective when used as an adjuvant for intradermal immunization with Bacillus anthracis protective antigen.* Vaccine, 2009. **27**(27): p. 3544-52.
17. McLachlan, J.B., et al., *Mast cell activators: a new class of highly effective vaccine adjuvants.* Nat Med, 2008. **14**(5): p. 536-41.
18. Gwinn, W.M., et al., *A comparison of non-toxin vaccine adjuvants for their ability to enhance the immunogenicity of nasally-administered anthrax recombinant protective antigen.* Vaccine, 2013. **31**(11): p. 1480-9.
19. Zeng, L., et al., *Compound 48/80 acts as a potent mucosal adjuvant for vaccination against Streptococcus pneumoniae infection in young mice.* Vaccine, 2015. **33**(8): p. 1008-16.
20. Zheng, M., et al., *Cross-protection against influenza virus infection by intranasal administration of nucleoprotein-based vaccine with compound 48/80 adjuvant.* Hum Vaccin Immunother, 2015: p. 0.
21. Schijns, V.E. and E.C. Lavelle, *Trends in vaccine adjuvants.* Expert Rev Vaccines, 2011. **10**(4): p. 539-50.
22. Borges, O., et al., *Uptake studies in rat Peyer's patches, cytotoxicity and release studies of alginate coated chitosan nanoparticles for mucosal vaccination.* J Control Release, 2006. **114**(3): p. 348-58.
23. Foged, C., et al., *Particle size and surface charge affect particle uptake by human dendritic cells in an in vitro model.* Int J Pharm, 2005. **298**(2): p. 315-22.
24. Dee, K.C., D.A. Puleo, and R. Bizios, *Protein-Surface Interactions*, in *An Introduction To Tissue-Biomaterial Interactions*2003, John Wiley & Sons, Inc. p. 37-52.
25. Oh, W.K., et al., *Cellular uptake, cytotoxicity, and innate immune response of silica-titania hollow nanoparticles based on size and surface functionality.* ACS Nano, 2010. **4**(9): p. 5301-13.
26. Bhattacharjee, S., et al., *Cytotoxicity and cellular uptake of tri-block copolymer nanoparticles with different size and surface characteristics.* Part Fibre Toxicol, 2012. **9**: p. 11.
27. Yu, K., et al., *Toxicity of amorphous silica nanoparticles in mouse keratinocytes.* Journal of Nanoparticle Research, 2009. **11**(1): p. 15-24.
28. Napierska, D., et al., *Size-dependent cytotoxicity of monodisperse silica nanoparticles in human endothelial cells.* Small, 2009. **5**(7): p. 846-53.
29. Karlsson, H.L., et al., *Size-dependent toxicity of metal oxide particles--a comparison between nano- and micrometer size.* Toxicol Lett, 2009. **188**(2): p. 112-8.
30. Kanchan, V. and A.K. Panda, *Interactions of antigen-loaded polylactide particles with macrophages and their correlation with the immune response.* Biomaterials, 2007. **28**(35): p. 5344-57.

CHAPTER 5

C48/80 associated with chitosan nanoparticles as a path to enhanced mucosal immunity

This chapter was adapted from:

Bento, D, HF Staats, Gonçalves T, Borges B. Development of a novel adjuvanted nasal vaccine: C48/80 associated with chitosan nanoparticles as a path to enhance mucosal immunity. Eur J Pharm Biopharm, 2015. 93: p. 149-64.

Abstract

In a time in which mucosal vaccines development has been delayed by the lack of safe and effective mucosal adjuvants, the combination of adjuvants has starting to be explored as a strategy to obtain potent vaccine formulations. This study describes a novel adjuvant combination as an effective approach for a nasal vaccine - the association of the mast cell activator compound 48/80 with chitosan based nanoparticles. It was hypothesized that mucoadhesive nanoparticles would promote the cellular uptake and prolong the antigen residence time on nasal cavity. Simultaneously, mast cell activation would promote a local microenvironment favourable to the devolvement of an immune response. To test this hypothesis, two different C48/80 loaded nanoparticles (NP) were prepared: Chitosan-C48/80 NP (Chi-C48/80 NP) and Chitosan/Alginate-C48/80 NP (Chi/Alg-C48/80 NP). The potential as a vaccine adjuvant of the two delivery systems was evaluated and directly compared. Both formulations had a mean size near 500 nm and a positive charge; however Chi-C48/80 NP was a more effective adjuvant delivery system when compared with Chi/Alg-C48/80 NP or C48/80 alone. Chi-C48/80 NP activated mast cells at a greater extent, was better internalized by antigen presenting cells than Chi/Alg-C48/80 NP and successfully enhanced the nasal residence time of a model antigen. Superiority of Chi-C48/80 NP as adjuvant was also observed *in vivo*. Therefore, nasal immunization of mice with *Bacillus anthracis* protective antigen (PA) adsorbed on Chi-C48/80 NP elicited high levels of serum anti-PA neutralizing antibodies and a more balanced Th1/Th2 profile than C48/80 in solution or Chi/Alg-C48/80 NP. The incorporation of C48/80 within Chi NP also promoted a mucosal immunity greater than all the other adjuvanted groups tested, showing that the combination of a mast cell activator with chitosan NP could be a promising strategy for nasal immunization.

5.1 Introduction

Mucosal vaccination offers several advantages over the parenteral strategy, such as no requirement for specialized medical personnel for the vaccine administration, the higher patient compliance and the ability to induce both systemic and mucosal immune responses [1]. With the vaccine development in the present being centered on poorly immunogenic subunit antigens instead of traditional whole-cells vaccines the concomitant use of adjuvants is required. This need of more effective and potent adjuvants has been delaying the development of mucosal vaccines.

Mast cells, best known for their function in allergy, have been recognized in recent years as important players in the development of protective immune responses [2-4]. These cells are strategically located at the host-environment interface and promptly respond to pathogen stimulation releasing preformed mediators that activate the innate immune system to mobilize various immune cells to the site of infection and to draining lymph nodes. Thus, the use of mast cell activators as new class of vaccine adjuvants began to be explored [5] and since then, additional studies confirmed the immunopotentiator properties of the mast cell activator C48/80 [6-8]. In fact, mast cells play a significant role in the immune response induced by other adjuvants such as Il-18 [9], the cholera toxin derived CTA1-DD [10], imiquimod [11] and alum [12] . Polymyxins have also shown the ability to induce mast cell degranulation *in vitro* and to increase antigen-specific immunity [13]. Therefore, several scientific reports indicate the possible involvement of mast cells in the immune responses induced by different adjuvants.

In addition to mast cell activators, particulate delivery systems represents a pathogen-mimicking formulation with some attractive features for vaccine development [14-16], such as promotion of a depot effect and increased uptake by antigen presenting cells (APCs) [17]. These delivery systems are particularly interesting for the design of mucosal vaccines by reducing the rate of dilution and degradation of antigen on mucosal tissues [18] . Among other polymers, chitosan, a biocompatible, biodegradable and non-toxic polysaccharide with immunostimulating properties, is considered to be very promising on the design of antigen delivery systems for mucosal surfaces [19, 20]. Its cationic nature and mucoadhesivity helps to reduce the antigen clearance rate in the nasal cavity. Besides, the ability of chitosan to open tight junctions promotes the antigen penetration through nasal mucosal surface and uptake by APCs [21, 22], a process usually hindered by the tight arrangement of the epithelial cells.

The combination of adjuvants, particularly strategies involving the association of particles with immunostimulatory compounds, has lately been appointed as a promising approach in

vaccine development [23], however, until recently, not very often explored. Besides the possibility of obtaining a more potent adjuvant formulation than each individual component, the delivery of an immunopotentiator molecule by particulate delivery systems can attenuate any potential toxic effect resultant of the immediate availability of the molecule [15, 24]. The ability of the mast cell activator C48/80 to promote an immune response *in vivo* was already established. However, the effect of the association of the mast cell activator with nanoparticles still lacks a thorough investigation. So our aim was to associate C48/80 with chitosan nanoparticles and assess the potential of this strategy as a combined vaccine adjuvant for the induction of a mucosal and systemic immunity. We hypothesize that chitosan-based nanoparticles would extend the residence time of both antigen and C48/80 on nasal cavity and, at the same time, the activation of mast cells would promote a local microenvironment favourable to the initiation of an immune response. Alginate, a biodegradable and anionic polysaccharide was also included in chitosan-based nanoparticles with the aim to facilitate the encapsulation of the cationic mast cell activator C48/80 compound. This polymer have been successfully used for vaccine delivery [25, 26] and had been reported to hold immunomodulatory properties [27]. To analyse if this combined effect would result in a better vaccine formulation we prepared and tested two chitosan based nanoparticles associated with the C48/80: C48/80 loaded chitosan nanoparticles (Chi-C48/80 NP) and C48/80 loaded chitosan/alginate nanoparticles (Chi/Alg-C48/80 NP). The potential of the two formulations were evaluated and compared first *in vitro* and then *in vivo* using the protective antigen of anthrax (PA) as a model antigen.

5.2 Materials and Methods

5.2.1 Materials

LMW Chitosan (deacetylation degree 95 %) was purchased from Primex BioChemicals AS (Avaldsnes, Norway) and used after a purification process described in chapter 3, section 3.3.2. Alginate (MANUCOL LB®) was kindly donated by ISP Technologies Inc. (Surrey, UK). Compound 48/80, MTT (3-[4, 5-dimethylthiazol-2-yl]-2,5-diphenyl tetrazolium bromide) were obtained from Sigma-Aldrich (Sintra, Portugal). BCA assay kit was obtained from Pierce Chemical Company (Rockford, IL, USA). Fluorescein isothiocyanate (FITC) was purchased from Santa Cruz Biotechnology (Santa Cruz, CA, USA). Trypsin-EDTA and fetal bovine serum (FBS) were obtained from Life Technologies Corporation (Paisley, UK). The nuclear stain Hoechst 33342, Alexa Fluor® 594 WGA and Alexa Fluor® 647 labeled ovalbumin were purchased from Invitrogen. Recombinant protective antigen of anthrax (PA) and recombinant

lethal factor (LF) were purchased from List Biologicals (Campbell, CA, USA). All other reagents used were of analytical grade.

5.2.2 Cell culture

5.2.2.1 Cell lines maintenance

Mouse RAW 264.7 macrophage cells (ECACC, Salisbury, UK) were maintained in Dulbecco's modified Eagle medium (DMEM) supplemented with HEPES 1 mM, sodium pyruvate 100 mM and 10 % of non-inactivated fetal bovine serum (FBS). A549 cell line (ATCC, Manassas, VA, USA) was cultured in F12 Ham nutrient mixture with 10 % of heat-inactivated FBS and supplemented with 1 % Penicillin/Streptomycin. The human mast cell line HMC-1 (gift from Dr Butterfield, Mayo Clinic, USA) was grown in Iscove's Modified Dulbecco's Medium (IMDM) with 25 mM HEPES, 3.024 g/L sodium bicarbonate supplemented with 2 mM glutamine, 1 % penicillin⁄streptomycin and 10 % defined, iron-supplemented bovine calf serum (Hyclone, Logan Utah). J774A.1 mouse macrophages (ATCC, Manassas, VA, USA) were maintained in DMEM with 4 mM L-glutamine, 4.5 g/L glucose, 1 mM sodium pyruvate, 1.5 g/L sodium bicarbonate and supplemented with 10 % of non-inactivated FBS and 1 % penicillin/streptomycin. All cell lines were maintained in a 5 % CO_2 humid atmosphere at 37 °C.

5.2.2.1 Generation of human dendritic cells from peripheral blood monocytes

Immature dendritic cells were generated from peripheral blood mononuclear cells (PBMCs) accordingly to an established method [28]. Briefly, PBMCs were isolated from fresh human blood on a density gradient with Lymphoprep (Axis-Shield, Oslo, Norway) by centrifugation at 1200 g for 20 min. The cell suspension was diluted 1:1 in PBS and washed 3 times, by centrifugation at 490 g, for 10 min at RT.

The cell suspension was resuspended in RPMI medium and seeded at 2.0 x 10^6 cells/mL in a 6-well plate. After 3 h of plastic adherence at 37 ºC, non-adherent cells were removed by washing 5 times. For differentiation of monocytes into immature DCs, hereafter called PBDCs (peripheral blood derived dendritic cells), the remaining adherent cell fraction was cultured in RPMI medium supplemented with 10 % heat-inactivated FBS, 5 ng/mL IL-4 (BD Biosciences, San Jose, CA, USA) and 10 ng/mL granulocyte–macrophage colony-stimulating factor (GM-CSF) (BD Biosciences, San Jose, USA). The cells were maintained at 37 °C and 5 % CO_2 and, on days 3 and 5 of culture, were fed with fresh medium and cytokines and used on day 6.

5.2.3 Preparation of C48/80 loaded nanoparticles

5.2.3.1 Chitosan nanoparticles

C48/80 loaded chitosan nanoparticles (Chi-C48/80 NP) were prepared by adding dropwise 3 mL of an alkaline solution (5 mM NaOH) of C48/80 and Na_2SO_4 (0.3 mg/mL and 2.03 mg/mL, respectively) to 3 mL of a chitosan solution (1 mg/mL in acetic acid 0.1 %) under high speed vortexing. The nanoparticles were formed after further maturation for 60 min under magnetic stirring. Blank chitosan particles (Chi NP) were obtained by preparing nanoparticles exactly in the same conditions but without C48/80.

5.2.3.2 Chitosan/alginate nanoparticles

C48/80 loaded Chitosan/alginate nanoparticles (Chi/Alg-C48/80 NP) were prepared using a two-step method modified from Rajaonarivony et al. [29]. First, 3 mL of a calcium chloride solution (2 mg/mL) was added dropwise to 47 mL of sodium alginate solution (0.063 %, pH 5.1) in a ultrasound bath while stirring for 15 min at 25000 rpm with a homogenizer (Ystral GmbH D-7801, Dottingen, Germany) in order to prepare a pregel. Then, Ca^{2+}/alginate pregel was stirred for further 20 min with a magnetic stirrer. Finally, the particles were formed upon mixing 3 mL of pregel with an equal volume of a solution containing chitosan and C48/80 (0.05 % and 0.3 mg/mL, respectively, at pH 5.4) during high-speed vortexing, followed by 30 min of maturation with magnetic stirring. Blank chitosan/alginate particles (Chi/Alg NP) were obtained by preparing the particles under the same conditions but without C48/80.

5.2.4 Characterization of nanoparticles

5.2.4.1 Morphology

Particle morphology was evaluated by cryo-scanning electron microscopy (cryo-SEM). The nanoparticles resuspended in milli-Q water were mounted on a sample-holder and frozen by immersion in liquid nitrogen. Then the sample holder was placed into the cryo-chamber where it was kept under vaccum at – 150 ºC. The samples were fractured and then the water sublimated at – 90 ºC for 2 min. Finally, the samples were cooled back down to -150 ºC, coated with gold and observed in FE-CryoSEM/EDS, JEOL JSM 6301F (JEOL, Peabody, MA, USA).

5.2.4.2 Size and Zeta Potential

Particle size and zeta potential were analyzed by dynamic light scattering and electrophoretic light scattering ELS, respectively, using a Delsa™ Nano C (Beckman Coulter, Miami, FL, USA). Size was measured by diluting the nanoparticle suspension in milli-Q water and for zeta potential nanoparticles were dispersed in 1 mM NaCl solution.

5.2.4.3 Loading efficacy of C48/80

In order to evaluate the loading efficacy (LE) of C48/80, nanoparticles were centrifuged 20 min at 8000 g and C48/80 was quantified in the supernatant using a method validated by our group [30]. Briefly, 25 µL of carbonate buffer pH 9.6 was added to 175 µL of sample in a 96-well plate. Subsequently, 50 µL of a 15 % acetaldehyde solution containing 1.5 % of sodium nitroprusside was added and the absorbance measured at 570 nm. The loading efficacy was calculated using equation 5.1.

$$\text{C48/80 LE (\%)} = \frac{\text{totalC48/80 (µg/mL)} - \text{freeC48/80 in supernatant (µg/mL)}}{\text{total C48/80 (µg/mL)}} \text{ x } 100 \quad \text{(Equation 5.1)}$$

5.2.5 Preparation of PA loaded nanoparticles

The loading of PA on nanoparticle surface was made by physical adsorption. After centrifugation for 30 min at 4500 g, nanoparticles were resuspended in 25 mM acetate buffer (pH 5.7) and incubated with PA at 167 µg/mL for 30 min. After incubation with the antigen, particles were centrifuged at 12000 g for 20 min and the supernatant collected to measured free PA using BCA assay. The PA loading efficacy (LE) was calculated by difference between the total amount of PA added to the medium and the amount of PA remaining in the nanoparticle supernatant, using the equation 5.2.

$$\text{PA LE (\%)} = \frac{\text{(total amount of PA (µg/mL)-non bound PA (µg/mL))}}{\text{total amount of PA (µg/mL)}} \times 100 \quad \text{(Equation 5.2)}$$

5.2.6 Cytotoxicity studies

Single cell suspensions of spleen cells from 8-week old female C57BL/6 mice (Charles River, France) were prepared as previously described [31]. Cells were seeded in a 96-well plate at a density of 1 x 10^6 cells/well in complete RPMI 1640 medium (supplemented with 10 % (v/v) fetal bovine serum, 2 mM glutamine, 1 % Penicillin/Streptomycin and 20 mM HEPES buffer) and different concentrations of C48/80 in solution or loaded in nanoparticles were added. After 24 h of incubation, cellular viability was assessed by MTT assay. Briefly, 20 µL of

MTT 5 mg/mL in PBS (pH 7.4) was added to each well and incubated for more 4 h. The plate was centrifuged for 25 min at 800 g and the supernatants removed. Finally, formazan crystals produced by metabolic active cells were solubilized with 200 μL of DMSO per well and the optical density measured at 540 nm with 630 nm as wavelength reference.

Cytotoxicity was also evaluated in A549 cell line. Cells were seeded in 96-well plate at a density of 1 x 10^4 cells/well in 100 μL of F-12 Ham medium and incubated overnight. In the next day, medium was replaced by fresh medium and formulations were added to a final volume of 200 μL/well. After incubation for 24 h, 20 μL of MTT was added and plates incubated for 2 h at 37 °C. Culture medium was discarded and formazan crystals were dissolved as described for spleen cells.

For both cells, the viability of non-treated cells (control) was defined as 100 % and the relative cell viability (%) calculated using equation 5.3.

$$\text{Cell viability (\%)} = \frac{\text{OD sample (540 nm) - OD sample (630 nm)}}{\text{OD control (540 nm) - OD control (630 nm)}} \times 100 \quad \text{(Equation 5.3)}$$

5.2.7 Uptake of nanoparticles by antigen presenting cells

5.2.7.1 Confocal microscopy

The synthesis of FITC-labeled chitosan was based on the reaction between the isothiocyanate group of FITC (Ex/Em – 490/525) and the primary amino group of chitosan. Briefly, chitosan was labeled by mixing 35 mL of dehydrated methanol containing 25 mg of FITC to 25 mL of a 1 % (w/v) chitosan in 0.1 M of acetic acid solution. After 3 h of reaction in the dark at RT, the FITC-labeled chitosan was precipitated with 0.2 M NaOH until pH 10. FITC-labeled chitosan was obtained by centrifugation for 30 min at 4500 g and the resultant pellet was washed 3 times with a mixture of methanol: water (70:30, v/v). The labeled chitosan was resuspended in 15 mL of 0.1 M acetic acid solution and stirred overnight. Polymer solution was dialyzed in the dark against 2.5 L of distilled water for 3 days before freeze-drying using a freeze dry system (FreezeZone 6, Labconco, Kansas City, MO, US).

To evaluate the cellular uptake of nanoparticles, RAW 264.7 macrophage cells were seeded on glass coverslips in 12-well plates at a density of 2.5 x 10^5 cells per well and incubated overnight. On the next day, media was replaced by fresh DMEM and FITC-Chi-C48/80 NP or FITC-Chi/Alg-C48/80 NP were added into the wells, at a final concentration of 100 μg/mL, and incubated for 0.5 h, 1 h or 4 h. At the end of incubation, RAW 264.7 cells were washed three times with PBS pH 7.4 and fixed with 4 % paraformaldehyde in PBS for 15 min at 37 ºC. The nucleus of the pre-fixed cells were labeled using Hoechst 33342 dye, according

to manufacturer's instructions. Then the cells were washed twice with PBS and the coverslips mounted in microscope slides with DAKO mounting medium. Samples were examined under an inverted laser scanning confocal microscope (Zeiss LSM 510 META, Carl Zeiss, Oberkochen, Germany), with a 63 x oil immersion objective, and images acquired with the LSM 510 imaging software.

5.2.7.2 Flow cytometry

The uptake of nanoparticles by macrophages and dendritic cells was also evaluated by FACS. RAW 264.7 and PBDCs were plated at a density of 3 x 10^5 cells and 1.5 x 10^5 cells per well, respectively, in a 24-well plate and incubated overnight. On the next day, culture medium was replaced with fresh one and cells were incubated for 2 h at 37 °C with FITC-labeled Chi-C48/80 NP or Chi/Alg-C48/80 NP. After the incubation period, cells were washed 3 times with PBS, collected using cell dissociation medium (NaCl 8 g/L, Na_2HPO_4 1.16 g/L, KH_2PO_4 0.2 g/L, EDTA 0.16 g/L) and finally resuspended in cold PBS for uptake analysis by flow cytometry. To quench external FITC, trypan blue at a final concentration of 0.2 % was added to each sample 5 min before FACS analysis. The intracellular fluorescence intensity was determined on Becton Dickinson FACSCalibur flow cytometer (San Jose, CA, USA) and data analyzed by the BD CellQuest Software. For each sample, 10 000 events were evaluated and uptake was expressed as % of FITC positive cells.

5.2.8 Mast cell activation studies

5.2.8.1 β-hexosaminidase release

HMC-1 cells were plated in 96-well flat bottom plates at a density of 4 x 10^5 cells/well in 180 µl of sterile Tyrode's solution (Sigma-Aldrich). Cells were stimulated for 60 min at 37 ºC with C48/80 at 20, 40 or 80 µg/mL (positive control) or with nanoparticles containing the equivalent amount of C48/80 as the control. Blank formulations, were also tested to evaluate the effect of the incorporation of the mast cell activator into nanoparticles. HMC-1 cells mixed with 0.5 % Triton-X 100 and cells without any stimulus were used to measure total β-hexosaminidase (β-hex) release and the basal release, respectively.

The protocol for measurement of β-hex released in the supernatant was adapted from methods previously described [32, 33]. Briefly, 20 µl of cell supernatant was incubated with 30 µL of substrate solution (1.3 mg/mL p-nitrophenyl-N-acetyl-β-D-glucosaminidine) in citrate buffer (pH 4.5, 0.1 M) for 90 min at 37 ºC. After this time, the enzymatic reaction was stopped and a color change induced by the addition of 100 µL carbonate buffer (0.1 M, pH

10). The absorbance at 405 nm was measured using a Multiskan EX 96-well plate reader (Thermo Electron Corporation, Vantaa, Finland). Percentage (%) of β-hex release was calculated using equation 5.4.

$$\beta\text{-hex release (\%)} = \frac{\text{OD sample} - \text{OD basal}}{\text{OD Triton X}-100} \text{ x } 100 \quad \text{(Equation 5.4)}$$

5.2.8.2 Confocal microscopy

HMC-1 cells were plated in 8 well ibiTreat μ-Slides (Ibidi, Germany) at a density of 2 x 10^4 cells/well and incubated overnight. On the next day, culture medium was discarded and the nucleus and cell membrane of live cells were labeled with Hoechst 33342 and Alexa Fluor ® 594 WGA respectively, according to manufacturer's instructions. Cells were washed twice with PBS (pH 7.4) and 230 μL of Tyrode's solution added to each well. Images of a pre-established microscope field were acquired before and 2 min after treatment of cells with Chi-C48/80 NP.

5.2.9 *In vivo* studies

Six-week-old SKH1 female mice and 6-8 week old C57BL/6NCr female mice from Charles River (National Cancer Institute, Frederick) were housed in filter top cages with food and water provided *ad libitum*. All experiments were performed according to protocols approved by Duke University Division of Laboratory Animal Resources and Duke University Institutional Animal Care and Use Committee (IACUC).

5.2.9.1 Nasal residence time of a model antigen

The use of hairless animals prevents the attenuation of the fluorescent signal on *in vivo* imaging. So, to evaluate the nasal clearance of a model antigen we used SKH1 hairless mice, an immune competent model that have blood counts, immunoglobulin levels, and CD4+ and CD8+ T cells comparable to C57Bl/6 strain [34]. Nasal residence time measurements were performed according to the method described elsewhere [35] with slight modifications. The mice (n = 7 for each formulation in a total of 2 independent experiments) were slightly anesthetized with isoflurane prior to the nasal administration of 15 μL (5 μg) of Alexa Fluor 647 conjugated OVA alone or formulated with 15 μg of C48/80 in solution or associated with nanoparticles. One control group received Chi NP at the same concentration of nanoparticles than Chi-C48/80 NP. The external surface of the mouse nose was cleaned with a paper towel to remove any nanoparticles adhering to the external surface of the nose and fluorescence

intensity was immediately determined with the IVIS Spectrum imaging system (Caliper Life Sciences, USA). Scans were performed in different time points (0, 0.5, 1, 2, 4, 6 and 24 h). In between scans, mice were put back in their cages to recover from anesthesia. Images were analyzed using Living Image 3.1 software from Caliper Life Sciences (Hopkinton, MA, USA). The image autofluorescent background was obtained with Ex 605/Em 680 and for the primary image Ex 640/Em 680 was used. The image math method was applied to obtain the background subtracted image used for the quantitative analysis via ROI (region-of-interest) analysis. Fluorescence intensity at t = 0 was defined as 100 %.

5.2.9.2 Nasal immunization

Mice (5 per group in 2 experiments, n=10) were intranasally immunized on days 0, 7 and 21 with 15 μL of vaccine formulation, 7.5 μL per nostril, under isoflurane anesthesia (IsoFlo, USP; SOLVAY Animal Health, Mendota Heights, MN). Vaccine groups are detailed in table 5.1 and included PA alone, PA + C48/80 in solution or incorporated in Chi-C48/80 NP and Chi/Alg-C48/80 NP, PA + Chi NP, PA + Chi NP + C48/80 (C48/80 not incorporated within the nanoparticles) and naïve group vaccinated with saline. Serum was collected on days 14, 21 and 42 and spleens, nasal washes, fecal material and vaginal lavage were collected on day 42 and processed as described below.

Table 5.1 – Description of the immunization study groups.

Group	NP formulation	C48/80 μg/mouse	PA μg/mouse	Route	Immunization schedule
Naïve	-	0	0	nasal	Days 0, 7 and 21
PA alone	-	0	2.5 μg	nasal	Days 0, 7 and 21
C48/80	-	15 μg [a]	2.5 μg	nasal	Days 0, 7 and 21
Chi-C48/80 NP	Chi-C48/80 NP	15 μg [b]	2.5 μg	nasal	Days 0, 7 and 21
Chi NP	Chi NP	0	2.5 μg	nasal	Days 0, 7 and 21
Chi NP + C48/80	Chi NP	15 μg [a]	2.5 μg	nasal	Days 0, 7 and 21
Chi/Alg-C48/80	Chi/Alg-C48/80 NP	15 μg [b]	2.5 μg	nasal	Days 0, 7 and 21

[a] C48/80 in solution, [b] C48/80 incorporated in the nanoparticle formulation

5.2.9.3 Sample collection

Blood samples were collected by the submandibular lancet method to microcentrifuge tubes and centrifuged at 7000 rpm for 15 min. Vaginal washes were collected from mice under isoflurane anesthesia. The vaginal cavity was washed by instilling 100 μL of sterile PBS and flush the lavage fluid in - out a few times before collect it to a microcentrifuge tube. Samples

were centrifuged at 13000 rpm during 10 min and supernatants collected. Fecal extracts were prepared by mixing the collected fecal pellets with fecal extraction buffer (phosphate-buffered saline [PBS], 10 % normal goat serum, 0.1 % Kathon) at 100 mg/mL and vortexing for 30 min to disrupt the fecal pellet. The vortexed mixture was centrifuged at 13000 rpm for 10 min and the supernatant collected. Nasal lavage samples were collected from euthanized mice. The lower jaw of the mice was cut way and the nasal lavage collected by instilling 1 ml of sterile PBS posteriorly into the nasal cavity. Fluid exiting the nostrils was collected and spun at 13000 rpm at 4 °C for 20 min. Collected and processed samples were stored at −20 °C until further analysis.

5.2.9.4 Measurement of antibodies by ELISA

The titers of PA-specific IgG, IgG1 and IgG2c isotypes, anti-PA IgE and anti-PA IgA antibodies were determined by ELISA as described by McLachlan et al. [5]. Black Maxisorp 384-well plates (Nalge Nunc International, Rochester, NY, USA) were coated with 2 μg/mL of PA diluted in 50 mM carbonate/bicarbonate buffer pH 9.5. After overnight incubation at 4 ºC, non-specific binding sites were blocked with 3 % nonfat dry milk in carbonate/bicarbonate buffer with 0.1 % v/v Kathon for at least 2 h. Plates were washed 4 times with wash buffer (0.1 % Kathon and 0.05 % Tween 20 in PBS) and samples serial diluted in sample diluent (1 % w/v bovine serum albumin, 1 % w/v nonfat dry milk, 5 % normal goat serum, 0.05 % Tween 20, 0.1 % Kathon in PBS) were added to the plate and incubated overnight at 4 ºC. Plates were washed and alkaline phosphatase conjugated goat anti-mouse secondary antibodies (Southern Biotech, Birmingham, AL, USA) 1:8000 diluted in secondary antibody diluent (0.5 % bovine serum albumin, 5 % normal goat serum, 0.05 % Tween 20 and 0.1 % Kathon) were added to the plates and incubated for 2 h at room temperature. Plates were washed and the fluorescent AttoPhos substrate (Promega, Madison, WI, USA) was added to each well and incubated for 15 min at RT. The plate was then read on a fluorescence microplate reader at 440 nm excitation and 570 nm emission. The end-point titer presented in the results represents the antilog of the last log2 dilution for which the relative light units were at least three-fold higher than the value of the naive sample equally diluted. The log 2 endpoint titers were used for statistical analysis. Samples with undetectable titers were assigned a titer of one less than the first dilution tested.

5.2.9.5 Spleen cell restimulation

Spleen cells were collected on day 42 and a single cell suspension of cells was prepared using a 70 μm cell strainer. The erythrocytes from each spleen were lysed with 1 mL of ACK lysing buffer (Lonza, Walkersville, MD, USA), the spleen cells were washed and resuspended in T cell media (RPMI 1640, 10 % FBS, 20 mM HEPES, 1 % Penicillin/Streptomycin, 50 μM 2-Mercaptoethanol, 1 % of 1 N NaOH, 1 % sodium pyruvate, 1 % MEM non-essential amino acids, 2 % MEM amino acids). For the restimulation assay, 500 μL of suspension was plated at 2.5×10^6 cells/mL in 48-well plates and 500 μL of either T cell media alone or 10 μg/mL PA in media (to a final concentration of 5 μg/ml) was added to the cells. The plates were incubated at 37 °C for 5 days to induce cytokine production by antigen-specific T-cells. Supernatants were harvested to 96-well deep well plates and stored at −80 °C until further analysis.

5.2.9.6 Cytokine profiles

Spleen cell restimulation cytokine profiles were determined using a multiplex bead assay from R&D (Minneapolis, MN, USA) according to the supplier's instructions. Cytokines measured included IL-2, IL-4, IL-10, IL-17, IL-22 and IFN-gamma. Samples with cytokine concentrations below the low value of the standard curve were assigned a value equal to a quarter of the low standard for statistical analysis. Data shown are the mean Ag-specific cytokine production for each group (i.e., PA-induced cytokine production − unstimulated cell cytokine production).

5.2.9.7 *In vitro* LeTx neutralization assay

A macrophage toxicity assay using J774A.1 mouse macrophage cell line was used to determine the ability of serum anti-PA antibodies to neutralize LeTx (lethal toxin). The assay was performed as previously described [36]. Briefly, serum samples (first diluted to 1:64 in media and then serially diluted 1:2, 12-folds) were incubated with LeTx and then added to the cells for a final concentration of 187.5 ng/ml for both PA and LF**.** The viability of the cells was determined using CellTiter 96 Aqueous (Promega, Madison, WI), according to the supplier's instructions. Percent neutralization (NT) was calculated using the equation 5.5.

$$\text{NT (\%)} = \frac{\text{OD sample - OD LeTx standard}}{\text{OD cells only - OD LeTx standard}} \text{ x } 100 \quad \text{(Equation 5.5)}$$

The optical density (OD) of a medium-only well (i.e., no cells) was subtracted from all values before percent neutralization was calculated. Fifty percent neutralization titers (NT50) were calculated by plotting percent neutralization vs. serum dilution and non-linear regression was used to calculate the dilution at which 50 % of the cells were viable, ie, serum dilution needed to neutralize 50 % of LeTx. Samples with an NT50 less than 1:128 were below our tested range and were assigned a value of 1:2 for graphical representation and statistical evaluation.

5.2.10 Statistical analysis

Statistical analysis was performed with GraphPad Prism v 5.03 (GraphPad Software Inc., La Jolla, CA, USA). Unless otherwise stated in the figures, ANOVA followed by Tukey's post-test was used for multiple comparisons. Comparisons of two samples were made using Student's t-test. Statistical analysis of cytokine secretion was performed using a Kruskal-Wallis non-parametric test followed by Dunns post-test. A p value < 0.05 was considered statistically significant.

5.3 Results and discussion

5.3.1 Characteristics of C48/80 loaded nanoparticles

Two C48/80 loaded delivery systems were prepared – Chi-C48/80 NP and Chi/Alg-C48/80 NP. Blank formulations, without the mast cell activator, were also obtained to investigate the effect of C48/80 incorporation on the characteristics of chitosan based nanoparticles. Mean particle diameter, polydispersity index (PI), zeta potential (ZP) and loading efficacy of C48/80 were summarized on table from figure 5.1A. C48/80 loaded and unloaded chitosan nanoparticles were both monodisperse (PI < 0.162) with sizes around 500 nm and 400 nm, respectively. Chi/Alg-C48/80 NP were slightly more polydisperse (PI = 0.280) but the average size (564 nm) was not statistically different than the Chi-C48/80 NP. On the other hand, was found that the unloaded Chi/Alg NP were highly polydisperse (PI > 1) with a mean diameter of around 5750 nm. Since the zeta potential of this particles was + 5.3 mV, and considering that particles with zeta potential close to zero have a great tendency to agglomerate, this mean size most likely corresponded to agglomerates of smaller particles. All the other particles were positively charged with zeta potential higher than + 21 mV which is important for the stability of the formulations and for interactions with cell membrane, promoting the uptake by APCs [37].

A

Formulation	Size (nm)	PI [a]	ZP (mV)[b]	% LE (C48/80)[c]
Chi-C48/80 NP	500.9 ± 65.2	0.161 ± 0.051	23.83 ± 3.76	18.65 ± 2.99
Chi NP	396.2 ± 35.0	0.156 ± 0.037	21.59 ± 2.81	- [d]
Chi/Alg-C48/80 NP	564.3 ± 201.4	0.280 ± 0.038	25.51 ± 4.04	29.56 ± 1.59
Chi/Alg NP	5752.3 ± 529.6	1.221 ± 0.248	5.33 ± 5.23	- [d]

[a] Polydispersity index, [b] Zeta Potential, [c] C48/80 loading efficacy, [d] without C48/80

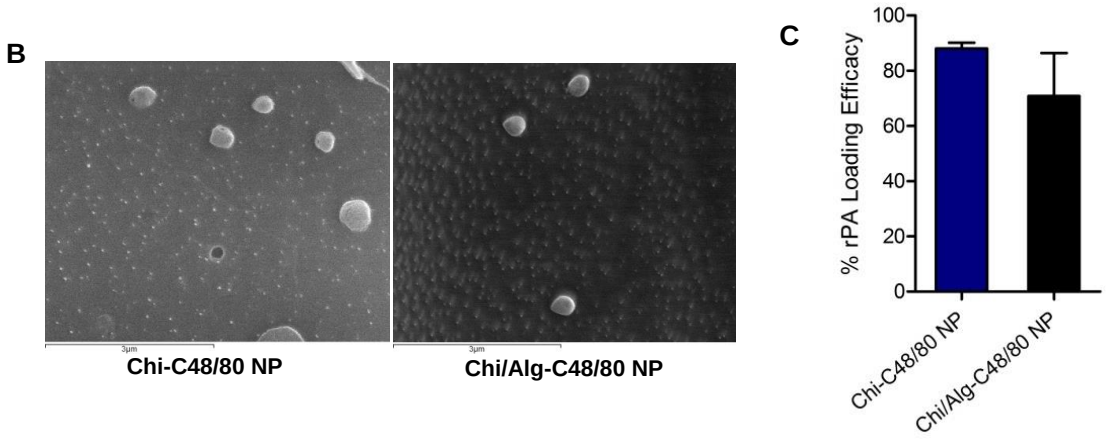

Figure 5.1 – Characteristics of C48/80 loaded chitosan based nanoparticles. (A) Particle size distributions in milli-Q water and the mean value of zeta potential of Chi-C48/80 NP, Chi/Alg-C48/80 NP and correspondent blank nanoparticles dispersed in 1 mM NaCl solution; mean ± SD, n ≥ 3. (B) Representative cryo-SEM images of Chi-C48/80 NP and Chi/Alg-C48/80 NP. Scale bar, 3 μm. (C) Loading efficacy of PA on nanoparticles. Nanoparticles were incubated with PA for 30 min in acetate buffer pH 5.7 at RT. The unbound protein was quantified in the supernatant using the BCA assay. Bars represent mean ± SD, n=4, ** $p < 0.01$.

While the incorporation of C48/80 into Chi NP only slightly affected the nanoparticle size, the same was not true for Chi/Alg NP. The incorporation of the cationic compound C48/80 into Chi/Alg NP significantly decreased particle size and significantly increased the zeta potential ($p < 0.001$), resulting in a greater stability of the nanoparticle suspension. The cryo-SEM images revealed that both C48/80 loaded NPs have a similar nearly spherical shape (Fig. 5.1B) and confirmed the mean size of Chi-C48/80 NP and Chi/Alg-C48/80 NP, measured by dynamic light scattering.

5.3.2 Incorporation of C48/80 on both nanoparticles decreases its cytotoxicity

Evaluation of the safety of adjuvants is an important step during the development and pre-clinical assessment of an adjuvanted vaccine. Data from *in vitro* studies contribute to the preliminary overall safety [38] and, at an initial phase of development, can provide information about the potential toxicity of the formulation reducing the number of animals

used [39]. The MTT assay was used to evaluate the cytotoxicity of C48/80 in solution or incorporated in NP in two different cell types: a primary culture of mice spleen cells – a good representative of the different cells of immune system [31] and A549 cell line, a carcinomic human alveolar cell line. This epithelial cell line is widely used for nanotoxicity studies [40, 41] and should more closely represent the primary exposure route for nanoparticles. The cellular viability was monitored after exposing cells to different concentrations of C48/80 for 24 h.

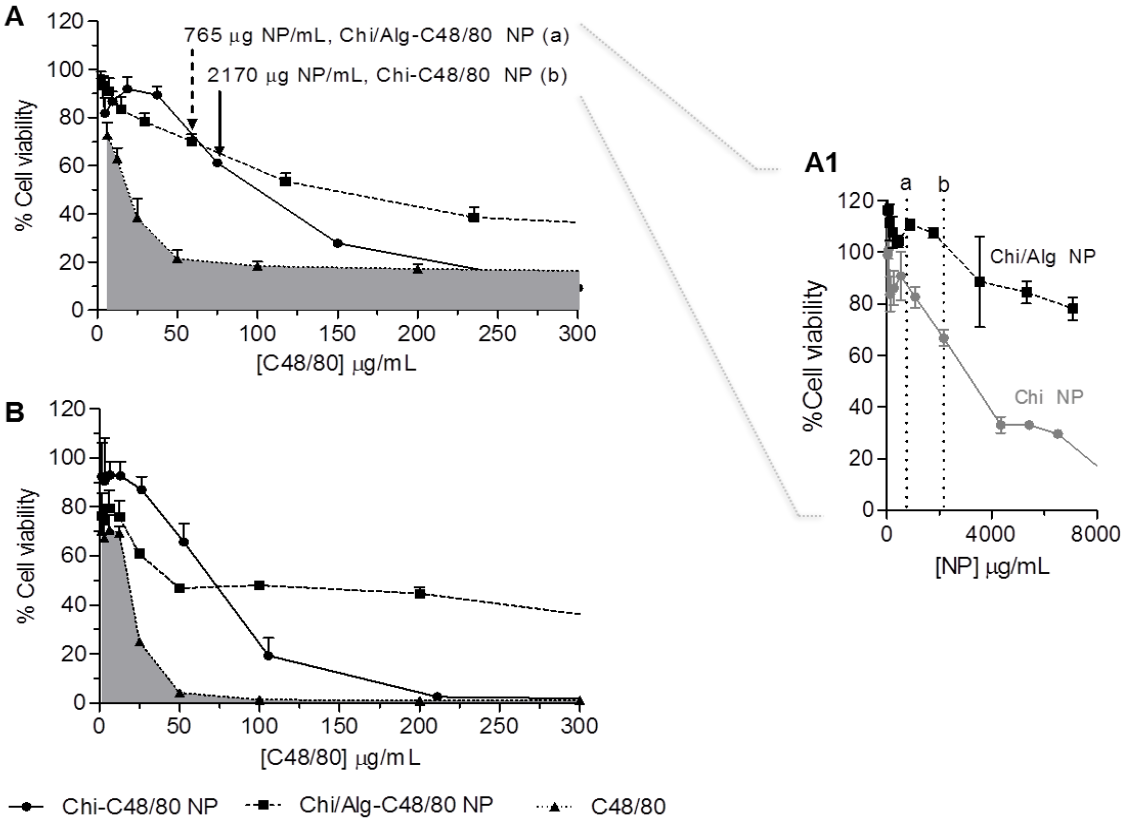

Figure 5.2 – Cytotoxicity of C48/80 free and C48/80 loaded into chitosan based particles. Different concentrations of C48/80 free or incorporated into NP were incubated for 24 h with (A) spleen cells or (B) A549 cells. Cell viability was measured by MTT assay after 24 h of incubation with samples. (A1) Cytotoxicity of blank Chi NP and blank Chi/Alg NP in mice spleen cells at 24 h. Each result is representative of at least two independent experiments performed in quadruplicate, mean ± SD.

Dose response curves (Fig. 5.2A and 5.2B) showed that cell viability decreased as the concentration of C48/80 in solution increased. However, the dose-response curve profile was not the same for the nanoparticle formulations. When C48/80 was incorporated into nanoparticles, cells survived exposure to higher concentrations of C48/80, resulting in higher cell viability than the same concentration of C48/80 in solution. It was also observed a more drastically decrease of cell viability with Chi-C48/80 NP than with Chi/Alg-C48/80 NP.

These differences can be explained by the differences in NP concentrations required to have a comparable amount of C48/80 (Fig. 5.2A, curves a and b), which is related with different C48/80 LE on both formulations (Fig. 5.1A). Therefore, the intrinsic cytotoxicity of nanoparticles also contribute to the differences observed since the comparison of cytotoxicity of blank Chi NP and Chi/Alg NP in spleen cells (Fig. 5.2A1) showed that Chi NP induced a decrease in cell viability at lower concentrations that Chi/Alg NP.

Overall, the results obtained with two different cell types indicate that the association with nanoparticles improves the biocompatibility of C48/80. This is in agreement with the idea that the association of an immunopotentiator with particles minimizes its toxicity, by limiting the systemic distribution of the immunopotentiator and decreasing the maximal available concentrations [15]. This is of utmost importance since one of the major challenges in adjuvant research is to gain potency while minimizing toxicity. However, the toxicity of adjuvants is a somewhat controversial topic. On the one hand, that is a huge concern about safety of vaccine adjuvants, and efforts are been made to establish methods to be used during the non-clinical screening of novel adjuvants to evaluate and to improve the toxicity profile of the candidates [42]. On the other hand, it was suggested that controlled cell death may be an effective strategy to provide safe and effective adjuvants [33]. In fact, the adjuvanticity of alum, a FDA-approved and the most widely used vaccine adjuvant, is mediated by cell death [43, 44], which suggests that a moderate cytotoxicity may be required for the adjuvant activity.

5.3.3 Chi-C48/80 NP are more efficiently taken up by antigen presenting cells than Chi/Alg-C48/80 NP

A nasal vaccine delivery system should efficiently interact with antigen presenting cells on NALT (nasal associated lymphoid tissue). Therefore we investigated the ability of both developed formulations to be internalized by different APCs – macrophages and PBDCs.

To visualize particle uptake by macrophages, cells were incubated with fluorescent Chi-C48/80 NP or Chi/Alg-C48/80 for different time points. Images from confocal microscopy showed that Chi-C48/80 NP were efficiently taken up by macrophages while the uptake of same concentration of Chi/Alg-C48/80 NP was barely detectable (Fig. 5.3A). The uptake of Chi-C48/80 NP increased with increasing incubation time. While at 30 min the NP were mainly adsorbed at the surface of cells, the amount of fluorescent particles inside the cells was successively higher after 1 h and 4 h of incubation. A considerable amount of nanoparticles remained attached to cell surface regardless of a thorough washing of the adhered cells. This membrane binding can also favor the development of an immune response by promoting a continuous release of the antigen as demonstrated by others [45]. On the other hand, only a

small amount of Chi/Alg-C48/80 NP was taken up by macrophages even after 4 h of incubation.

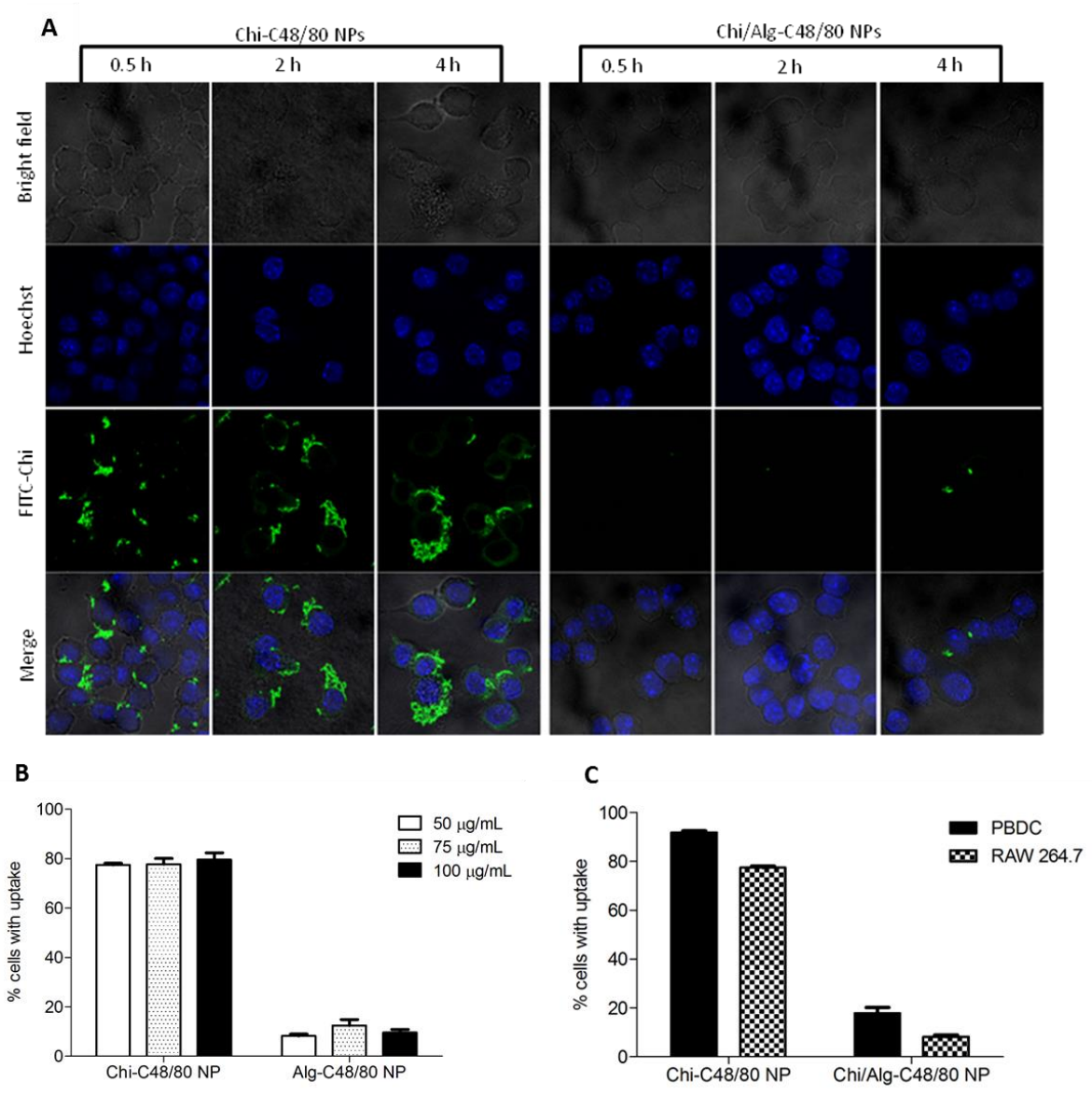

Figure 5.3 – Evaluation of cellular uptake of different C48/80 loaded nanoparticles by APCs. (A) Confocal images of RAW 264.7 cells after incubation with C48/80 loaded FITC-chitosan nanoparticles (green). Cells were labeled with Hoechst 33342 (blue) to identify the nucleus. (B) Nanoparticles uptake by RAW 264.7 macrophages after 2 h incubation. Percentage of cells with internalized particles was determined by FACS. (C) Nanoparticles internalization by different antigen presenting cells was assessed after incubation of PBDCs and RAW 264.7 with 50 µg/mL of Chi-C48/80 NP or Chi/Alg-C48/80 for 2 h. Bars represent mean ± SD, n=3.

Subsequently, FACS was used to confirm the confocal microscopy results and to quantify the uptake by macrophages and dendritic cells after 2 h incubation. To ensure that the fluorescence detected was from internalized particles and not from particles attached to cell surface, trypan blue was used to quench the external fluorescence of FITC. To evaluate the effect of the amount of nanoparticles in the uptake, 3 different concentrations of Chi-C48/80 NP and Chi/Alg-C48/80 NP were incubated with RAW 264.7 (50, 75 and 100 μg/mL). The concentration of nanoparticles did not significantly affect the uptake by macrophages (Fig. 5.3B). So, the lowest concentration was selected to quantify and compare nanoparticle uptake by DCs and macrophages. The results are in agreement with the observed on confocal studies. In both cell types, the uptake of Chi-C48/80 NP was significantly higher than the uptake of Chi/Alg-C48/80 NP (Fig. 5.3C). Even if the size and zeta potential of the two formulations were similar, its ability to interact with APCs was completely different. These results confirm the premise that not only the size and charge of the nanoparticles but also their surface characteristics play a role in the internalization by cells [46]. The lower amount of chitosan in Chi/Alg-C48/80 NP when compared with Chi-C48/80 NP could result in a less mucoadhesive formulation, and may have hindered the uptake of Chi/Alg-C48/80 NP. This could also explain why Chi/Alg-C48/80 NP were less toxic; these particles are less internalized and adhered less to cell surface.

Considering that the generation of a primary adaptive immune response initially involves the uptake by APCs [23], the high uptake achieved by Chi-C48/80 NP indicates its suitability as a vaccine delivery system for mucosal surfaces.

5.3.4 Chitosan nanoparticles activate mast cells inducing β-hexosaminidase release

After successful incorporation of a mast cell activator into nanoparticles, the next step was to evaluate if the C48/80 was still able to interact with mast cells inducing degranulation. The ability of the formulations to activate mast cells was assessed in a human mast cell line (HMC-1) by the β-hex release assay. This assay is routinely used to evaluate the mast cell degranulation and was recently described as a tool to detect novel potential adjuvant compounds [33].

Different concentrations of C48/80 in solution or incorporated in nanoparticles were assessed. Blank nanoparticles (without C48/80) were also tested as a control to analyze the effect of the particles itself. C48/80 in solution, used as positive control for degranulation, induced a β-hex release between 0.7 % and 1.6 % (Fig. 5.4),values that are in accordance with

those described in the literature [33]. When C48/80 was incorporated in Chi NP, a significantly higher β-hex release was observed – values between 2.0 % and 9.0 % for the lower and higher concentrations tested, respectively. Results also showed that blank Chi NP by itself induced mast cell activation higher than C48/80 in solution but lower than Chi-C48/80 NP. On the other hand, the β-hex release triggered by C48/80 in Chi/Alg NP was not significantly different from C48/80 alone and the respective blank formulation induced only a minor mediator release – lower than 0.2 %. To rule out the possibility of mast cell activation being mediated by a potential endotoxin contamination, HMC-1 cells were stimulated with different concentrations of LPS (between 0.5 and 100 ng/mL) and the β-hex release measured in the supernatant. None of the tested concentrations induced a β-hex release significantly higher than the basal value (data not shown).

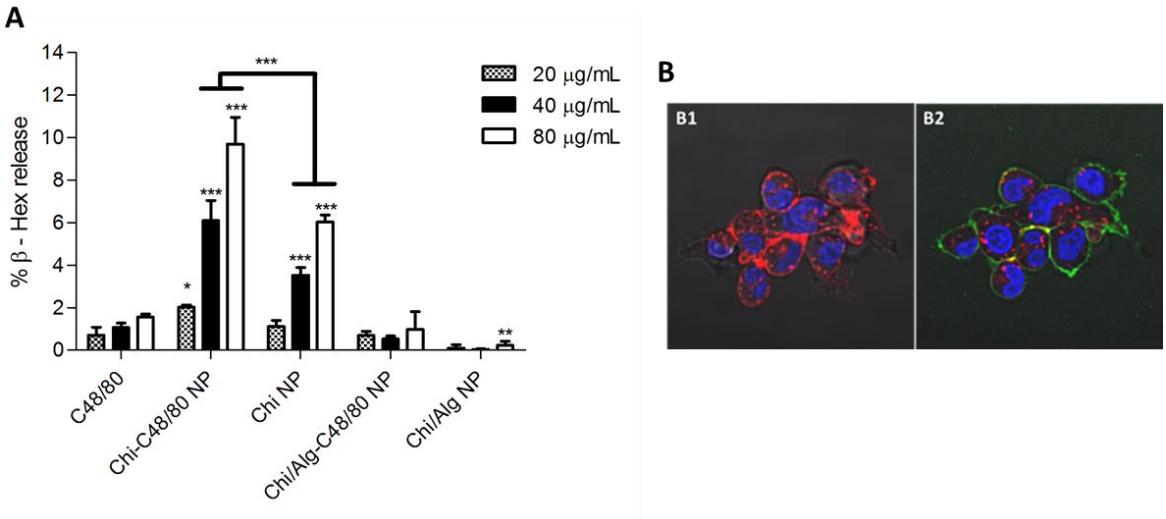

Figure 5.4 – Evaluation of mast cell activation by nanoparticles. (A) Degranulation of the mast cell line HMC-1 was evaluated by a β-hex release assay. Cells were stimulated with C48/80 at 20, 40 or 80 μg/mL in solution or incorporated in nanoparticles. Blank Chi NP and Chi/Alg NP were used as controls at the same concentration of nanoparticles tested with C48/80 loaded particles. Data are representative from three independent experiments performed in triplicate or quadruplicate, mean ± SD, n = 3. Symbols above bars indicate the differences relative to C48/80 in solution, * $p < 0.05$, ** $p < 0.01$, *** $p < 0.001$ 2-way ANOVA. (B) Confocal images of HMC-1 before (B1) and 2 min after treatment with FITC labeled Chi-C48/80 NP (green) at a dose correspondent to 40 μg/mL of C48/80 in Tyrode's solution (B2). Cells were labeled with Hoechst 33342 (blue) for nuclei and with Alexa Fluor ® 594 WGA to identify cell membrane. Images showed that Chi-C48/80 immediately adsorbed on cell surface.

The stimulation of mast cells by chitosan implants was recently described [47] but to our knowledge the effect of chitosan nanoparticles on mast cells was not evaluated before. Our results demonstrate that chitosan NP also activate mast cells inducing β-hex release. Besides,

the incorporation of C48/80 into these nanoparticles resulted in enhanced mast cell activation when compared with both C48/80 in solution or blank Chi NP. On the other hand, the combination of C48/80 with Chi/Alg NP did not significantly affect the β-hex release. One of the pathways of mast cell activation is the basic secretagogues mediated pathway. These secretagogues comprise a large number of molecules, including C48/80, that only have in common their cationic property [48]. It was suggested that the response of mast cells to secretagogues could be mediated by an initial binding of this molecules to negatively charged sialic acid residues on the cell surface [49], which could also be the case for the positively charged chitosan nanoparticles. This idea is supported by the fact that chitosan nanoparticles extensively adsorbed on mast cells surface immediately after being added to the cells (Fig. 5.4B), suggesting a possible role of chitosan bioadhesivity in mast cell activation. Our results are in agreement with Farrugia et al. that demonstrated the ability of chitosan polymer to adhere and stimulate mast cells [47]. But other authors showed on the RBL-2H3 cell line, a basophilic leukemia cell line that has been used as a model of mast cell activation [50], that chitosan oligosaccharides and chitosan coated nanoparticles had an inhibitory effect on IgE-mediated mast cell activation [51, 52]. So, it is possible that chitosan has the ability to inhibit mast cells through downregulation of FcERI, as shown with the chitosan oligosaccharides [51] but also the ability to activate mast cells via an IgE independent pathway. Additionally, as explained by Farrugia, water soluble chitosan oligosaccharides have their cellular adhesion and interaction diminished which, according with same authors, may contribute to explain the observed absence of the effect. This hypothesis should be investigated in future studies. Indeed, mast cell degranulating peptide (MCDP), a basic secretagogue, also exhibits this double activity thought to be related to the fact the MCDP shows both IgE-independent effects on mast cells as well as IgE-mediated action [53].

According to our data, activation of mast cells may be one of the mechanisms that contribute to the immunostimulating properties of chitosan nanoparticles. This would support the idea of mast cells as a common player in the modulation of immunity induced by different molecules with adjuvant properties [33] as already demonstrated for C48/80 [5], IL-18 [9], the cholera toxin derived CTA1-DD [10], imiquimod [11], alum [12] and polymyxins [13].

5.3.5 The nasal residence time of a model antigen is increased by the co-administration with mucoadhesive chitosan nanoparticles but not with chitosan/alginate nanoparticles

One of the proposed mechanisms by which nanoparticles act as an adjuvant is their ability to form slow release depots [23]. However, in the nasal cavity the mucociliary clearance limits the nasal residence time of the particles and practically nullifies the benefit of the depot effect [54, 55]. The use of mucoadhesive particles should overcome the negative effect of the mucociliary clearance by allowing a prolonged residence time of the adjuvant and antigen on nasal cavity. To evaluate if the developed chitosan based formulations were able to increase the nasal residence time of the antigen, the decay of fluorescence in the nasal cavity was quantified overtime (Fig. 5.5). Each adjuvanted group received 15 μg of C48/80 either in solution or associated with nanoparticles (Chi-C48/80 NP and Chi/Alg-C48/80 NP). A control group received Chi NP at the same concentration of nanoparticles than Chi-C48/80 NP to evaluate the effect of the incorporation of C48/80.The dose of C48/80 was chosen based on a previously study that used 15 μg of this mast cell activator as adjuvant for nasal immunization [56]. After 1 h, about 50 % of OVA administered alone or with C48/80 was cleared from the nasal cavity (Fig. 5.5A and 5.5B). Nevertheless, a strong fluorescence signal was detected even 6 h after the administration of Chi-C48/80 NP and Chi NP, while less than 10 % of the OVA remained in the groups that received OVA or OVA + Chi/Alg-C48/80 NP at this time point (Fig. 5.5B). The co-administration of OVA with C48/80 slightly delayed the clearance of the antigen. However, only Chi-C48/80 NP and Chi NP resulted in a significantly higher OVA residence time. The results obtained clearly show that the loading of OVA on Chi-C48/80 NP or with Chi NP decreases the rate of antigen clearance from nasal cavity. These results are in accordance with others that demonstrated that chitosan was able to increase the antigen residence time in nasal cavity of sheep [57] and humans [58], an effect attributed to the tight adhesion of the positively charged particles to the negative sialic acid residues of the glycoprotein mucins that constitute the mucus. The similarity between the C48/80 loaded and unloaded delivery systems indicated that the incorporation of C48/80 did not affect the mucoadhesive properties of chitosan.

Alginate is also a mucoadhesive polymer [59], however nanoparticles with alginate were not as successful as chitosan at enhancing nasal residence time of the antigen. Instead, the association of alginate with chitosan negatively affected the mucoadhesive properties of chitosan resulting in a weaker adhesion of nanoparticles on the nasal surface. Moreover, as was discussed previously, the nanoparticle uptake in cells was also affected by the introduction of the alginate on formulation. This observation agrees with a previous study in which, using

an *in situ* mucoadhesion test with beads, it was demonstrated that the increased mass ratio chitosan:alginate, enhanced the bioadhesivity of the formulation [60].

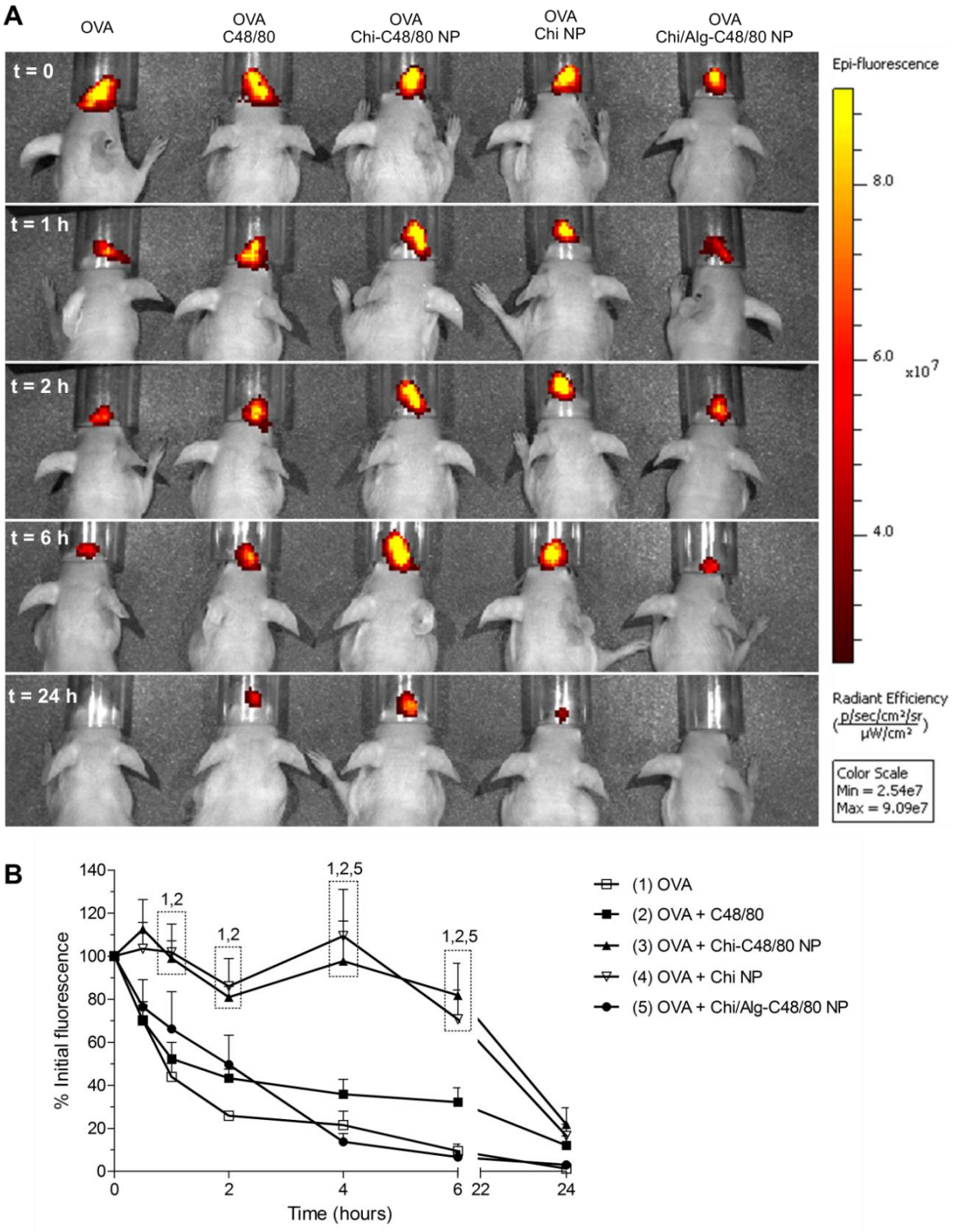

Figure 5.5 – Nasal residence time of Alexa Fluor 647 labeled OVA (a) Representative example of the detected fluorescence intensity after nasal administration of 5 µg of Alexa Fluor 647 labeled OVA in solution or with nanoparticles formulations. Fluorescence intensity in the nasal cavity was measured at different points and compared with the fluorescence at

time = 0 h. (b) Average relative fluorescence intensity, calculated as % of initial fluorescence. Mean ± SE, n=7. The numbers (1, 2, and 3) indicate which groups are significantly different from the indicated groups, $p < 0.05$.

C48/80 is also a positively charged polymer and a polyamine. The presence of amine groups on the molecules favors bioadhesion through hydrogen bonds formation [61] but to our knowledge, nothing was previously described about the mucoadhesive properties of this compound. Even if its chemical characteristics may have contributed for a decrease in clearance observed between 2 h and 6 h, at the tested concentration this mast cell activator by itself did not significantly increase the residence time of the antigen.

An increased nasal residence time of the antigen is associated with an enhanced uptake of the antigen on nasal cavity [62, 63] and with effective mucosal and humoral immunity [63]. So, the results obtained strongly indicate the potential of Chi-C48/80 NP as a new nasal antigen carrier.

5.3.6 Association of C48/80 with chitosan nanoparticles induced high titers of neutralizing antibodies and a more balanced Th1/Th2 profile than Chi/Alg-C48/80 NP or C48/80 alone

The *in vitro* screening and the nasal clearance study suggested that Chi-C48/80 NP is a more effective delivery system than Chi/Alg-C48/80 NP. The next step was to see if these results would translate in a better immunogenicity of the Chi-C48/80 NP formulation *in vivo*. Mice were intranasally immunized with PA plus Chi-C48/80 NP or PA plus Chi/Alg-C48/80 NP at days 0, 7 and 21 (Fig. 5.6A) and serum anti-PA IgG analyzed at 3 different time points (Fig. 5.6B). Control groups included the PA alone and the PA + C48/80 in solution. To better evaluate the advantage of incorporating C48/80 in nanoparticles, two extra groups of mice were also included in this study. One group received PA plus Chi NP alone and other was vaccinated with the mast cell activator mixed with Chi NP but not incorporated within the nanoparticles (Chi NP + C48/80).

Results showed that PA alone at 2.5 μg was not able to induce specific-IgG in serum at any of the time points tested. After the first boost, at day 14, significantly higher anti-PA IgG was detectable in mice adjuvanted with C48/80, Chi-C48/80 NP, Chi NP and Chi NP plus C48/80 when compared with PA alone group. However, Chi/Alg-C48/80 NP required a second boost to induce comparable anti-PA antibody titers to the ones induced by the other groups. At day 42, high levels of specific IgG was detected in the serum of all adjuvanted groups, but these titers were significantly higher in the groups immunized with PA plus C48/80 in solution or incorporated in Chi NP. To see if the different formulations influenced

the quality of the immune response, anti-PA IgG1 and IgG2c at day 42 were monitored (Fig. 5.6D). All the adjuvants induced comparable levels of IgG1 significantly higher than PA alone. However, even if all the groups showed a Th2 biased immune response, the administration of the antigen with Chi-C48/80 NP or Chi NP + C48/80 significantly enhanced the IgG2c titers when compared with C48/80 in solution and Chi/Alg-C48/80 NP.

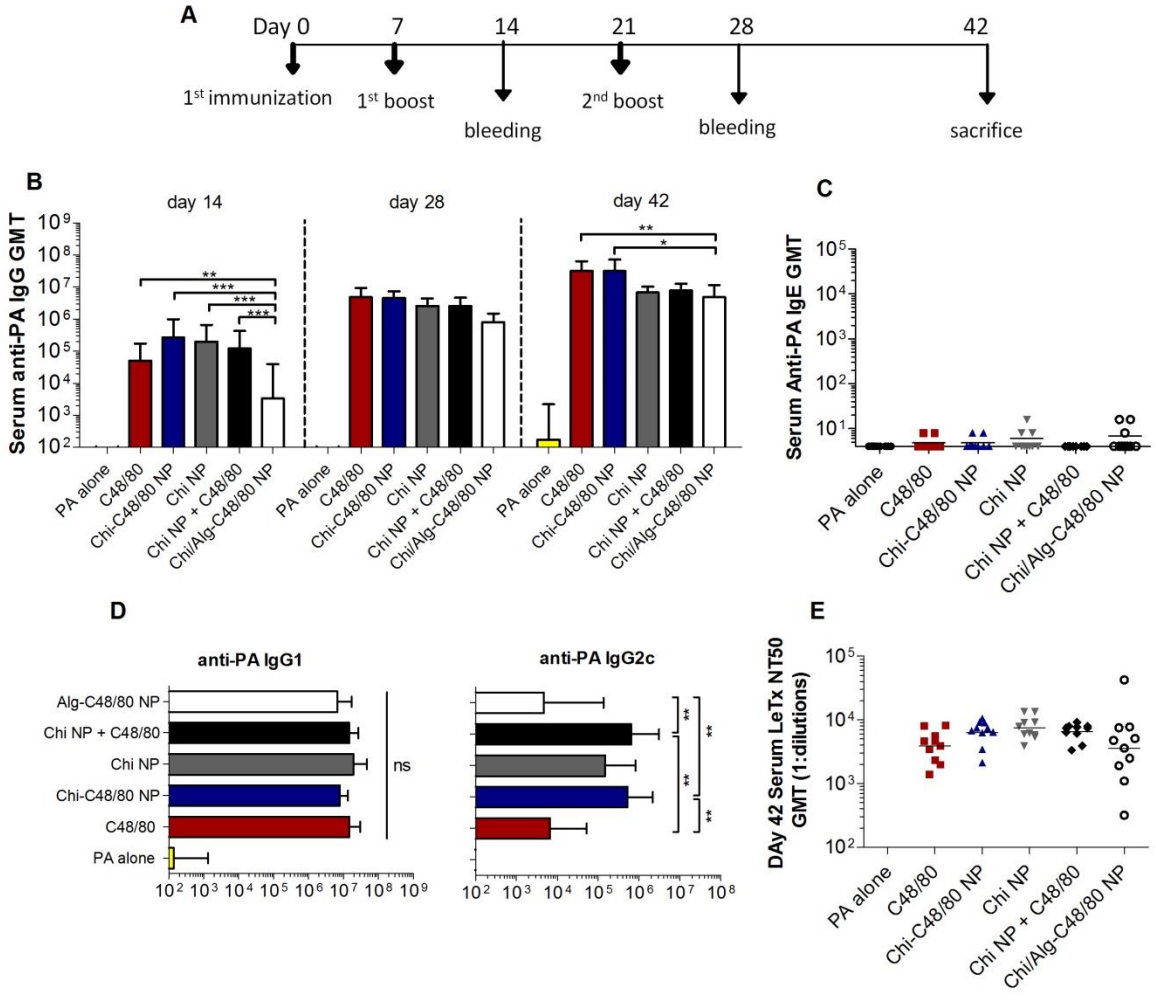

Figure 5.6 – Immune responses after vaccination with C48/80 loaded nanoparticles. (A) Immunization schedule. C57BL/6 mice were immunized with 2.5 μg of PA alone or plus different adjuvants on days 0, 7 and 21 and on day 42 mice were sacrificed. Serum was collected at day 14, 28 and 42 and antibody titers measured by ELISA. (B) Serum anti-PA IgG overtime from immunized mice. (C) Day 42 serum specific IgE. (D) Day 42 serum specific IgG subtypes. Results are expressed as the antilog of the last log2 dilution for which the relative light units were at least 3-fold higher than the value of the naive sample equally diluted. (E) A lethal toxin (LeTx) neutralization assay with J774A.1 macrophages was performed to measure functional anti-PA antibody responses in serum at day 42. Results are expressed as serum dilution required for a 50 % inhibition of LeTx-induced J774A.1 cell death (LeTx NT50). Bars represent geometric mean titer (GMT) ± 95 % CI. Results represent two experiments with 5 mice in each group for a total of 10 mice per group. Two-way ANOVA followed by Bonferroni post-test was used to assess significant differences in anti-PA IgG

titers among groups at different time points. * $p < 0.05$, ** $p < 0.01$, *** $p < 0.001$.

One of the reasons why PA antigen was used as a model was the possibility to evaluate the functionality of the antibodies induced using an *in vitro* challenge study which is important because not always the immune response measured by ELISA correlates with a protective capacity of vaccine-induced antibodies [56]. So, the ability of the induced anti-PA serum antibodies to neutralize anthrax lethal toxin (LeTx) was tested using an *in vitro* macrophage toxicity assay (Fig. 5.6E). LeTx neutralization titers were presented as the serum dilution required to neutralize 50 % of the LeTx (NT50). At day 42, all adjuvanted formulations exhibited high LeTx-neutralizing activity and were significantly greater than with PA alone but no statistical significant differences were detected between the adjuvanted groups. However, the association of C48/80 with Chi NP resulted in a lower dispersion of the response when compared with the groups immunized with C48/80 alone or Chi/Alg-C48/80 NP.

Overall, the results showed that Chi-C48/80 NP was as effective as C48/80 in solution at generating high levels of serum specific IgG while the Chi/Alg-C48/80 NP required an extra boost to induce comparable titers. Moreover, anti-PA IgG titers induced by Chi/Alg-C48/80 NP did not last as long as the ones induced by C48/80 in solution or incorporated in Chi NP. Co-administration of C48/80 with chitosan did not significantly enhance antibody production, possibly due to the strength of the ability of C48/80 and Chi NP to induce antibody production by itself. However, this association was favorable to the induction of anti-PA IgG2c. Administration of C48/80 together with Chi NP, either incorporated or mixed, elicited a more balanced Th1/Th2 profile suggesting that the co-administration of the two adjuvants potentiates the induction of a mixed humoral and cellular response. The more balanced profile induced by chitosan nanoparticles can possibly be related with the increased antigen residence time on nasal cavity promoted by this formulations. It was already suggested before that the gradual release of the antigen on the mucosa after nasal administration promotes a Th1 biased immune response due to the longer antigen residence time and enhancement of antigen permeation [6]. This would also explain why Chi/Alg-C48/80 NP was not so successful at inducing anti-PA IgG2c antibodies.

IgE induction by vaccine adjuvants is an important concern in vaccine safety due to the potential to induce anaphylactic reactions [64]. It is known that the mast cell activator C48/80 does not induce IgE when used as an adjuvant [5, 7, 56] but to certify that the incorporation of C48/80 in nanoparticles would not increase its toxicity, serum specific IgE was analyzed after vaccination with the different adjuvant combinations (Fig. 5.6C). None of the vaccine formulations induced elevated serum antigen specific IgE at day 42 showing that the

developed formulations exert their adjuvant effect without inducing potentially detrimental IgE.

5.3.7 Co-administration of C48/80 with chitosan in the same nanoparticle induced strong mucosal immunity

One of the greatest advantages of mucosal vaccines is the possibility to induce not only serum antibodies but also a mucosal immune response at the local of entry of pathogens. To evaluate the ability of the developed adjuvant combinations to enhance the induction of antigen-specific IgA in the mucosae, nasal washes, fecal pellets and vaginal washes were collected on day 42 and analyzed (Fig. 5.7).

Chi-C48/80 NP induced PA-specific IgA titers in the nasal mucosa significantly higher than all the other groups tested. On vaginal washes, the greater IgA production was also observed in the group adjuvanted with C48/80 incorporated in Chi NP. Chi-C48/80 NP induced vaginal anti-PA IgA titers significantly higher than PA alone or PA plus Chi NP or Chi/Alg-C48/80 NP. None of the other groups was significantly different from the non-adjuvanted one. Day 42 fecal anti-PA IgA titers were significantly elevated in C48/80, Chi-C48/80 NP, Chi NP and Chi NP + C48/80 adjuvanted groups but not in the Chi/Alg-C48/80 NP group. Besides, both formulations that combined chitosan and C48/80 (Chi-C48/80 NP and Chi NP + C48/80) were significantly superior to Chi/Alg-C48/80 NP. The importance of a mucosal immunity for protection against pathogens that enter the body across mucosal surfaces was established by different studies. For instances, mucosal IgA antibodies demonstrated to be better than IgG at protecting primates from a mucosal challenge with a simian-human immunodeficiency virus (SHIV) [65] and were absolutely essential for the development of a protective immune response to rotavirus, a common enteropathogenic virus [66]. In this study, Chi-C48/80 NP was the only adjuvant that induced mucosal anti-PA IgA titers significantly higher than PA alone in all the mucosal surfaces tested. Besides, in nasal mucosal Chi-C48/80 NP promoted specific IgA titers significantly higher than all the other adjuvants tested. So, these results suggest that the incorporation of C48/80 in Chi NP was the most effective strategy for the induction of a mucosal immunity.

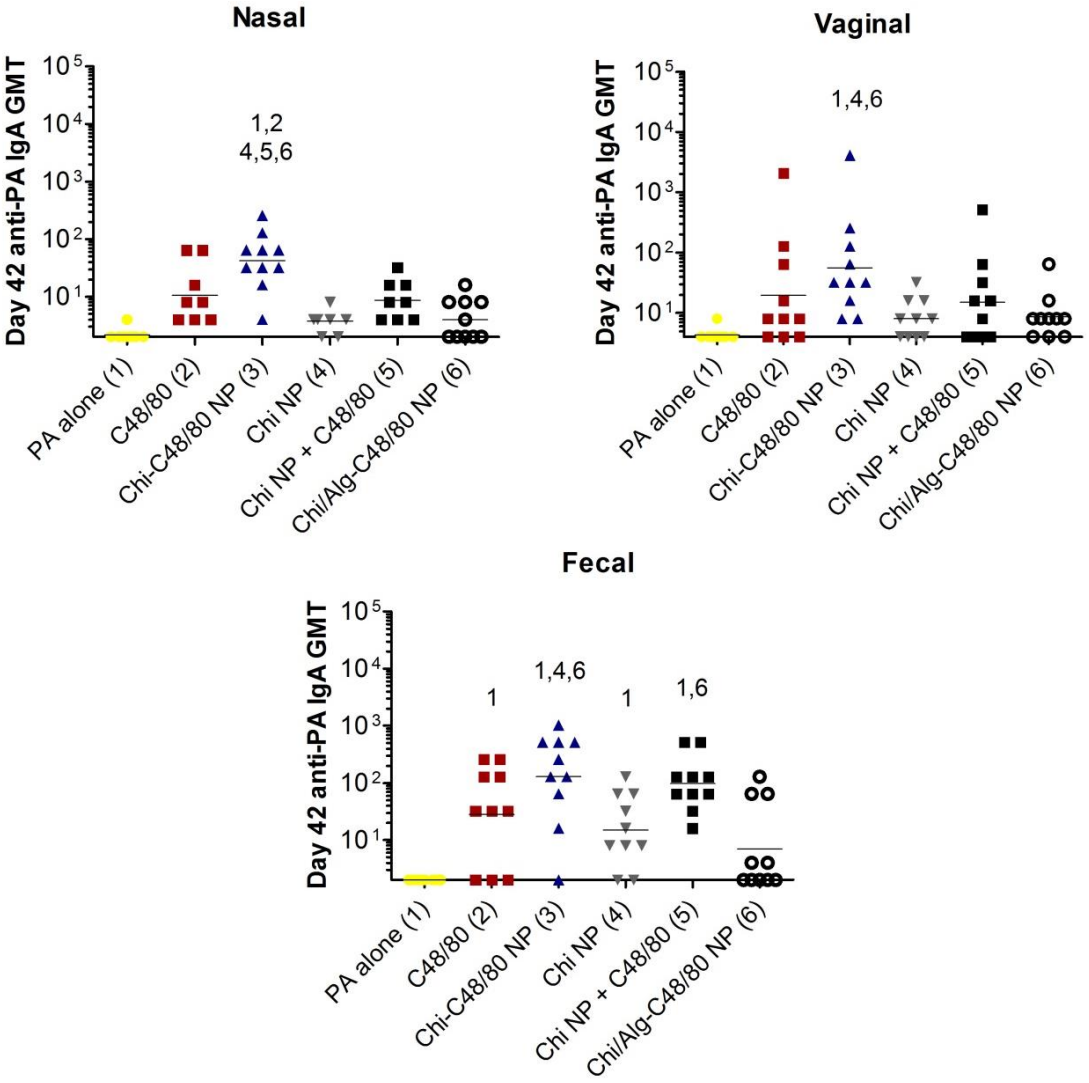

Figure 5.7 – Mucosal immunity in nasal washes, vaginal washes and fecal extracts after vaccination with C48/80 loaded nanoparticles. C57BL/6 mice were immunized with 2.5 μg of PA alone or plus different adjuvants on days 0, 7 and 21. On day 42 mice were sacrificed and mucosal samples were collected and processed as described in Methods section. Anti-PA IgA titers were measured by ELISA. Results are expressed as the antilog of the last log2 dilution for which the relative light units were at least 3-fold higher than the value of the naive sample equally diluted. Geometric mean titer (GMT) ± 95 % CI. Results represent two independent experiments with 5 mice in each group for a total of 10 mice per group. Numbers above bars indicate results significantly different ($p < 0.05$).

5.3.8 Chitosan nanoparticles but not chitosan/alginate or C48/80 alone promote the production of Th17 type cytokines by spleen cells

To further understand the immune response elicited by the different formulations, *ex vivo* cytokine release profile was evaluated by analyzing Th2 (IL-4, IL-10), Th1 (IL-2, IFN-gamma) and Th17 (IL-17, IL-22) type cytokines in the supernatant of spleen cells re-stimulated with PA (Fig. 5.8).

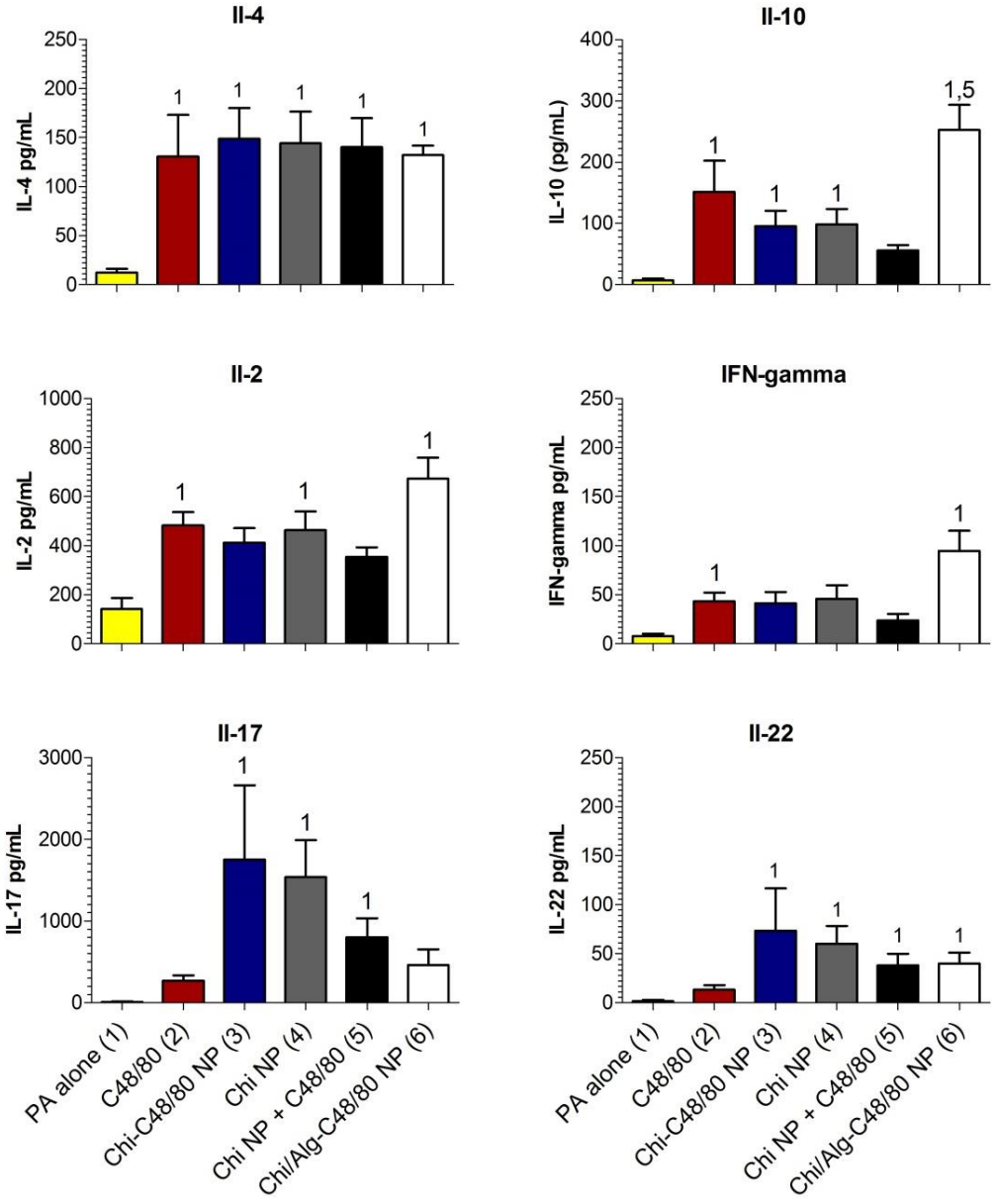

Figure 5.8 – Antigen-specific lymphocyte cytokine responses after nasal immunization with PA. Mice were immunized with 2.5 μg of PA alone or plus different adjuvants on days 0, 7 and 21. At day 42, splenocytes were harvested and cultured at 1.25×10^6 cells per well in T-cell culture medium (48 well plate) with or without PA (5 μg/ml) to induce recall cytokine secretion by antigen-specific T cells. Supernatants were collected after 5 days of re-stimulation and IL-4, IL-2, IL-10, IFN-gamma, IL-17 and IL-22 levels were measured using a multiplex bead assay. Data shows the antigen-specific cytokine production for each group (i.e., PA induced cytokine production –minus the individual values of non-stimulated cells). Bars represent mean ± SD. Results represent two experiments with 5 mice in each group for a total of 10 mice per group. The numbers above the error bars indicate which groups (1–6) are significantly different from the indicated group, $p < 0.05$.

Groups vaccinated with PA alone secreted negligible amounts of each tested cytokine. Cells harvested from the different adjuvanted groups produced significantly higher levels of IL-4 than PA alone, which correlate with the high levels of serum IgG1 observed in all these groups. The highest levels of IL-10 were detected in cells from Chi/Alg-C48/80 NP vaccinated group. Regarding the production of the Th1-type cytokines IL-2 and IFN-gamma, no significant differences were observed between the adjuvanted groups but C48/80 and Chi/Alg-C48/80 NP induced significantly higher IFN-gamma than PA alone. High levels of IL-17 were secreted by restimulated cells harvested from mice immunized with Chi-C48/80 NP, Chi NP and Chi NP + C48/80. Similarly, all the groups adjuvanted with nanoparticles significantly induced greater production of the Th17 cytokine IL-22 than PA alone, contrasting with the observed with C48/80 in solution. This IL-17 and IL-22 production driven by chitosan nanoparticles is consistent with a recent study that demonstrated chitosan as a Th17 promoting adjuvant [67]. Th17 cells have a key role in the host defense against pathogens at mucosal surfaces [68]. In fact, it was demonstrated that Th17 cells mediate the mucosal adjuvant effect of the potent mucosal immunopotentiator cholera toxin [69]. In this study Chi-C48/80 NP was not only the adjuvant formulation promoting the highest secretion of Th17 type cytokines but also the one inducing the greatest mucosal anti-PA IgA titers. So, it is possible that the strong mucosal immunity induced by Chi-C48/80 NP is associated with its ability to drive Th17 type cytokines.

5.4 Conclusion

Safe and effective adjuvants which enhance immune responses to poorly immunogenic subunit antigens are required for the vaccine development. A combination strategy, involving the association of mucoadhesive nanoparticles with an immunostimulatory compound, will most likely result in a more potent adjuvant formulation for mucosal vaccination. Moreover, depending of the immunopotentiators and antigen delivery system chosen, it may be possible to modulate the immune response to obtain Th1, Th2 or a mixed immune response or even to stimulate mucosal and/or systemic antibodies. In the present study, two different chitosan based nanoparticles associated with the mast cell activator C48/80 were developed and compared: Chi-C48/80 NP and Chi/Alg-C48/80 NP. This is the first time that this combination of adjuvants is tested. Despite some similarities between the two formulations, in most of *in vitro* studies, and in the nasal residence time study, Chi-C48/80 NP outperformed Chi/Alg-C48/80 NP. So, *in vitro* the incorporation of alginate in the nanoparticles did not reveal any major advantage. *In vivo* the differences between Chi/Alg-C48/80 NP and Chi-

C48/80 NP were not as marked but the results still suggested the superiority of Chi-C48/80 NP. Based on serum specific IgG1 and neutralizing antibodies all formulations seemed similar. However, when considering IgG2c, Chi NP + C48/80 and Chi-C48/80 NP induced significantly higher IgG2c titers than C48/80 in solution and Chi/Alg-C48/80 NP. Regarding mucosal immunity, Chi-C48/80 NP induced significantly higher IgA titers than Chi/Alg-C48/80 NP in nasal, vaginal and fecal samples. So, even if Chi/Alg-C48/80 NP was as effective as Chi-C48/80 NP at inducing specific IgG and LeTx neutralizing antibodies, overall Chi-C48/80 NP outperformed Chi/Alg-C48/80 NP inducing a faster immune response with a more balanced Th1/Th2 immune profile and a significantly stronger mucosal immunity. Still, the strength of the immune response induced by Chi/Alg-C48/80 NP is quite surprisingly considering the *in vitro* performance of this adjuvant. This suggests that even if an *in vitro* screening may be helpful to decrease the number of animals used in vaccine development the results should be carefully analyzed. While in most of the experiments Chi NP mixed with C48/80 in solution was as good as Chi-C48/80 NP, the benefit of incorporating C48/80 in the nanoparticles was observed in the mucosal immune response. Chi-C48/80 NP induced significantly higher specific IgA levels in the nasal mucosa than all the other adjuvants tested and was the only adjuvant able to significantly elevate the anti-PA IgA in vaginal mucosa. Our results stress the potential advantage of an adjuvant combination strategy but also show that this benefit is not independent of the delivery system. For example, the adjuvant effect of Chi/Alg-C48/80 NP was comparable to C48/80 in solution in all the experiments performed. Therefore, understanding the mechanisms of the adjuvants is of utmost importance on the rational design of adjuvant associations. In this particular case, the incorporation of C48/80 in the mucoadhesive Chi NP and the increased production of Th17 type cytokines induced by Chi-C48/80 NP maybe associated with the improved mucosal immunity induced by this formulation. But further studies in mast cell deficient mice could be helpful to clarify the involvement of mast cells in the adjuvant effect of these nanoparticles. So, the current study highlights the adjuvant combination Chi-C48/80 NP as an effective and promising strategy for nasal vaccination eliciting a strong systemic immunity and mucosal immunity.

References

1. Borges, O., et al., *Mucosal vaccines: recent progress in understanding the natural barriers.* Pharm Res, 2010. **27**(2): p. 211-23.
2. Abraham, S.N. and A.L. St John, *Mast cell-orchestrated immunity to pathogens.* Nat Rev Immunol, 2010. **10**(6): p. 440-52.

3. Metz, M. and M. Maurer, *Mast cells--key effector cells in immune responses.* Trends Immunol, 2007. **28**(5): p. 234-41.
4. Marshall, J.S., *Mast-cell responses to pathogens.* Nat Rev Immunol, 2004. **4**(10): p. 787-99.
5. McLachlan, J.B., et al., *Mast cell activators: a new class of highly effective vaccine adjuvants.* Nat Med, 2008. **14**(5): p. 536-41.
6. Staats, H.F., et al., *Mucosal targeting of a BoNT/A subunit vaccine adjuvanted with a mast cell activator enhances induction of BoNT/A neutralizing antibodies in rabbits.* PLoS One, 2011. **6**(1): p. e16532.
7. McGowen, A.L., et al., *The mast cell activator compound 48/80 is safe and effective when used as an adjuvant for intradermal immunization with Bacillus anthracis protective antigen.* Vaccine, 2009. **27**(27): p. 3544-52.
8. Wang, S.H., et al., *Stable dry powder formulation for nasal delivery of anthrax vaccine.* J Pharm Sci, 2012. **101**(1): p. 31-47.
9. Kayamuro, H., et al., *Interleukin-1 family cytokines as mucosal vaccine adjuvants for induction of protective immunity against influenza virus.* J Virol, 2010. **84**(24): p. 12703-12.
10. Fang, Y., et al., *Mast cells contribute to the mucosal adjuvant effect of CTA1-DD after IgG-complex formation.* J Immunol, 2010. **185**(5): p. 2935-41.
11. Heib, V., et al., *Mast cells are crucial for early inflammation, migration of Langerhans cells, and CTL responses following topical application of TLR7 ligand in mice.* Blood, 2007. **110**(3): p. 946-53.
12. McKee, A.S., et al., *Alum induces innate immune responses through macrophage and mast cell sensors, but these sensors are not required for alum to act as an adjuvant for specific immunity.* J Immunol, 2009. **183**(7): p. 4403-14.
13. Yoshino, N., et al., *Polymyxins as novel and safe mucosal adjuvants to induce humoral immune responses in mice.* PLoS One, 2013. **8**(4): p. e61643.
14. Smith, D.M., J.K. Simon, and J.R. Baker, Jr., *Applications of nanotechnology for immunology.* Nat Rev Immunol, 2013. **13**(8): p. 592-605.
15. De Temmerman, M.L., et al., *Particulate vaccines: on the quest for optimal delivery and immune response.* Drug Discov Today, 2011. **16**(13-14): p. 569-82.
16. Sahdev, P., L.J. Ochyl, and J.J. Moon, *Biomaterials for Nanoparticle Vaccine Delivery Systems.* Pharm Res, 2014.
17. Zhao, L., et al., *Nanoparticle vaccines.* Vaccine, 2013.
18. Vajdy, M., et al., *Mucosal adjuvants and delivery systems for protein-, DNA- and RNA-based vaccines.* Immunol Cell Biol, 2004. **82**(6): p. 617-27.
19. Arca, H.C., M. Gunbeyaz, and S. Senel, *Chitosan-based systems for the delivery of vaccine antigens.* Expert Rev Vaccines, 2009. **8**(7): p. 937-53.
20. Jabbal-Gill, I., P. Watts, and A. Smith, *Chitosan-based delivery systems for mucosal vaccines.* Expert Opin Drug Deliv, 2012. **9**(9): p. 1051-67.
21. Wu, Y., et al., *Novel thermal-sensitive hydrogel enhances both humoral and cell-mediated immune responses by intranasal vaccine delivery.* Eur J Pharm Biopharm, 2012. **81**(3): p. 486-97.
22. Woodrow, K.A., K.M. Bennett, and D.D. Lo, *Mucosal vaccine design and delivery.* Annu Rev Biomed Eng, 2012. **14**: p. 17-46.
23. Schijns, V.E. and E.C. Lavelle, *Trends in vaccine adjuvants.* Expert Rev Vaccines, 2011. **10**(4): p. 539-50.
24. Mutwiri, G., et al., *Combination adjuvants: the next generation of adjuvants?* Expert Rev Vaccines, 2011. **10**(1): p. 95-107.
25. Borges, O., et al., *Alginate coated chitosan nanoparticles are an effective subcutaneous adjuvant for hepatitis B surface antigen.* Int Immunopharmacol, 2008. **8**(13-14): p. 1773-80.

26. Mata, E., et al., *Enhancing immunogenicity to PLGA microparticulate systems by incorporation of alginate and RGD-modified alginate.* Eur J Pharm Sci, 2011. **44**(1-2): p. 32-40.
27. Yang, D. and K.S. Jones, *Effect of alginate on innate immune activation of macrophages.* J Biomed Mater Res A, 2009. **90**(2): p. 411-8.
28. Bender, A., et al., *Improved methods for the generation of dendritic cells from nonproliferating progenitors in human blood.* J Immunol Methods, 1996. **196**(2): p. 121-35.
29. Rajaonarivony, M., et al., *Development of a new drug carrier made from alginate.* J Pharm Sci, 1993. **82**(9): p. 912-7.
30. Bento, D., et al., *Validation of a new 96-well plate spectrophotometric method for the quantification of compound 48/80 associated with particles.* AAPS PharmSciTech, 2013. **14**(2): p. 649-55.
31. Borges, O., et al., *Uptake studies in rat Peyer's patches, cytotoxicity and release studies of alginate coated chitosan nanoparticles for mucosal vaccination.* J Control Release, 2006. **114**(3): p. 348-58.
32. Lee, J. and K.T. Lim, *Inhibitory effect of phytoglycoprotein (24kDa) on allergy-related factors in compound 48/80-induced mast cells in vivo and in vitro.* Int Immunopharmacol, 2010. **10**(5): p. 591-9.
33. Staats, H.F., et al., *A Mast Cell Degranulation Screening Assay for the Identification of Novel Mast Cell Activating Agents.* Medchemcomm, 2013. **4**(1): p. 88-94.
34. Schaffer, B.S., et al., *Immune competency of a hairless mouse strain for improved preclinical studies in genetically engineered mice.* Mol Cancer Ther, 2010. **9**(8): p. 2354-64.
35. Hagenaars, N., et al., *Role of trimethylated chitosan (TMC) in nasal residence time, local distribution and toxicity of an intranasal influenza vaccine.* J Control Release, 2010. **144**(1): p. 17-24.
36. Staats, H.F., et al., *In vitro and in vivo characterization of anthrax anti-protective antigen and anti-lethal factor monoclonal antibodies after passive transfer in a mouse lethal toxin challenge model to define correlates of immunity.* Infect Immun, 2007. **75**(11): p. 5443-52.
37. Foged, C., et al., *Particle size and surface charge affect particle uptake by human dendritic cells in an in vitro model.* Int J Pharm, 2005. **298**(2): p. 315-22.
38. Montomoli, E., et al., *Current adjuvants and new perspectives in vaccine formulation.* Expert Rev Vaccines, 2011. **10**(7): p. 1053-61.
39. Stewart-Tull, D.S., *Harmful and Beneficial Activities of Immunological Adjuvants*, in *Vaccine Adjuvants*, D. O'Hagan, Editor 2000, Springer New York. p. 29-48.
40. Lanone, S., et al., *Comparative toxicity of 24 manufactured nanoparticles in human alveolar epithelial and macrophage cell lines.* Part Fibre Toxicol, 2009. **6**: p. 14.
41. Davoren, M., et al., *In vitro toxicity evaluation of single walled carbon nanotubes on human A549 lung cells.* Toxicol In Vitro, 2007. **21**(3): p. 438-48.
42. Mastelic, B., et al., *Mode of action of adjuvants: implications for vaccine safety and design.* Biologicals, 2010. **38**(5): p. 594-601.
43. Marichal, T., et al., *DNA released from dying host cells mediates aluminum adjuvant activity.* Nat Med, 2011. **17**(8): p. 996-1002.
44. Jacobson, L.S., et al., *Cathepsin-mediated necrosis controls the adaptive immune response by Th2 (T helper type 2)-associated adjuvants.* J Biol Chem, 2013. **288**(11): p. 7481-91.
45. Kanchan, V. and A.K. Panda, *Interactions of antigen-loaded polylactide particles with macrophages and their correlation with the immune response.* Biomaterials, 2007. **28**(35): p. 5344-57.
46. Csaba, N., M. Garcia-Fuentes, and M.J. Alonso, *Nanoparticles for nasal vaccination.* Adv Drug Deliv Rev, 2009. **61**(2): p. 140-57.

47. Farrugia, B.L., et al., *The localisation of inflammatory cells and expression of associated proteoglycans in response to implanted chitosan.* Biomaterials, 2014. **35**(5): p. 1462-77.
48. Ferry, X., et al., *G protein-dependent activation of mast cell by peptides and basic secretagogues.* Peptides, 2002. **23**(8): p. 1507-15.
49. Mousli, M., et al., *Activation of rat peritoneal mast cells by substance P and mastoparan.* J Pharmacol Exp Ther, 1989. **250**(1): p. 329-35.
50. Passante, E., et al., *RBL-2H3 cells are an imprecise model for mast cell mediator release.* Inflamm Res, 2009. **58**(9): p. 611-8.
51. Vo, T.-S., et al., *Protective effect of chitosan oligosaccharides against FcεRI-mediated RBL-2H3 mast cell activation.* Process Biochemistry, 2012. **47**(2): p. 327-330.
52. Tahara, K., et al., *The suppression of IgE-mediated histamine release from mast cells following exocytic exclusion of biodegradable polymeric nanoparticles.* Biomaterials, 2012. **33**(1): p. 343-51.
53. Buku, A., *Mast cell degranulating (MCD) peptide: a prototypic peptide in allergy and inflammation.* Peptides, 1999. **20**(3): p. 415-20.
54. Slutter, B., et al., *Antigen-adjuvant nanoconjugates for nasal vaccination: an improvement over the use of nanoparticles?* Mol Pharm, 2010. **7**(6): p. 2207-15.
55. Utkarshini Anand, T.F., Remigius U. Agu, *Novel Mucoadhesive Polymers for Nasal Drug Delivery*, in *Recent Advances in Novel Drug Carrier Systems*, A.D. Sezer, Editor 2012, InTech: http://www.intechopen.com/books/recent-advances-in-novel-drug-carrier-systems/novel-mucoadhesive-polymers-for-nasal-drug-delivery.
56. Gwinn, W.M., et al., *A comparison of non-toxin vaccine adjuvants for their ability to enhance the immunogenicity of nasally-administered anthrax recombinant protective antigen.* Vaccine, 2013. **31**(11): p. 1480-9.
57. Soane, R.J., et al., *Clearance characteristics of chitosan based formulations in the sheep nasal cavity.* Int J Pharm, 2001. **217**(1-2): p. 183-91.
58. Soane, R.J., et al., *Evaluation of the clearance characteristics of bioadhesive systems in humans.* Int J Pharm, 1999. **178**(1): p. 55-65.
59. Deat-Laine, E., et al., *Efficacy of mucoadhesive hydrogel microparticles of whey protein and alginate for oral insulin delivery.* Pharm Res, 2013. **30**(3): p. 721-34.
60. Tahtat, D., et al., *Oral delivery of insulin from alginate/chitosan crosslinked by glutaraldehyde.* Int J Biol Macromol, 2013. **58**: p. 160-8.
61. Smart, J.D., *The basics and underlying mechanisms of mucoadhesion.* Adv Drug Deliv Rev, 2005. **57**(11): p. 1556-68.
62. Pawar, D., et al., *Development and characterization of surface modified PLGA nanoparticles for nasal vaccine delivery: Effect of mucoadhesive coating on antigen uptake and immune adjuvant activity.* Eur J Pharm Biopharm, 2013.
63. Nochi, T., et al., *Nanogel antigenic protein-delivery system for adjuvant-free intranasal vaccines.* Nat Mater, 2010. **9**(7): p. 572-8.
64. Ko, S.Y., et al., *alpha-Galactosylceramide can act as a nasal vaccine adjuvant inducing protective immune responses against viral infection and tumor.* J Immunol, 2005. **175**(5): p. 3309-17.
65. Watkins, J.D., et al., *Anti-HIV IgA isotypes: differential virion capture and inhibition of transcytosis are linked to prevention of mucosal R5 SHIV transmission.* AIDS, 2013. **27**(9): p. F13-20.
66. Blutt, S.E., et al., *IgA is important for clearance and critical for protection from rotavirus infection.* Mucosal Immunol, 2012. **5**(6): p. 712-9.
67. Mori, A., et al., *The vaccine adjuvant alum inhibits IL-12 by promoting PI3 kinase signaling while chitosan does not inhibit IL-12 and enhances Th1 and Th17 responses.* Eur J Immunol, 2012. **42**(10): p. 2709-19.

68. Khader, S.A., S.L. Gaffen, and J.K. Kolls, *Th17 cells at the crossroads of innate and adaptive immunity against infectious diseases at the mucosa.* Mucosal Immunol, 2009. **2**(5): p. 403-11.
69. Datta, S.K., et al., *Mucosal adjuvant activity of cholera toxin requires Th17 cells and protects against inhalation anthrax.* Proc Natl Acad Sci U S A, 2010. **107**(23): p. 10638-43.

CHAPTER 6

Effect of Chi-C48/80 NP on the anthrax protective antigen dose required for effective nasal vaccination

This chapter was adapted from:

Bento D, Staats HF, Borges O. Effect of particulate adjuvant on the anthrax protective antigen dose required for effective nasal vaccination. Vaccine, 2015. 33(31): p. 3609-13.

Abstract

Successful vaccine development is dependent on the development of effective adjuvants since the poor immunogenicity of modern subunit vaccines typically requires the use of potent adjuvants and high antigen doses. In recent years, adjuvant formulations combining both immunopotentiators and delivery systems have emerged as a promising strategy to develop effective and improved vaccines. In this study we investigate if the association of the mast cell activating adjuvant compound 48/80 (C48/80) with chitosan nanoparticles would promote an antigen dose sparing effect when administered intranasally. Even though the induction of strong mucosal immunity required higher antigen doses, incorporation of C48/80 into nanoparticles provided significant dose sparing when compared to antigen and C48/80 is solution with no significant effect on serum neutralizing antibodies titers. These results suggest the potential of this novel adjuvant combination to improve the immunogenicity of a vaccine and decrease the antigen dose required for vaccination.

6.1 Introduction

Strategies to reduce the antigen dose in vaccines are highly desirable since they could reduce the vaccine manufacturing cost, improve its availability and therefore increase the supply of vaccines worldwide. This is particularly relevant for mucosally-administered vaccines that usually require high antigen doses due to enzymatic degradation on the mucosae. The use of potent vaccine adjuvants is one of the strategies able to provide antigen sparing. More recently there has been a growing recognition of the potential of adjuvant combinations in vaccine development [1-4]. However, the advantage, in terms of antigen dose-sparing, of having an immunopotentiator co-delivered by nanoparticles instead of its soluble form has not yet been thoroughly evaluated. The aim of this study was to investigate if having an effective immunopotentiator incorporated within nanoparticles would increase adjuvant potency resulting in an antigen dose sparing effect. To test this hypothesis, compound 48/80 (C48/80), a mast cell activator with well established immunopotentiator properties [5-10], was associated with mucoadhesive chitosan nanoparticles. Mice were intranasally vaccinated with different doses of protective antigen of anthrax (PA) plus compound 48/80 (C48/80), in solution or incorporated in nanoparticles, and the respective immune response evaluated. To our knowledge, this is the first report that shows the effect of combining C48/80 and the antigen in chitosan nanoparticles on the antigen dose required for induction of the desired immune response.

6.2 Materials and Methods

6.2.1 Materials

Low molecular weight chitosan (deacetylation degree 95 %), was purchased from Primex BioChemials AS (Avaldsnes, Norway) and used after a purification process described in chapter 3, section 3.2.2. Compound 48/80 was purchased from Sigma-Aldrich (St Louis, MO, USA). Recombinant protective antigen of anthrax (PA) and recombinant lethal factor (rLF) were purchased from List Biologicals (Campbell, CA, USA).

6.2.2 Nanoparticle preparation and characterization

C48/80 loaded chitosan nanoparticles (Chi-C48/80 NP) were prepared by adding dropwise 3 mL of an alkaline solution (5 mM NaOH) of C48/80 and Na_2SO_4 (0.3 mg/mL and 2.03 mg/mL, respectively) to 3 mL of a chitosan solution (1 mg/mL in 0.1% acetic acid) under high speed vortexing. The nanoparticles were formed after further maturation for 60 min under magnetic stirring and PA was loaded by physical adsorption after incubation for 30 min

with Chi-C48/80 NP. Particle size and zeta potential were measured in a Zetasizer Nano ZS (Malvern). Loading efficacy of C48/80 and PA were determined according to the method described in section 3.2.2 and Pierce BCA protein assay, respectively. Endotoxin content of materials and nanoparticles was evaluated using the PYROGENT™ Gel Clot LAL assay.

6.2.3 Nasal immunization

Six- to eight-week-old C57BL/6NCr female mice were purchased from Charles River (National Cancer Institute, Frederick, MD). Mice (5 per group) were intranasally immunized on days 0, 7 and 21 with 0.4 μg, 1 μg or 2.5 μg of PA adjuvanted with 15 μg of C48/80 in solution or C48/80 incorporated in Chi NP. Controls included a naïve group that received saline and an antigen alone group vaccinated with 2.5 μg of PA. Each mouse received 15 μL of vaccine formulation, 7.5 μL per nostril, under isoflurane anesthesia. Serum was collected on days 14, 21 and 42. Nasal washes, fecal material and vaginal lavage were collected on day 42 and processed as previously described in section 5.9.3.3. All animal procedures were approved by Duke University Division of Laboratory Animal Resources and Duke University Institutional Animal Care and Use Committee (IACUC).

6.2.3.1 Measurement of antibodies by ELISA

Titers of PA-specific IgG, IgG isotypes and IgA antibodies were determined by ELISA as previously described in section 5.9.2.4. The log 2 endpoint titers were used for statistical analysis. Samples with undetectable titers were assigned a titer of one less than the first dilution tested.

6.2.3.2 LeTx neutralization assay

A macrophage toxicity assay using J774A.1 mouse macrophages (ATCC, Manassas, VA) was used to determine the ability of serum anti-PA antibodies to neutralize lethal toxin (LeTx). The assay was performed as previously described in section 5.9.2.7. LeTx neutralizing titers for each mouse were calculated as 50 % neutralization titers (NT50), i.e., the serum dilution needed to neutralize 50 % of LeTx. Samples with an NT50 less than 1:128 were below our tested range and were assigned a value of 1:64 for graphical representation and statistical evaluation.

6.2.4 Statistical analysis

Statistical analysis was performed with GraphPad Prism v 5.03 (GraphPad Software Inc., La Jolla, CA, USA). Student's t-test and one-way ANOVA followed by Tukey's post-test were used for two samples or multiple comparisons, respectively. A P value < 0.05 was considered statistically significant.

6.3 Results and Discussion

6.3.1 Anthrax protective antigen was efficiently adsorbed on the surface of Chi-C48/80 particles

Previous work demonstrated that nasal immunization with Chi-C48/80 NP as adjuvant resulted in high levels of protective antibodies and significantly higher nasal IgA titers than those induced by C48/80 in solution or Chi NP. Fecal and vaginal IgA levels were also significantly greater in mice immunized with Chi-C48/80 NP when compared to the responses induced by Chi NP (Chapter 5) [11]. Having demonstrated the potent adjuvant activity of Chi-C48/80 NP, the focus of this study was to assess if the incorporation of C48/80 in Chi NP had the further advantage of providing an antigen dose sparing effect when compared with C48/80 in solution.

A

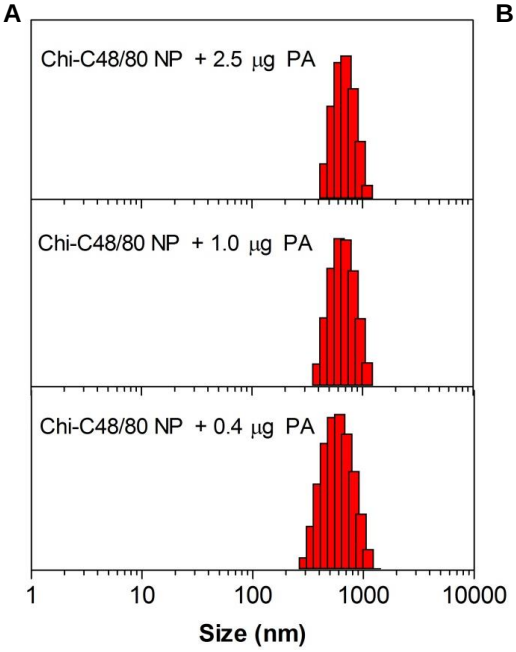

B

Vaccine Formulation	Size (nm)	PI	ZP (mV)
NP + PA 2.5 µg	633 ± 126	0.166 ± 0.063	26.4 ± 2.4
NP + PA 1.0 µg	678 ± 54	0.081 ± 0.043	28.3 ± 0.4
NP + PA 0.4 µg	557 ± 115	0.101 ± 0.060	29.2 ± 0.9

C

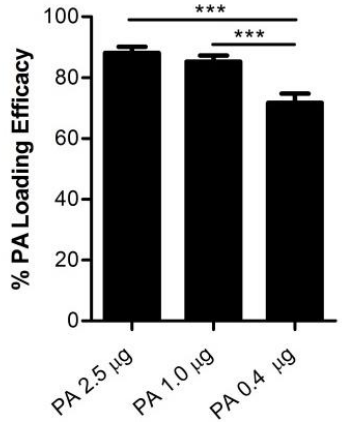

Figure 6.1 – Characterization of nanoparticle formulations used in the dose response study. (A) Representative size distribution by intensity of Chi-C48/80 NP loaded with different doses of PA. (B) Size, polydispersity index (PI) and zeta potential (ZP) of vaccine formulation and nanoparticles alone. (C) Loading efficacy of PA on nanoparticles surface for each dose of antigen tested, mean ± SD, n = 3.

Chi-C48/80 NP were prepared by a method optimized in our laboratory. The loading efficacy of C48/80 on NP was 18.7 ± 3.0 % which corresponded to a loading capacity of 35.3 μg of C48/80 per 1 mg of nanoparticles. These nanoparticles were thereafter loaded with different amounts of PA by physical adsorption to obtain vaccine formulations with the desired antigen doses. The vaccine formulations displayed a unimodal size distribution (Fig. 6.1A) with an average size in the range of 550 nm to 680 nm and were positively charged (Fig. 6.1B). All formulations had more than 70 % of the PA adsorbed to the particles and the remaining antigen was free on the nanoparticle suspension (Fig. 6.1C). The loading of different quantities of antigen on nanoparticle surface did not significantly affect the size and charge of the formulations ($p > 0.05$). To rule out the possibility of endotoxin contamination of the nanoparticles, endotoxin in the final formulation were evaluated and found to be below the level of detection (0.125 EU/ml) of the assay.

6.3.2 Incorporation of C48/80 in nanoparticles lowers the antigen dose required for the induction of serum Lethal Toxin neutralizing antibody responses

To evaluate if the incorporation of C48/80 in nanoparticles would improve its adjuvanticity leading to an antigen sparing effect, mice were intranasally immunized with 0.4 μg, 1 μg or 2.5 μg of PA adjuvanted with 15 μg of C48/80 in solution or incorporated in Chi NP (Chi-C48/80 NP). After the first boost (day 14), all adjuvants induced serum anti-PA IgG titers significantly greater than those induced by immunization with 2.5 μg PA alone (Fig. 6.2A). Chi-C48/80 NP plus 2.5 μg or 1 μg of PA induced anti-PA serum IgG titers significantly higher than all the other vaccine formulations while 0.4 μg of PA plus C48/80 in solution induced the lowest levels of PA-specific IgG. The beneficial effect of the encapsulation of the C48/80 was also observed by the direct comparison of C48/80 in solution with Chi-C48/80 NP at each antigen dose. Chi-C48/80 NP was more effective at inducing serum anti-PA IgG than C48/80 at all antigen doses tested. After the second boost (at day 42), 0.4 μg of PA plus C48/80 was again the group with lower anti-PA IgG when compared with all other adjuvanted groups (Fig. 6.2B). On the other hand, high levels of PA-specific IgG were detected in the serum of mice vaccinated with Chi-C48/80 NP even with only 0.4 μg of antigen. The increase in serum anti-PA IgG titers after the second boost was particularly evident in the group immunized with the lowest dose of PA adjuvanted with Chi-C48/80 NP. In fact, 0.4 μg of PA plus Chi-C48/80 NP induced PA-specific IgG titers significantly higher than the IgG responses induced by any dose of PA adjuvanted with C48/80 in solution.

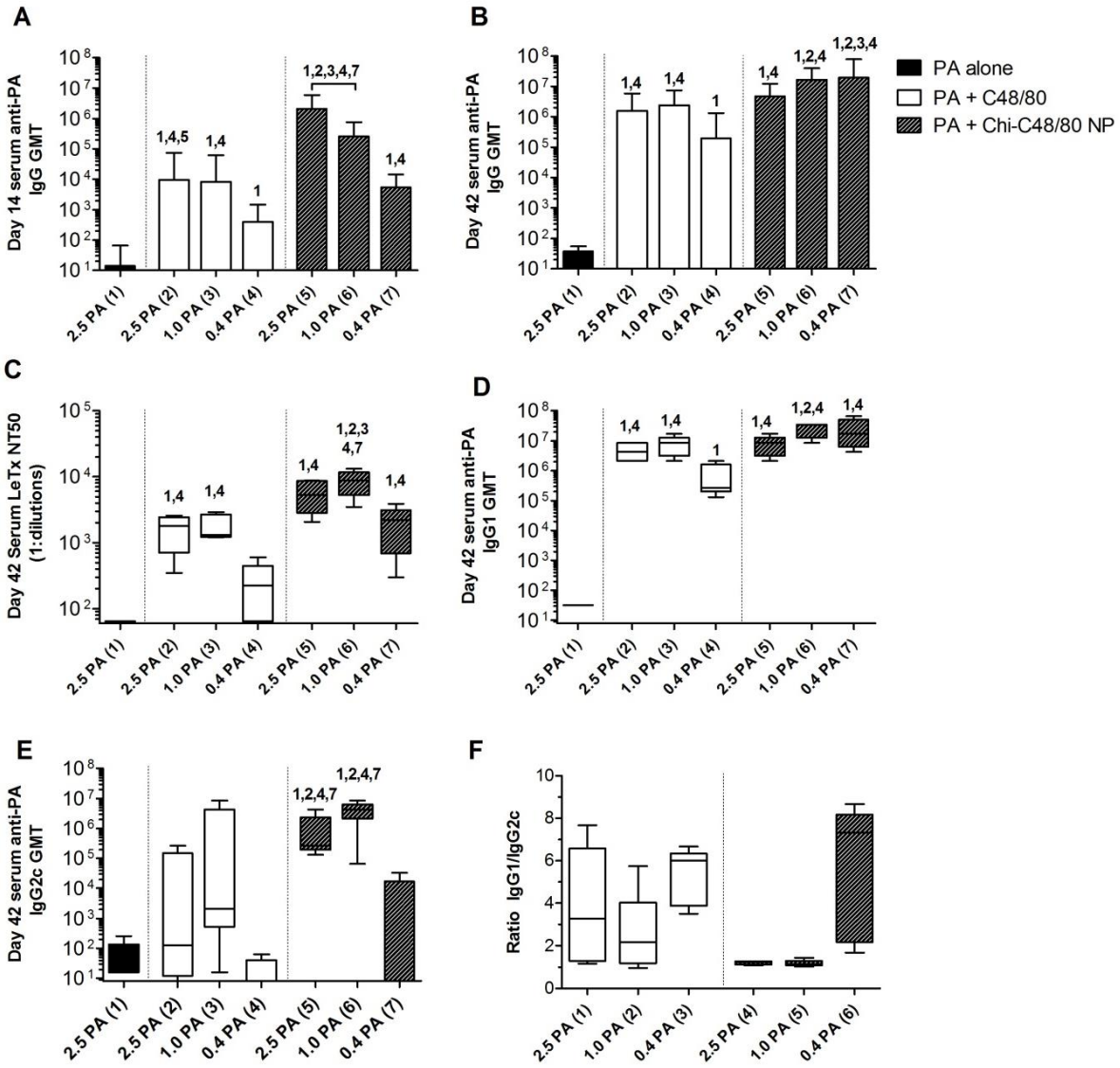

Figure 6.2 – Systemic immune responses after vaccination with different doses of PA alone or plus adjuvants. C57BL/6 mice were immunized on days 0, 7 and 21 with three doses of PA (2.5 μg, 1.0 μg and 0.4 μg) adjuvanted with C48/80 in solution or associated with nanoparticles. A non-adjuvanted group received 2.5 μg of PA. (A) Serum anti-PA IgG was evaluated by ELISA in samples from day 14 and (B) day 42. (C) A lethal toxin (LeTx) neutralization assay with J774A.1 macrophages was performed to measure functional anti-PA antibody responses in serum taken on day 42. Results are expressed as serum dilution required for a 50 % inhibition of LeTx-induced J774A.1 cell death (LeTx NT50). (D) Day 42 serum specific IgG1 and (E) IgG2c were measured and (F) IgG1/IgG2c ratio calculated. Antibody titers results are expressed as the antilog of the last log2 dilution for which the relative light units were at least 3-fold higher than the value of the naive sample equally diluted. Bars represent geometric mean titer (GMT) ± 95 % Confidence Interval. The numbers above the bars indicate which groups (1–7) are significantly different from the indicated group, $P < 0.05$, n = 5.

The use of PA allowed us to evaluate the functionality of the immune response using an *in vitro* macrophage toxicity assay that assesses the ability of the induced anti-PA serum antibodies to neutralize LeTx. While vaccination with 0.4 μg of PA plus free C48/80 failed to induce LeTx neutralizing titers significantly higher than those observed in mice immunized with antigen alone, the administration of C48/80 incorporated into nanoparticles resulted in strong LeTx-neutralizing activity even when using a lower dose of antigen (Fig. 6.2C). Interestingly, 1 μg of PA co-administered with Chi-C48/80 NP induced LeTx neutralizing titers significantly higher than those induced by any dose of PA adjuvanted with C48/80 in solution. The influence of antigen dose on the quality of the immune response was assessed by monitoring anti-PA IgG1 and IgG2c titers at day 42. All adjuvant formulations induced levels of anti-PA IgG1 significantly higher than IgG1 titers in mice immunized with PA alone but the group vaccinated with 0.4 μg PA plus free C48/80 had lower anti-PA IgG1 titers than all the other adjuvant groups (Fig. 6.2D). Immunization with 2.5 μg or 1.0 μg of PA plus Chi-C48/80 NP resulted in high levels of anti-PA IgG2c production with low variation between mice of the same group (Fig. 6.2E). In fact, while the other groups showed a Th2 biased immune response, the IgG1/IgG2c ratio on these two groups of mice was close to 1 (Fig. 6.2F) suggesting the induction of a mixed Th1/Th2 response by C48/80 incorporated into nanoparticles.

In summary, the vaccine-induced serum responses demonstrated that the incorporation of C48/80 in nanoparticles resulted in a more potent vaccine adjuvant than C48/80 in solution, allowing a reduction of the antigen dose from 2.5 μg to 0.4 μg without affecting the levels of functional serum antibodies. The induction of adaptive immune response with only 0.4 μg of PA in three doses (1.2 μg in total) is remarkable considering that much higher total PA amounts have been used in other studies, for example 15 μg with liposome-protamine-DNA (LPD) particles [12] or even 40 μg of PA adjuvanted with a nanoemulsion [13]. Boyaka et al [14] used from 10 μg up to 40 μg of PA per dose in a 3 times nasal immunization schedule and observed that the IgG subclass pattern was not affected by the antigen dose when using cholera toxin as the adjuvant. However, using much lower doses of PA we showed that the quality of the immune response was affected by both antigen dose and adjuvant formulation. While vaccination with the immunopotentiator in solution induced mainly anti-PA IgG1 antibodies, the incorporation of C48/80 into nanoparticles resulted in a production of both anti-PA IgG1 and IgG2c. This mixed response was not observed when mice were vaccinated with the lowest PA dose (Chi-C48/80 NP plus 0.4 μg of PA), suggesting that the induction of anti-PA IgG2c is dependent on the antigen dose.

6.3.3 Improvement of the mucosal immune response induced by incorporation of C48/80 into nanoparticles was dependent on the antigen dose

To investigate if the association of C48/80 with chitosan nanoparticles would improve vaccine-induced mucosal immunity antigen-specific IgA was analyzed in nasal washes, vaginal lavage and fecal extracts collected on day 42.

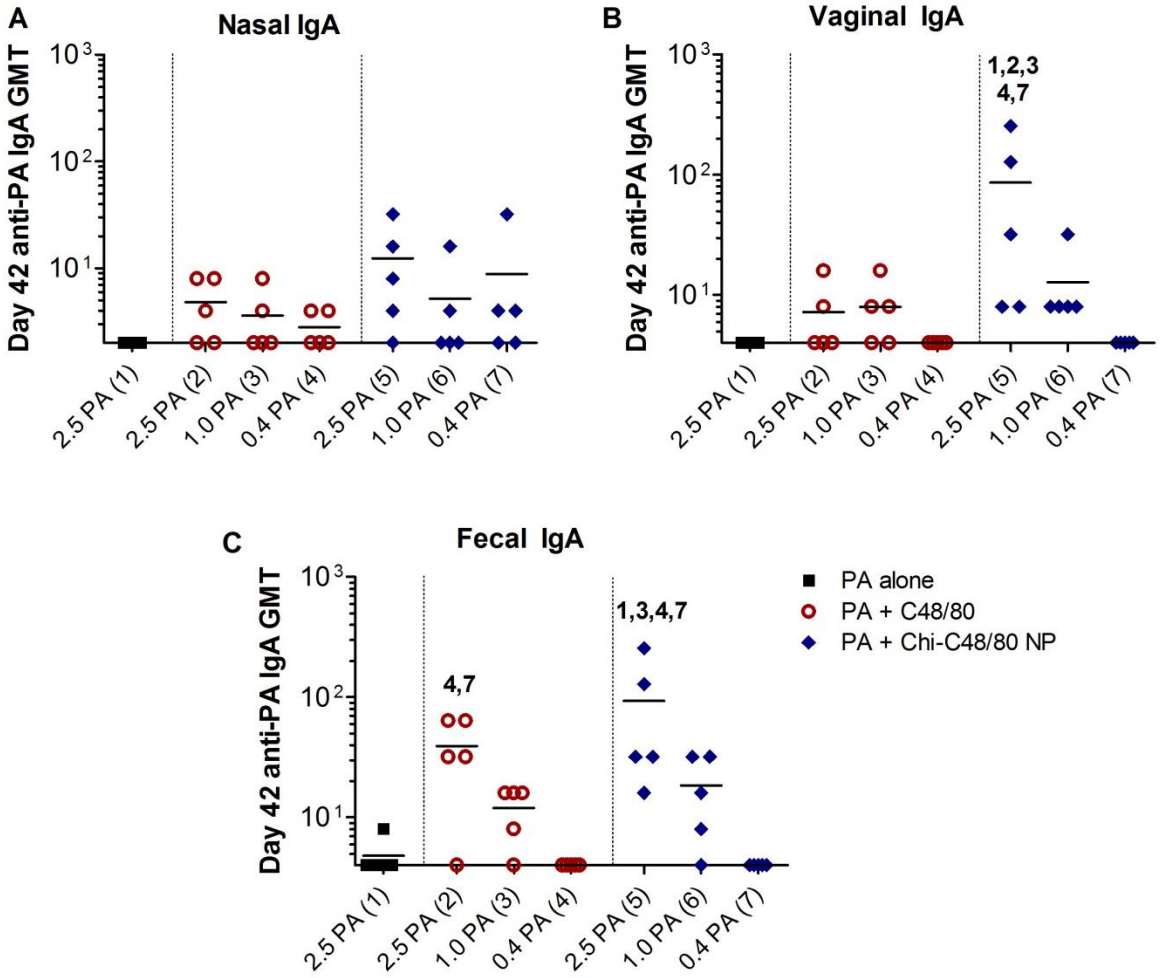

Figure 6.3 – Anti-PA IgA titers in (A) nasal washes, (B) vaginal lavage and (C) fecal extracts of immunized mice. C57BL/6 mice were immunized on days 0, 7 and 21 with three doses of PA (2.5 μg, 1.0 μg and 0.4 μg) adjuvanted with C48/80 in solution or associated with nanoparticles. Non-adjuvanted control included PA alone at 2.5 μg. On day 42, mice were sacrificed and mucosal samples collected for measurement of anti-PA IgA titers by ELISA. Results are expressed as the antilog of the last log2 dilution for which the relative light units were at least 3-fold higher than the value of the naive sample equally diluted. The numbers above the bars indicate which groups (1–7) are significantly different from the indicated group, $P < 0.05$, n = 5.

Vaccination with PA plus C48/80 in solution induced low titers of anti-PA mucosal IgA even at the highest dose of antigen tested (Fig. 6.3A to 6.3C) and responses were highly variable within groups. Although the anti-PA IgA responses in the NP groups also showed titer variability, high individual titers were observed, especially in vaginal (Fig. 6.3B) and fecal samples (Fig. 6.3C). Statistical analysis of the results determined that immunization with 2.5 μg of PA plus Chi-C48/80 NP induced fecal anti-PA IgA titers significantly higher than those induced by immunization with PA alone and vaginal anti-PA IgA antibodies significantly higher than those induced by PA alone or plus C48/80. In general, vaccination with PA plus nanoparticles produced detectable levels of antigen-specific IgA in more mice than the induced by immunization with PA adjuvanted with C48/80 in solution. However, the mucosal immunity was dependent on the antigen dose. The 2.5 μg of PA was required to induce IgA secretion significantly higher than PA alone, and a progressive reduction of mucosal immunity was observed in mice vaccinated with the lower doses of antigen. These results are in agreement with a previously study that showed that mucosal immunity was greatly dependent on the antigen dose [14]. However, while the described study used PA doses up to 40 μg, Chi-C48/80 NP induced mucosal immunity with only 2.5 μg of the same antigen which represents a relevant antigen dose sparing.

6.4 Conclusion

In this study, the potential of the novel adjuvant combination Chi-C48/80 NP to reduce the antigen dose required for mucosal vaccination was evaluated *in vivo*. The nasal administration of PA loaded Chi-C48/80 NP resulted in a lower dose of antigen required to achieve similar humoral immunity. However, mucosal immune response was dependent on the antigen dose, indicating that the maintenance of a strong mucosal immunity requires a higher antigen dose or a further optimization of the immunization scheme/adjuvant dose. In summary, our results demonstrate that the use of adjuvanted nanoparticles provides an effective strategy to maximize the induction of humoral immunity while reducing the antigen dose when using the intranasal route of immunization. The antigen dose sparing provided by adjuvanted nanoparticles represents a potential strategy to reduce the cost of vaccines while maintaining effective induction of humoral immunity.

References

1. Wilson, H.L., et al., *A novel triple adjuvant formulation promotes strong, Th1-biased immune responses and significant antigen retention at the site of injection.* Vaccine, 2010. **28**(52): p. 8288-99.

2. Kovacs-Nolan, J., et al., *The novel adjuvant combination of CpG ODN, indolicidin and polyphosphazene induces potent antibody- and cell-mediated immune responses in mice.* Vaccine, 2009. **27**(14): p. 2055-64.
3. Bradney, C.P., et al., *Cytokines as adjuvants for the induction of anti-human immunodeficiency virus peptide immunoglobulin G (IgG) and IgA antibodies in serum and mucosal secretions after nasal immunization.* J Virol, 2002. **76**(2): p. 517-24.
4. Schijns, V.E. and E.C. Lavelle, *Trends in vaccine adjuvants.* Expert Rev Vaccines, 2011. **10**(4): p. 539-50.
5. Staats, H.F., et al., *Mucosal targeting of a BoNT/A subunit vaccine adjuvanted with a mast cell activator enhances induction of BoNT/A neutralizing antibodies in rabbits.* PLoS One, 2011. **6**(1): p. e16532.
6. McGowen, A.L., et al., *The mast cell activator compound 48/80 is safe and effective when used as an adjuvant for intradermal immunization with Bacillus anthracis protective antigen.* Vaccine, 2009. **27**(27): p. 3544-52.
7. McLachlan, J.B., et al., *Mast cell activators: a new class of highly effective vaccine adjuvants.* Nat Med, 2008. **14**(5): p. 536-41.
8. Gwinn, W.M., et al., *A comparison of non-toxin vaccine adjuvants for their ability to enhance the immunogenicity of nasally-administered anthrax recombinant protective antigen.* Vaccine, 2013. **31**(11): p. 1480-9.
9. Zeng, L., et al., *Compound 48/80 acts as a potent mucosal adjuvant for vaccination against Streptococcus pneumoniae infection in young mice.* Vaccine, 2015. **33**(8): p. 1008-16.
10. Zheng, M., et al., *Cross-protection against influenza virus infection by intranasal administration of nucleoprotein-based vaccine with compound 48/80 adjuvant.* Hum Vaccin Immunother, 2015: p. 0.
11. Bento, D., et al., *Development of a novel adjuvanted nasal vaccine: C48/80 associated with chitosan nanoparticles as a path to enhance mucosal immunity.* European Journal of Pharmaceutics and Biopharmaceutics, 2015. **93**(0): p. 149-164.
12. Sloat, B.R. and Z. Cui, *Strong mucosal and systemic immunities induced by nasal immunization with anthrax protective antigen protein incorporated in liposome-protamine-DNA particles.* Pharm Res, 2006. **23**(2): p. 262-9.
13. Bielinska, A.U., et al., *Mucosal immunization with a novel nanoemulsion-based recombinant anthrax protective antigen vaccine protects against Bacillus anthracis spore challenge.* Infect Immun, 2007. **75**(8): p. 4020-9.
14. Boyaka, P.N., et al., *Effective mucosal immunity to anthrax: neutralizing antibodies and Th cell responses following nasal immunization with protective antigen.* J Immunol, 2003. **170**(11): p. 5636-43.

CHAPTER 7

Concluding remarks and future perspectives

The evolution of emerging infectious diseases and appearance of pathogens resistant to antimicrobial drugs emphasize the importance of the continuous development of new efficient vaccination strategies. Furthermore, development of vaccines against diseases for which successful vaccines are not currently available would bring huge benefits for public health and for the society. One of the unmet goals in vaccine development is to induce an effective immune response against potential pathogens at mucosal surfaces. Considering this, together with the recent success of the adjuvant combination strategy to increase the efficacy of subunit vaccines, this project aimed at developing a novel delivery system for nasal vaccination composed by two highly promising adjuvant candidates: chitosan nanoparticles and the mast cell activator C48/80. This was the first time that the effects of the association of a mast cell activator with nanoparticles on the induction of an immune response were investigated.

One of the initial challenges of this project was the development of a method to quantify the C48/80 after being associated to the chitosan-based particles, to support the formulation development of C48/80 loaded nanoparticles. Therefore, we developed and validated a UV-Vis spectrophotometric method to quantify C48/80. The method was validated according to the recommendations of ICH Guidelines for specificity, linearity, range, accuracy, precision and detection and quantification limit. This C48/80 quantification method was optimized for 96-well plates, requiring only a small volume of sample and allowing the simultaneous analysis of a large number of samples, which is very helpful during formulation development.

Two C48/80 loaded chitosan-based delivery systems were successfully developed: Chi-C48/80 NP and Chi/Alg-C48/80 NP, with mean particle size of 501 nm and 564 nm, respectively. While incorporation of C48/80 in Chi NP did not significantly change the size and charge of the particles, the same was not true for Chi/Alg NP. The association of C48/80 with Chi/Alg significantly affected both, size and zeta potential of the formulation. The main objective of this project was to prepare C48/80 loaded nanoparticles to use as an enhanced adjuvant delivery system. However, in some *in vitro* tests, namely cytotoxicity and mast cell activation studies, it was important to evaluate the effect of the association of the C48/80 with the nanoparticles and therefore particles without C48/80 were also developed and tested. Since unloaded Chi NP had very similar characteristics to Chi-C48/80 NP, it is safe to assume that any differences observed between these formulations, either *in vitro* or *in vivo*, were due to the presence of C48/80. However, unloaded Chi/Alg NP was not a stable formulation and had a significantly higher particle size and lower zeta potential than Chi/Alg-C48/80 NP. We could have optimized Chi/Alg NP to a more stable formulation and with a size similar to

Chi/Alg-C48/80 NP. But this formulation would have a totally different amount of the polymers chitosan and alginate when compared with the loaded nanoparticles, so it would not be suitable as a control for the above described experiments. Even if Chi/Alg NP were not ideal we consider that they were the best control possible for the studies performed.

In vitro studies showed that Chi-C48/80 NP were more efficiently internalized by APCs than Chi/Alg-C48/80 NP. Similarly to unloaded Chi NP, Chi-C48/80 NP showed low cytotoxicity even at high concentrations. On the other hand, Chi/Alg-C48/80 NP were more cytotoxic than unloaded Chi/Alg NP. Nevertheless, incorporation of C48/80 in both formulations resulted in a decreased toxicity of the immunopotentiator compared with C48/80 in solution. This is particularly important for prophylactic vaccines because since most of the vaccines are given to a healthy population, a risk-benefit analysis of vaccination favors safety over efficacy.

Since we were using a mast cell activator as immunopotentiator, we wanted to see if the incorporation of C48/80 with nanoparticles would interfere with its ability to activate mast cells. We observed that the association of C48/80 with Chi NP but not with Chi/Alg NP resulted in enhanced *in vitro* mast cell activation when compared with C48/80 in solution. The results also revealed the ability of Chi NP of its own to activate mast cells. This was a surprising result, since there was, at the time, no report in the literature showing the ability of chitosan to activate mast cells. More recently, a study published by Farrugia et al. supported our findings by demonstrating the ability of chitosan to adhere and stimulate mast cells [1].

One of the aims of the project was to develop a mucoadhesive delivery system that would extend the residence time of the antigen in the nasal cavity. That, together with the adjuvant properties of chitosan itself, was the main reason why this polymer was selected as the basis of our prototypic delivery system for nasal vaccination. Therefore, to see if the developed delivery systems could successfully decrease the clearance of the antigen, an *in vivo* imaging study using fluorescently labelled ovalbumin was performed. The results revealed that Chi-C48/80 NP but not Chi/Alg-C48/80 NP significantly enhanced the nasal residence time of the model antigen.

Although the incorporation of alginate in chitosan-based nanoparticles efficiently increased the loading efficacy of the cationic C48/80, the results from *in vitro* studies and from the nasal residence study, suggested that Chi-C48/80 NP was a more valuable vaccine adjuvant candidate than Chi/Alg-C48/80 NP. To assess if these results would translate into Chi-C48/80 NP being a better vaccine adjuvant, we compared the ability of both formulations to enhance the immunogenicity of nasally-administered anthrax protective antigen (PA). In Chi-

C48/80 NP, C48/80 was incorporated in the nanoparticles during the preparation as detailed in the chapter 3. To analyze if the observed effects were due to the incorporation of C48/80 in NP or simply a result of the additive effects of chitosan plus C48/80, we also include in our experimental design a group with Chi NP plus C48/80 in solution. Vaccination studies confirmed that Chi-C48/80 NP is better nasal adjuvant candidate than Chi/Alg-C48/80 NP. Nasal immunization of mice with PA adsorbed on Chi-C48/80 NP elicited high levels of serum anti-PA neutralizing antibodies and more anti-PA IgG2c antibodies than C48/80 in solution or Chi/Alg-C48/80 NP. The incorporation of C48/80 within Chi NP also promoted a greater mucosal immunity than all the other adjuvanted groups tested, including the Chi NP + C48/80 adjuvanted group. This suggests that the actual incorporation of C48/80 in Chi NP was more beneficial than the simply combination of both adjuvants.

It would be interesting to see if the *in vitro* mast cell activation results translate into the *in vivo* differences observed between Chi-C48/80 NP and Chi NP. In other words, although Chi-C48/80 NP was a better adjuvant than Chi NP we do not know for sure if the differences observed *in vivo* are due to mast cell activation. It is known that mast cells play a role in the *in vivo* adjuvant activity of C48/80 but mast cell activation does not explain all of the adjuvant activity of C48/80. McLachlan et al. demonstrated that C48/80 still had some adjuvant activity in mast cell deficient ($Kit^{W}/Kit^{W\text{-}v}$) mice, although the adjuvant activity in these mice was less than the adjuvant activity in wild type mice [2]. Immunization of mast cell deficient mice with Chi-C48/80 NP and Chi NP would allow us to understand if the differences observed between these formulations are to some extent mediated by mast cell activation. Furthermore, since mast cell activation by chitosan is a recent discovery, the immunization of mast cell deficient mice and wild-type mice in parallel would be important to assess the mast cell involvement in the adjuvant effect of chitosan nanoparticles.

Considering the novelty of Chi-C48/80 NP it would also be very interesting to determine the cytokines produced by different cell subsets using intracellular cytokine staining, a flow cytometry based assay. Additionally, it would be worth assessing antigen-specific T cell responses using MHC tetramer staining, particularly investigate if antigen specific CD8+ T cells are stimulated using MHC class I tetramers. This would be difficult using PA as antigen, but we could use OVA as antigen since this protein was also used as a model antigen for part of the characterization studies.

Given the great potential of Chi-C48/80 NP demonstrated in the nasal immunization studies, we wanted to further investigate if the association C48/80 with chitosan nanoparticles would promote an antigen dose sparing effect. Chi-C48/80 NP were indeed able to provide

significant dose sparing when compared to antigen and C48/80 is solution, representing a potential strategy to reduce the cost of vaccines while maintaining effective induction of humoral immunity. However, is noteworthy that the induction of a mucosal immune response was dependent on the antigen dose. This suggests that maintenance of a strong mucosal immunity requires a higher antigen dose. It would be interesting to assess if an optimization of the immunization scheme and/or an increase of the adjuvant dose could restore the mucosal immune response while retaining the antigen dose sparing effect.

The use of PA from *Bacillus anthracis* allowed us to evaluate the functionality of the immune response using an *in vitro* macrophage toxicity assay that assesses the ability of the induced anti-PA serum antibodies to neutralize LeTx. Additionally, PA has the grand advantage of being a clinically relevant antigen and the development of a new nasal vaccine against anthrax is highly desired. Anthrax is considered by US Centers for Disease Control and Prevention as one of the most likely agents to be used as a biological weapon [3]. There are two anthrax vaccines currently licensed for human use, the US licensed anthrax vaccine adsorbed (AVA or Biothrax) and the analogous UK licensed anthrax vaccine precipitated (AVP). While these vaccines are effective, they have several drawbacks such as an intensive dosing schedule, relatively high rates of adverse reactions and an undefined composition. Therefore, efforts have been made to develop a more effective and tolerable anthrax vaccine. Ideally, a new anthrax vaccine should be needle-free to facilitate mass vaccination and stable at room temperature to avoid cold-chain requirements. Additionally, since the most severe form of anthrax is inhalational anthrax, a new anthrax vaccine should induce mucosal immunity conferring protection at the local of entry of the pathogen. The results of this project showed that needle-free nasal immunization using anthrax protective antigen adjuvanted with Chi-C48/80 NP efficiently induced both high levels of serum anti-PA neutralizing antibodies and mucosal antibodies, which would be highly beneficial in an anthrax vaccine. Furthermore, our studies showed that Chi-C48/80 NP were stable at room temperature for at least 4 months, after lyophilization with trehalose as cryoprotectant. This indicates that this adjuvant combination can potentially be used to develop a vaccine formulation to avoid cold chain requirements. However, to more completely assess the storage stability of a Chi-C48/80 NP adjuvanted vaccine, the nanoparticles should be lyophilized after antigen adsorption and stored under different temperature and different moisture levels. Stability of the vaccine should then be assessed by determining not only its physicochemical characteristics but also its biological activity. In the particular case of PA, an *in vitro* macrophage toxicity assay could be used to assess the functionality of the antigen [4].

To conclude, the aim of this project was achieved. Two C48/80 loaded chitosan-based delivery systems were successfully developed and tested as adjuvants for nasal vaccines. Chi-C48/80 NP revealed to be a better nasal adjuvant than Chi/Alg-C48/80 NP inducing high mucosal and systemic immune responses to PA following nasal immunization. Overall, the results from this thesis show that the combination of two mucosal adjuvants C48/80 and chitosan resulted in an improved adjuvant formulation and is a promising strategy for the development of nasal vaccines. Chi-C48/80 NP could be an attractive adjuvant prototype to develop a new stable and effective subunit vaccine against anthrax or other mucosally transmitted diseases.

References

1. **Farrugia, B.L., et al., *The localisation of inflammatory cells and expression of associated proteoglycans in response to implanted chitosan.* Biomaterials, 2014. 35(5): p. 1462-77.**
2. **McLachlan, J.B., et al., *Mast cell activators: a new class of highly effective vaccine adjuvants.* Nat Med, 2008. 14(5): p. 536-541.**
3. **Statistics, C.-N.C.f.H. *Anthrax - Bioterrorism*. 2016 August 1, 2014 [cited 2016 July 1, 2016]; Available from: http://www.cdc.gov/anthrax/bioterrorism/threat.html.**
4. **Wang, S.H., et al., *Stable dry powder formulation for nasal delivery of anthrax vaccine.* J Pharm Sci, 2012. 101(1): p. 31-47.**